This is to certify that the
dissertation entitled

REGULATION OF SUBSARCOLEMMAL CA^{2+}
OSCILLATIONS AND MYOGENIC TONE IN THE
MICROCIRCULATION

presented by

ERIKA BOERMAN WESTCOTT

has been accepted towards fulfillment
of the requirements for the

Ph.D. degree in Pharmacology and Toxicology

Major Professor's Signature

11/22/10

Date

REGULATION OF SUBSARCOLEMMAL CA^{2+} OSCILLATIONS AND MYOGENIC TONE IN THE MICROCIRCULATION

By

Erika Boerman Westcott

A DISSERTATION

Submitted to
Michigan State University
In partial fulfillment of the requirements
for the degree of

DOCTOR OF PHILOSOPHY

Pharmacology and Toxicology

2010

ABSTRACT

REGULATION OF SUBSARCOLEMMAL CA^{2+} OSCILLATIONS AND MYOGENIC TONE IN THE MICROCIRCULATION

By

Erika Boerman Westcott

Ryanodine receptors (RyR) and inositol 1,4,5, trisphosphate receptors (IP_3R) importantly contribute to Ca^{2+} signals and myogenic tone in arteries, but their roles in the microcirculation remain unclear. The purpose of this study was to determine the function of both RyR and IP_3R in Ca^{2+} signals and myogenic tone in hamster and mouse cremaster muscle feed arteries and downstream arterioles using confocal imaging and pressure myography and to test the hypothesis that the expression and localization of RyR isoforms may account for differences in the roles played by RyR in feed arteries and down stream arterioles. In both species, feed arteries displayed Ca^{2+} sparks and Ca^{2+} waves, both of which were inhibited by the RyR antagonist, ryanodine (10 μM). Despite the inhibition of sparks and waves, ryanodine increased global intracellular Ca^{2+} and constricted the feed arteries. Blockade of IP_3R with xestospongin D (5 μM) or 2-aminoethoxydiphenyl borate (2-APB; 100 μM), or inhibition of phospholipase C (PLC) using U73122 (10 μM) also eliminated Ca^{2+} waves in feed arteries from both hamsters and mice. However, the IP_3R and PLC antagonists decreased global intracellular Ca^{2+} and dilated feed arteries without affecting Ca^{2+} sparks.

In contrast, cremaster arterioles from both species displayed only Ca^{2+} waves: Ca^{2+}sparks were not observed, and ryanodine (10-50 μM) affected neither Ca^{2+} signals nor arteriolar tone, despite the presence of functional RyR as assessed by responses to the RyR agonist, caffeine (10 mM). Arteriolar Ca^{2+} waves were abolished by xestospongin D (5 μM), 2-APB (100 μM) and U73122 (10 μM), all of which also decreased global intracellular Ca^{2+} and dilated the arterioles from both hamsters and mice. Quantitative, real-time, reverse transcriptase polymerase chain reaction applied to smooth muscle cells enzymatically isolated from mouse cremaster feed arteries and arterioles showed that RyR1 was not expressed feed artery or arteriole smooth muscle cells, that the relative abundance of transcripts for RyR2 was greater than that for RyR3, and importantly that RyR2 was more highly expressed in feed artery than arteriole smooth muscle, whereas transcripts for RyR3 were more abundant in arteriole than feed artery smooth muscle cells. Immunofluorescence staining with an anti-RyR1/2 antibody showed dense, clustered labeling in feed arteries, in contrast to more diffuse, uniform cytoplasmic staining in cremaster arterioles. These findings highlight the contrasting roles played by RyR and IP_3R in Ca^{2+} signals and myogenic tone in feed arteries, and demonstrate important differences in the function of RyR between feed arteries and downstream arterioles. Differences in RyR isoform expression and RyR protein localization may be responsible for the functional differences in RyR function between feed arteries and downstream arterioles.

ACKNOWLEDGEMENTS

I would first like to thank my mentor, Dr. Bill Jackson for taking the time to really help me grow as a student, researcher, and thinker. I owe many of my successes to your excellent training, and I hope I can continue on this path and be as wonderful a scientist and person as you.

Thank you to my committee members, coworkers and fellow students for your help making all my research possible. I would especially like to thank Erica Lange for her outstanding technical expertise and overall support.

I would also like to thank my parents and brother for their lifelong support and love. Without that foundation, I would never have been able to achieve this goal, and your examples of hard work and support kept me going whenever I had tough times.

Finally, thank you to my fantastic husband, Martin. You have been there for all the highs and lows of my time in graduate school, and I can't imagine doing any of it without you. Our relationship makes me better and more balanced personally and professionally. You get me, and I love you for that.

TABLE OF CONTENTS

LIST OF TABLES

LIST OF FIGURES

(some images are presented in color)

LIST OF ABBREVIATIONS

0 Ca^{2+} PSS	Calcium-free physiological salt solution
2-APB	2-aminoethoxydiphenyl borate
AC	Adenylate cyclase
BK_{Ca}	Large conductance calcium-activated potassium channels
CamKII	Calmodulin kinase II
cAMP	Cyclic adenosine monophosphate
CCE	Capacitative calcium entry
cGMP	Cyclic guanylyl monophosphate
CICR	Calcium-induced calcium release
Cl_{Ca}	Calcium-activated chloride channels
Cl_{VR}	Voltage-regulated chloride channels
DAG	Diacyl glycerol
DHPR	Dihydropyridine receptors
DMSO	Dimethyl sulfoxide
FDHM	Full duration at half-maximal amplitude
FKBP	FK506-binding protein
FWHM	Full width at half-maximal amplitude
HCA	Hamster cremaster arterioles
HFA	Hamster feed arteries
IHC	Immunohistochemistry
IK_{Ca}	Intermediate-conductance calcium-activated potassium channels

IP_3	Inositol (1,4,5) trisphosphate
IP_3R	Inositol (1,4,5) triphosphate receptors
K_{2P}	Two pore domain potassium channels
K_{ATP}	Adenosine triphosphate-sensitive potassium channel
K_{IR}	Inwardly-rectifying potassium channel
K_V	Voltage-regulated potassium channel
MCA	Mouse cremaster arterioles
MFA	Mouse feed arteries
MLC	Myosin light chain
MLCK	Myosin light chain kinase
PBS	Phosphate-buffered saline
PIP_2	Phosphatidyl inositol (4,5) bisphosphate
PKA	Protein kinase A
PKG	Protein kinase G
PLC	Phospholipase C
PMT	Photomultiplier tube
P_o	Probability of channel opening
PSS	Physiological salt solution
ROI	Region of interst
RyR	Ryanodine receptor
SAC	Stretch activated cation channel

SK_{Ca}	Small-conductance calcium-activated potassium channel
SMC	Smooth muscle cells
SOC	Store-operated cation channel
SR	Sarcoplasmic reticulum
STOC	Spontaneous transient outward current
TEA	Tetraethyl ammonium
TRP	Transient receptor potential
VGCC	Voltage-gated calcium channel

CHAPTER 1: INTRODUCTION

Skeletal muscle constitutes 40 % of body mass, and the vasculature in these muscles is essential in the regulation of cardiovascular homeostasis throughout the body (17, 98, 182, 198). Arterioles in the circulation are particularly important, as they are the major regulators of blood flow in these tissues (61). This regulation is achieved largely through modulation of myogenic tone and its underlying signaling pathways in the vascular smooth muscle cells, but the exact mechanisms of regulation are not clear (63). First observed by Bayliss (14), myogenic tone contributes to cardiovascular homeostasis by regulating blood flow, blood pressure, and exchange (61). The myogenic response allows for blood pressure-induced changes in tone to protect from end-organ damage, and steady state tone contributes to the maintenance total peripheral resistance and transcapillary exchange (62, 70, 224, 240). Ion channels, both in the plasma membrane and on the sarcoplasmic reticulum (SR) are critical to the regulation of myogenic tone (133). They provide the major source of activator Ca^{2+} that importantly regulates smooth muscle contraction(124). Ion channels in the plasma membrane also determine and modulate membrane potential (133). Membrane potential, in turn, determines the open state probablility of voltage-gated calcium channels (VGCC), Ca^{2+} influx, and hence myogenic tone. In addition, membrane potential influences Ca^{2+} release from internal stores (260) and may also affect Ca^{2+} sensitivity (285). Thus, ion channels play a central role

in the function of smooth muscle and the regulation of myogenic tone. This project focuses on the role of two SR Ca^{2+} release channels, ryanodine receptors and inositol (1,4,5) triphosphate receptors, and their specific roles in the regulation of subsarcolemmal Ca^{2+} signals and myogenic tone in cremaster muscle arterioles and their upstream feed arteries.

1. Ryanodine Receptors (RyR)

1.1. Structure.

Ryanodine receptors (RyR) are the largest known ion channel proteins (113) . They are composed of four identical ~560 kDa subunits and form, ryanodine-sensitive Ca^{2+} channels located on intracellular membranes such as the endoplasmic reticulum and the mitochondria (113). The bulk of the subunits are located on the cytoplasmic side of the membrane and form the large pore region, which allows the release of Ca^{2+} from intracellular stores into the cytoplasm (21, 113, 114, 174, 297). Despite numerous studies looking at the transmembrane and pore region topology (67, 110, 114, 255, 266, 297, 306) the specific structure of these regions has yet to be resolved. However, the C- and N- terminal ends of the protein are assumed to be on the cytoplasmic side of the membrane, and therefore the number of transmembrane domains is widely presumed to be an even number (174). The proposed number of transmembrane domains varies between four (255), six (266) eight (67) or ten (306), although the six- and eight-transmembrane domain models are favored due to the newer technology used to

resolve the structures, including high resolution electron microscopy and x-ray crystallography (114). The three-dimensional structure of RyR, shown in **Figure 1** from Perkel (219), suggests that the cytoplasmic portion, or "head" of the receptor, contains approximately 80% of their total mass (69). Each of the four subunits of the cytoplasmic "head" contain a clamp-shaped area that may allow the receptor to interact with other RyR or with RyR-associated proteins (23, 114). The "stem" of the receptor consists of the transmembrane assembly and accounts for only about 20% of the total mass (69). Within the "stem," four high-density columns surrounding a low-density region suggest the location of the pore, and a structure in the center of this channel (the "plug") may be important for channel gating (229).

1.2. Isoforms.

Ryanodine receptors exist in three isoforms (RyR1, RyR2 and RyR3), with nomenclature based on the chronological order in which they were discovered (113, 114, 297). The three isoforms are the product of distinct genes (RYR1-RYR3), and all three isoforms have relatively high sequence homology (66% between RyR1 and RyR2, 67% between RyR1 and RyR3 and 70% between RyR2 and RyR3) (110, 255, 306). In addition, the three-dimensional structures of the isoforms appear nearly identical (211, 243, 245). The sequence differences between the isoforms are contained mainly in three distinct regions of

the receptor. These divergent regions, termed D1, D2 and D3 are all located in the large cytoplasmic portion of the RyR, and these regions may be responsible for any functional differences observed between the isoforms (69). The D3 region of RyR1 is of particular interest because it uniquely contains a long chain of negatively charged residues thought to give the isoform a low-affinity calcium binding site that inactivates the receptor (174).

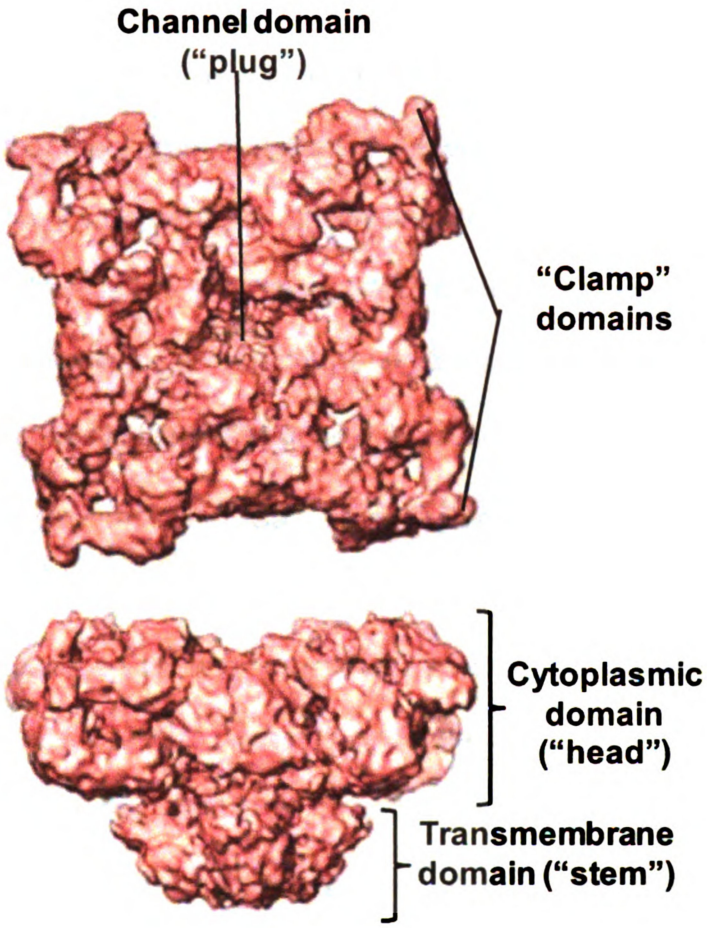

Figure 1. Three dimensional structure of ryanodine receptors

The top picture shows a top-down view of a ryanodine receptor, with the channel and clamp regions highlighted. The bottom image shows a side view of the receptor with the large cytoplamic domain ("head") and the smaller transmembrane domain ("stem") labeled accordingly. Adapted from Perkel 2009 (219).

1.3. Related Diseases.

Important insights into the unique functions of RyR isoforms have been gleaned from diseases that result from mutations in the genes encoding these receptors and alterations in posttranslational modifications of RyR, particularly for RyR1. Malignant hyperthermia is a pharmacogenetic disorder triggered by inhaled anesthetics or depolarizing muscle relaxants (232). The underlying genetic defects are mutations in the RYR1 gene that cause increased Ca^{2+} mobilization from the endoplasmic reticulum (Ca^{2+} "leak") when triggered by the above-stated drugs. The resulting condition is characterized by a rapid increase in body temperature, muscle rigidity and sometimes hyperkalemia, arrhythmia and metabolic acidosis (16, 209). Over 60 point mutations in RYR1 have been linked to malignant hyperthermia, and most of them are clustered into three specific regions of the gene near the N-terminal (Cys^{35}-Arg^{614}), the central (Asp^{2129}-Arg^{2458}), and near the C-terminal (Ile^{3916}-Ala^{4942}) domains of the channel (16). Despite the differences in location of these mutations, the resulting malignant hyperthermia is generally physiologically similar in terms of its clinical manifestations (16). Another condition, central core disease, also results from mutations in the RYR1 gene in these regions. Central core disease also results from excessive Ca^{2+} release from intracellular stores and leads to muscle weakness and motor deficiency. In both malignant hyperthermia and central core disease, the more severe myopathies are associated with RYR1 mutations on the C-terminus (154, 209). Mutations in RYR2 are not linked as conclusively

with disease as mutations in RYR1, but RYR2 is thought to play a role in the development of catecholaminergic polymorphic ventricular tachycardia, a rare condition brought on by periods of intensive exercise or stress (158). RyR2 is also loosely linked to congestive heart failure due to the hyperphosphorylation of RyR2 observed in some cases of heart failure (16).

1.4. Expression.

Ryanodine receptors are widely expressed throughout the body. In general, RyR1 is predominantly expressed in the skeletal muscle, RyR2 in the heart and RyR3 in the brain and other locations in lower amounts (92, 165, 230). However, many studies have shown that all three isoforms are expressed in many types of tissues at variable levels, and the improving technical ability to detect lower levels of expression has shown the presence of each of the ryanodine receptor isoforms in locations where they were previously undetectable (93, 175, 297). The widespread expression and distribution of RyR suggests that they participate in Ca^{2+} signaling and regulation in most tissues throughout the body (92).

In vascular smooth muscle, the expression and distribution of the RyR isoforms has not been clearly defined, and expression patterns appear to vary somewhat between studies and vessel types (237, 267, 269, 290). Recently, studies by Vaithianathan et al. (267), in cerebral artery smooth muscle found greater RyR2 message and protein expression compared to RyR1 or RyR3, which were both present at lower levels. In contrast, Salomone et al. (237), found expression of

RyR3, but not RyR1 or RyR2 in cerebral artery smooth muscle cells. Yang et al. (290), found that in intact rat aorta and pulmonary arteries, mRNA for all three isoforms were expressed, but RyR2 was much more abundant than RyR1 or RyR3, which were expressed in similar levels. However, in cultured aortic smooth muscle cells, Vallot et al. (269), demonstrated expression of all three isoforms in aortic smooth muscle cells, with RyR3 being most highly expressed, followed by RyR2 and RyR1, respectively. Studies in primary cultures of portal vein smooth muscle cells by Coussin et al. (54), showed similar expression of RyR1 and RyR2, with a lesser expression of RyR3. Zheng et al. (302) characterized RyR isoform expression in smooth muscle from rat pulmonary conduit arteries, pulmonary resistance arteries, and mesenteric arteries. All isoforms were expressed in similar levels in the pulmonary resistance arteries, while both pulmonary conduit arteries and mesenteric arteries expressed RyR1 and RyR2 at levels much higher than RyR3. These studies show that there are important differences in the expression of RyR isoforms in different types of vascular smooth muscle that may correlate to differences in the regulation of Ca^{2+} signaling. RyR from microvascular smooth muscle are particularly understudied, and they need to be better characterized in order to define the functional significance of each subtype in these cells.

1.5. Splice Variants.

In addition to differences in expression of the three isoforms of RyR, there are also splice variants of these receptors that may be important in some vascular

smooth muscle. Two known splice variants exist for RyR1: ASI and ASII (Alternative Splice sites I and II), which are located on separate exons within the gene (90). These splice variants appear in mouse heart, brain and skeletal muscle but vary in distribution based on tissue type and developmental timeline (90). The RyR1 splice variants exist in a region of the receptor responsible for inhibitory inter-domain interaction, and it has been proposed that they result in increased channel activity due to removal of this inhibition (150, 151). RyR3 also has splice variants that can occur in as many as seven known regions of the gene and have been documented in many tissues, including vascular smooth muscle (167, 185, 197). Of particular significance is the finding by Jiang et al. (146), that one of the splice variants of RyR3 (AS-8a, with a deletion in exon 8) is unique to smooth muscle cells. The deletion of a 29 amino acid fragment in a transmembrane region of the channel that leads to an incomplete channel with decreased capacity for Ca^{2+} release (58, 146). There is some evidence from heterologous expression studies in HEK 293 cells, however, that the function of these channels can be restored if they heterodimerize with wild type channels (58, 146). However, there is also evidence that the RyR3 AS-8a variant has a dominant negative effect, in which it heterodimerizes with functional RyR2 and suppresses the activity of that channel (146). The unique properties and specificity to smooth muscle of the RyR3 AS-8a splice variant makes it a potentially important area for future studies into the role of RyR subtypes and variants in Ca^{2+} handling in vascular and other smooth muscle cells.

1.6. Regulation.

Calcium. Calcium ions have a complex effect on RyR that varies based on the concentration and location of Ca^{2+} as well as the RyR subtype (52, 143, 164, 217, 262). All RyR isoforms are activated by cytosolic Ca^{2+} concentrations in the range of 1-10 μM (44, 113, 114, 147), and RyR1 are inhibited by cytosolic Ca^{2+} concentrations of 1 mM or higher, which suggests the possible presence of multiple Ca^{2+} binding sites on RyR1 (114, 147). RyR2 and RyR3 also can be inhibited by Ca^{2+}, but much higher concentrations, that are less physiologically relevant, are required (43, 238). The role of Ca^{2+} in RyR1 is also unique because sensitivities to a given Ca^{2+} concentration vary between individual RyR1 receptors within the same cell, whereas single RyR2 and RyR3 both respond the same when presented with identical Ca^{2+} stimuli (164, 217). Although many investigators have published proposed sites for the Ca^{2+} binding sites on RyR1-3, there is still not a definitive consensus on their locations (45, 69, 91, 278).

In addition to cytosolic Ca^{2+}, luminal calcium within the endoplasmic reticulum also affects RyR (85, 105, 164). Single-channel studies demonstrate clear changes in RyR function based on the Ca^{2+} load in the stores, but the exact mechanisms remain unclear. Some studies suggest that the increased luminal Ca^{2+} leads to increased RyR sensitivity to interaction with some of its associated

proteins (105), while other investigators think that the increased Ca^{2+} in the stores causes interaction with the cytosolic Ca^{2+} binding sites that leads to altered receptor activity (262).

Phosphorylation. Many phosphorylation sites exist on all three isoforms of RyR that have the potential to alter the receptor's activity, but there is still no consensus on the exact effect that phosphorylation of each of these sites has on each of the RyR isoforms, or RyR in general. (85, 114, 254, 297). Protein kinase A (PKA), calcium-calmodulin kinase II (CamKII), and various cAMP- and cGMP-dependent kinases are all capable of phosphorylating RyR, but PKA and CamKII appear to be the most important in modulating the properties of RyR (69, 297). These two kinases are also the only kinases known to have specific anchoring regions on RyR (13, 184). Despite the large number of studies documenting kinases and their phosphorylation sites on RyR, there is still a great deal of conflicting information regarding the functional effects of phosphorylation. The overall effect of both CamKII and PKA phosphorylation of RyR appears to be increased RyR activity (85, 276, 283, 297). Because of its potential role in heart failure, phosphorylation of RyR2 has been studied in much greater detail than RyR1 or RyR3, and the results of these studies are somewhat contradictory (16, 71, 175). Some studies suggest that hyperphosphorylation of RyR2 over long periods of time causes dissociation of FKBP12.6, a RyR-associated protein, leading to a Ca^{2+} leak through the channel (274, 275). However, studies looking at the effects of acute phosphorylation of RyR2 have reported increased activity

(108), decreased channel opening (268), and no change in RyR Ca^{2+} handling (169). The effects of phosphorylation of RyR are clearly complicated, and it is likely that conditions used in these various *in vitro* studies may have impacted the results. More information is needed, especially for RyR1 and RyR3, in order to clearly define the role of phosphorylation on the function of these receptors.

Oxidation. Because RyRs contain nearly 100 cysteine residues in each monomer, they are very sensitive to oxidation (69). Extensive studies by Dulhunty et al. (68, 69, 72, 73, 106), have demonstrated that, in skeletal and cardiac muscle, about half of the cysteines can be oxidized, *in vivo*, and chemical oxidation of about 15 of these cysteines lead to an increase in the open-state probability of RyR. They also found that further oxidation of at least 10 more cysteine residues actually led to inhibition of RyR activity, but these studies were done under conditions that are unlikely to be encountered in a typical cell (68, 69). In both cases, it has been proposed that redox actions on the channel lead to altered interaction of RyR with RyR-associated proteins which ultimately leads to a change in receptor function (298). Further studies should be done to define the exact locations of redox-sensitive residues on each RyR subtype, although it will be difficult to determine whether oxidation or reduction of RyR represents important regulatory mechanisms in specific tissues, *in vivo*.

Calmodulin and Sorcin. Calmodulin, short for Ca^{2+} modulated protein, is a 17 kDa calcium-binding protein expressed in all cells of the body (49). Each protein

contains four EF hand motifs that are able to associate with RyRs near the pore region of the channel (271). Calmodulin's interaction with RyR can increase or decrease channel activity, depending on the conformation of calmodulin (i.e. whether Ca^{2+} is bound) (85). In general, micromolar Ca^{2+} leads to increased binding of calmodulin to RyR, which leads to inhibition of RyR activity, while nanomolar concentrations of Ca^{2+} lead to decreased binding by calmodulin to RyR and increased RyR activity (114). However, the specific concentrations of Ca^{2+} needed to cause a calmodulin-mediated increase or decrease in RyR activity appears to vary somewhat based on RyR isoform (113). RyR1 and RyR3 appear to be more easily activated by calmodulin in the presence of low Ca^{2+} concentrations, while inhibitory effects of calmodulin on RyR2 occur at lower Ca^{2+} concentrations compared to RyR1 or RyR3 (88, 89). Relatively few studies have looked at these effects, and the details of calmodulin-mediated changes in RyR activity in specific isoforms remains controversial and warrants further investigation. Another calmodulin-based regulatory mechanism has been observed, specifically related to RyR1: calmodulin is capable of disrupting the interaction between RyR1 and L-type calcium channels due to the presence of calmodulin binding sites on both proteins (241). While the physiological significance of this interaction is not clear (69), more recent studies suggest it may be related to, but not essential for excitation-contraction coupling in skeletal muscle cells (12, 47).

Sorcin, another Ca^{2+}-binding EF hand motif protein, is also capable of modulating RyR function by binding to and inhibiting RyR under high Ca^{2+} conditions (69). Although its exact binding location on RyR is not known, their interaction has been confirmed through coimmunoprecipitation in cardiac myocytes (and therefore RyR2) (194). Rueda et al. (234) showed that aorta and cerebral artery smooth muscle expressed more sorcin but less RyR than cardiac myocytes, suggesting an increased role for sorcin-RyR interaction on those cells. They also demonstrated that sorcin decreased the frequency, amplitude and spatial spread of Ca^{2+} sparks from RyR. Farrell et al. (78, 79) suggested that the physiological function of sorcin may be to prevent the propogation of Ca^{2+} sparks to adjacent RyR by quickly responding to the local increase in Ca^{2+} from a spark, binding to nearby RyR, and inhibiting spark formation in those adjacent receptors.

FKBP12/FKBP12.6. FKBP's are immunophillin proteins named for their ability bind the immunosuppressant drug, FK506. Although there are at least 20 members of the FKBP family, only FKBP12 and FKBP12.6 (numbered according to molecular mass and also referred to as calstabin 1 and 2, respectively) appear to be important to the regulation of RyR (5, 42). The specific binding site of FKBP's on RyR has not been absolutely defined, but multiple studies suggest that it is likely on the cytosolic side of the receptor near the clamp region (35, 41, 272). Regardless of the isoform, one FKBP binds to each monomer of RyR with such a high affinity that the two proteins can be experimentally co-purified (181).

Both FKBP12 and FKBP12.6 are able to bind to all three RyR isoforms, but RyR1 and RyR3 appear to preferentially bind FKBP12, while RyR2 binds to FKBP12.6 (181). The functional result of FKBP binding to RyR appears to be a decrease in channel activity (42), but the exact mechanisms are still not clear. There is a consensus that in RyR1, removal of FKBP12 causes increased channel activity, but there are little data for RyR2 or RyR3 (85). Studies have been done (largely in RyR1 only) showing that FKBPs may lead to a stabilized closed or subconductance state of RyRs (6, 32, 184), or synchronization of groups of RyR, allowing them to open and close simultaneously (183). Despite what is known about the physical linkage of these proteins and the effects on channel gating, the greater physiological significance of their interaction is still debatable. Many regions of RyR1 related to malignant hyperthermia are near the FKBP binding site (42), suggesting that the Ca^{2+} leaks observed in the disease leading to disrupted E-C coupling could be related to the RyR-FKBP interaction. Similarly, hyperphosphorylation of RyR2 has been linked to displacement of FKBP12.6, causing Ca^{2+} leak and ultimately contributing to heart failure (16, 71). FKBPs are also linked to changes in the properties of Ca^{2+} sparks produced by RyR: overexpression of FKBP12 in cardiac myocytes decreases the amplitude and duration of sparks(144), and blocking FKBPs pharmacologically in bladder smooth muscle also led to increased spark amplitude and frequency (187). This indicates that immunophillins may be important modulators of Ca^{2+} signaling in smooth muscle cells.

Scaffolding and anchoring proteins. These proteins can regulate the function of RyR through interaction with RyR on the cytoplasmic side of the SR membrane (42). Homer, a scaffolding protein, regulates the coupling between membrane receptors and intracellular Ca^{2+} stores by binding to proline-rich sequences of many proteins, including RyR1, but not RyR2 or RyR3, which lack the consensus sequence (69). Studies of RyR1 in skeletal muscle show that the interaction with Homer proteins leads to an increase in channel activity (82), but the significance of these proteins in vascular smooth muscle is still not clear. Anchoring proteins, such as Protein Kinase A Anchoring Proteins (AKAP) function to tether PKA to specific subcellular locations, including to RyR. RyR2 coimmunoprecipitates with AKAP in cardiac muscle, suggesting a close association in those muscle cells (183). In skeletal muscle, mAKAP increases phosphorylation of RyR1, which increases Ca^{2+} release and facilitates muscle contraction (235). Like the literature for Homer proteins, there is a lack of information about the role of AKAP in vascular smooth muscle, making their role in those cells difficult to elucidate.

1.7. Pharmacology.

There are many pharmacological agents, both endogenous and exogenous, that have been shown to affect the function of RyR (297). However, despite the existence of this wide array of effectors that work by different mechanisms, no isoform-specific RyR modulators are currently available (297). **Table 1** lists the activators and inhibitors of RyR as well as their mechanisms of action, if known.

Table 1. Common pharmacological modulators of ryanodine receptors

Compound	Concentration	Ca^{2+} Release	Effect on RyR
Ryanodine	nM	(+)	locks RyR in partially open configuration (245)
Ryanodine	μM	(-)	fully closes RyR (245)
Caffeine	mM	(+)	increased P_O and open time; increased Ca^{2+} sensitivity (289)
4-chloro-m-cresol	μM	(+)	increased P_O and open time; increased Ca^{2+} sensitivity (308)
sulmazole	μM	(+)	increased P_O and open time by Ca^{2+} dependent and independent mechanisms (191)
Suramin	μM	(+)	increased P_O and stabilization of open state (247)
Halothane	< 3.8%	(+)	increased duration of open events; decreased lifetime of closed state (308)
Tetracaine	μM	(-)	decreased P_O (289)
Ruthenium red	nM	(-)	dncreased time in closed state without a change in open-state conductance (289)
FK-506, rapamycin	μM	(+)	increased P_O ; causes a long-lasting subconductance state (308)
Dantrolene	μM	(-)	unclear; may stabilize domain interactions (156)
Imperatoxin A	nM	(+)	Mimics DHPR-RyR interaction (104)

(+) = increased RyR activity

(-) = decreased RyR activity

Table 1. Common pharmacological modulators of ryanodine receptors

Compound	Concentration	Ca^{2+} Release	Effect on RyR
Ryanodine	nM	(+)	locks RyR in partially open configuration (245)
Ryanodine	μM	(-)	fully closes RyR (245)
Caffeine	mM	(+)	increased P_O and open time; increased Ca^{2+} sensitivity (289)
4-chloro-m-cresol	μM	(+)	increased P_O and open time; increased Ca^{2+} sensitivity (308)
sulmazole	μM	(+)	increased P_O and open time by Ca^{2+} dependent and independent mechanisms (191)
Suramin	μM	(+)	increased P_O and stabilization of open state (247)
Halothane	< 3.8%	(+)	increased duration of open events; decreased lifetime of closed state (308)
Tetracaine	μM	(-)	decreased P_O (289)
Ruthenium red	nM	(-)	dncreased time in closed state without a change in open-state conductance (289)
FK-506, rapamycin	μM	(+)	increased P_O ; causes a long-lasting subconductance state (308)
Dantrolene	μM	(-)	unclear; may stabilize domain interactions (156)
Imperatoxin A	nM	(+)	Mimics DHPR-RyR interaction (104)

(+) = increased RyR activity

(-) = decreased RyR activity

1.8. General role in muscle cells.

Skeletal Muscle. In skeletal muscle, RyR play an essential role in excitation-contraction (E-C) coupling, in which an electrical signal (depolarization) of the cell membrane is translated into SR calcium release and ultimately contraction of the cell (159). In skeletal muscle there is a specific arrangement between RyR1 in the SR and the dihydropyridine receptors (DHPR) of L-type Ca^{2+} channels (CaV1.1) in the t-tubule membranes (227). Four DHPR in the t-tubule membranes group together in skeletal muscle, forming a tetrad, and are connected to every other RyR1 on the SR, making a specific arrangement of RyR1-DHPR complexes which allow for signal transduction between the plasma membrane and SR without the need for calcium influx through the L-type Ca^{2+} channels (293). Instead, the voltage-sensing region of the L-type channels can detect membrane depolarization and through the DHPR directly activate the coupled RyR1 (39). The significance of the RyR not coupled to DHPR and their role in E-C coupling in skeletal muscle is still unclear. Because RyR1 and RyR3 are both expressed in skeletal muscle, and only RyR1 associates with DHPR, RyR3 may be overrepresented in the uncoupled RyR of some skeletal muscle, although the significance of this hypothesis is also unknown (249). Regardless of the isoform of RyR not coupled to DHPR, there is some evidence that these RyR function through Ca^{2+}-induced Ca^{2+}-release (CICR), opening in response to increased intracellular Ca^{2+} (236, 239)

Cardiac Muscle. Cardiac muscle RyR are also needed for excitation-contraction coupling, but they accomplish this goal using a different mechanism because they lack the mechanical coupling between RyR2 and L-type Ca^{2+} channel DHPR (227). The directly-coupled RyR-DHPR arrangement seen in skeletal muscles cannot be achieved in cardiac muscle for two reasons: The L-type Ca^{2+} channels in cardiac muscle cells (CaV1.2) do not form tetrads (159), and cardiac muscle only expresses RyR2, which cannot couple directly to DHPR (293). As a result, these cells rely on CICR to generate release of Ca^{2+} from the SR and subsequent contraction. In CICR, influx of Ca^{2+} through cardiac L-type Ca^{2+} channels (CaV1.2) is required in order to activate RyR2 in the SR membranes, causing the release of Ca^{2+} from intracellular stores in the form of Ca^{2+} sparks (227), which summate to form the global Ca^{2+} release event observed in cardiac myocytes. Although they are not physically coupled, the RyR-L-type Ca^{2+} channel relationship is still tightly regulated, and there is some evidence that opening of one L-type channel leads to the production of one Ca^{2+} spark (173).

Smooth Muscle. The physiological role of RyR in smooth muscle cells is more variable and less understood then either skeletal or cardiac muscle (51), possibly because these cells express all three RyR isoforms in varying amounts, depending on the specific tissue type (237, 267, 269, 290). Like skeletal and cardiac muscle, RyR may be involved in E-C coupling, but they do not rely on a particular arrangement of RyR with Ca^{2+} channels in order to do so (102).

Instead, the RyR may serve to amplify Ca^{2+} signals from other ion channels in the SR and plasma membrane. CICR stimulated by activation of L-type Ca^{2+} channels has been demonstrated in some smooth muscle types (51, 99, 118, 128, 129), but it may not be essential, as many smooth muscles contract at Ca^{2+} concentrations lower than those needed to induce CICR (102). In addition, the RyR antagonist, ryanodine, actually contracts some smooth muscle, suggesting that there is more heterogeneity in the role of RyR in smooth muscle compared to skeletal or cardiac muscle (11). Some evidence also suggests that smooth muscle RyR may amplify Ca^{2+} signals coming from nearby IP_3R on the SR membrane (22, 26), although this is still controversial. Guerrero-Hernandez et al. (234) suggest in a recent review that either the majority of smooth muscle RyR may not be sensitive enough to detect Ca^{2+} released from IP_3R or that IP_3R decrease the Ca^{2+} sensitivity of RyR by decreasing ER luminal Ca^{2+} concentration. Finally, RyR appear to play an important role in smooth muscle relaxation and the regulation of smooth muscle tone as part of an important negative feedback mechanism (46, 139, 202). This pathway is reviewed in greater detail in the subsequent section regarding Ca^{2+} sparks.

1.9. Calcium sparks.

Calcium sparks are the result of the rapid opening of one or more RyRs on the sarcoplasmic reticulum, leading to a transient, microdomain increase in cytoplasmic Ca^{2+} without a significant effect on global intracellular Ca^{2+}

concentration (76). They occur in many cell types, including skeletal, smooth, and cardiac myocytes (39) and neurons (46). In skeletal (153) and cardiac muscle (249), they are critical for excitation-contraction coupling, and although they may be important for Ca^{2+}-dependent exocytosis of neurotransmitters in neurons (126, 208), the role of sparks in these latter cells is still not clear .

Role in smooth muscle. In some vascular smooth muscle, Ca^{2+} sparks are a critical component of a negative feedback mechanism that regulates myogenic tone (46, 139, 202). In these cells, Ca^{2+} sparks activate nearby large conductance, Ca^{2+}-activated K^+ (BK_{Ca}) channels, increasing the efflux K^+ ions, hyperpolarizing the plasma membrane, and reducing smooth muscle cell excitability. The BK_{Ca} channel activity resulting from Ca^{2+} sparks is known as a spontaneous transient outward current (STOC) (27). The increased membrane potential from the STOC leads to closure of voltage-gated Ca^{2+} channels on the plasma membrane and therefore relaxation of the smooth muscle cell (46, 139, 202). In addition to BK_{Ca} channels, Ca^{2+}-activated Cl^- (Cl_{Ca}) channels can also be activated via Ca^{2+} sparks to produce spontaneous transient inward currents (STIC) (46). Because these currents actually depolarize cells, it has been proposed that the coupling between RyR and Cl_{Ca} channels may serve to stabilize membrane potential and smooth muscle tone rather than relax cells, as seen with BK_{Ca} channels (304). Despite the prominent role of Ca^{2+} sparks in the regulation of vascular tone in some vessel types, there are some types of smooth

muscle in which sparks are not a critical part of Ca^{2+} signaling. Studies in both rat uterine smooth muscle (37) and first order rat cremaster arterioles (291) provide examples of smooth muscle in which sparks are not observed at all, suggesting that the role of Ca^{2+} sparks in intact blood vessels may be more complex than originally proposed.

Morphology. The physical properties of Ca^{2+} sparks studied in various cell types are often quantified using several specific measurements (46). The amplitude of a spark refers to the peak increase in microdomain Ca^{2+} concentration as a result of the spark. It is often reported as $\Delta F/Fo$, which is the maximum increase in fluorescence (of a calcium-indicating dye) from baseline resulting from the Ca^{2+} spark. The width of a Ca^{2+} spark describes the spatial spread of the Ca^{2+} increase caused by a spark. The width can be calculated as the full-width at half-maximum (FWHM), which is the width of the area (usually in micrometers) with an increased Ca^{2+} concentration when the spark is at half of its peak amplitude. Duration of Ca^{2+} sparks is often reported as the full duration at half-maximum (FDHM). Similar to FWHM, this represents the temporal duration of the sparks at half of their maximum amplitude. Each of these morphological values is shown in the representative traces in **Figure 2.**

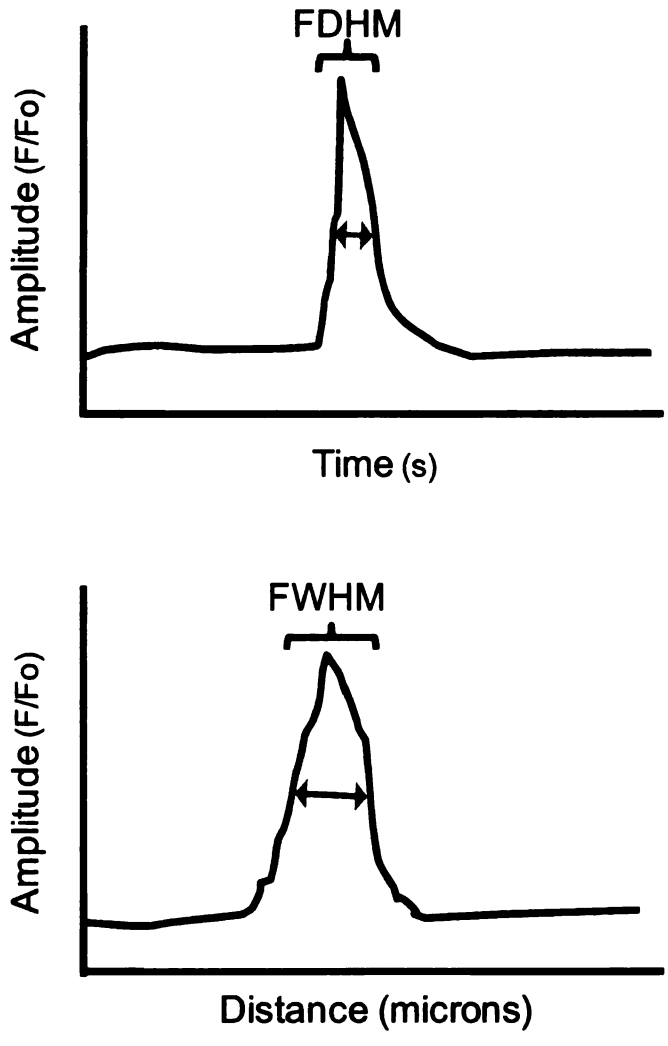

Figure 2. Morphology of a stylized Ca^{2+} spark

(Top) Generalized SparkAn output showing the amplitude and FDHM of a single Ca^{2+} spark from a cremaster feed artery smooth muscle cell. (Bottom) Generalized representative plot profile along the length of a feed artery smooth muscle cell demonstrating the amplitude and spatial spread of the Ca^{2+} spark

within a single smooth muscle cell. See Chapter 2, Methods, for details of Ca^{2+} spark analysis.

The morphology of $Ca^{2=}$ sparks has been characterized in smooth muscle cells from many different vascular beds (**Tables 2-4**). The majority of studies have focused on isolated cells, and nearly all of the studies looked at smooth muscle cells from the cerebral (29, 77, 97, 137, 171, 202, 234, 279, 300), mesenteric (228, 301, 302) or pulmonary (231, 290, 299, 302) vasculature. Across all of these studies, a wide range of spark morphological properties have been observed: frequencies ranged from 0.3 – 2.85 Hz, amplitudes from 1.2 – 3.2 (F/Fo), FWHM from 0.85 – 4.03 μm and FDHM from 13.3 – 190 ms (**Table 3**). Significantly fewer studies have investigated the properties of sparks in intact vessels, and most of these have focused on vessels that were unpressurized, either without myogenic tone (55, 56, 97, 139, 142) or with tone artificially generated with a high K^+ solution (48, 288) (**Table 4**). In these studies, the spark properties also varied: frequency from 0.12 – 1.53 Hz, amplitude from 1.36 – 1.93 (F/Fo) and FDHM from 27 – 60.7 ms. (**Table 4**). Only two of these studies looked at FWHM and observed spatial spreads of 1.25 μm (55) and 1.59 μm (56). Four studies, in cerebral (119, 180) or mesenteric (160, 195) vessels, have investigated Ca^{2+} spark properties in intact, pressurized vessels, and three of these studies used vessels that had significant myogenic tone (119, 180, 195) (**Table 3**). Three of the above studies also measured only the frequency of Ca^{2+} sparks, making comparisons between the studies difficult (**Table 5**). Looking at

the 27 studies summarized in **Tables 2-4**, it is clear that there is variability in the morphology of Ca^{2+} sparks observed. Many of these studies used vessels or isolated cells from different vascular beds and different species of animals, and experimental conditions varied significantly between the groups. Therefore, it is difficult to determine whether the differences in spark morphology are species-related, vascular bed related, or simply due to differences in the tools used to study these cells experimentally. It is likely a combination of all these factors, and more work needs to be done, especially in intact vessels, in order to clearly define the properties of Ca^{2+} sparks in native vascular smooth muscle cells.

Table 2. Ca^{2+} spark properties in single smooth muscle cells

	Study Details				*Calcium Spark Properties*			
Reference	**Spec.**	**Vessel Type**	**M.T.**	**Temp.**	**Freq. (Hz)**	**Amp. (F/Fo)**	**FWHM (μm)**	**FDHM (ms)**
Nelson, 1995 (202)	Rat	Cerebral arteries	NA	RT		3.03 ± 0.1	2.38 ± 0.14	48 ± 2.6
Lohn, 2000 (171)	Rat	Cerebral arteries	NA	RT	0.025 ± 0.003*	2.1 ± 0.2	2.89 ± 0.21	45.2 ± 2.6
Balasubra-manian, 2007 (11)	Rat	Renal arteries	NA	RT	0.36 ± 0.07	1.5 ± 0.02	0.7 ± 0.03	13.3 ± 0.03
Bonev, 1997 (29)	Rat	Basilar arteries	NA	RT	2.85 ± 0.40	1.78 ± 0.03	4.03 ± 0.15	65.2 ± 2.7
Essin, 2007 (77)	Mouse	Basilar arteries	NA	RT	1.1 ± 0.1	3.21 ± 0.2	3.3 ± 0.1	51.6 ± 4.4
Wellman, 2002 (279)	Human	Cerebral arteries	NA	RT	0.8 ± 0.1	2.02 ± 0.04	8.2 ± 0.5 ∞	
Remillard, 2002 (231)	Rat	Pulmonary arteries	NA	RT	0.30 ± 0.04	1.46 ± 0.01	1.760 ± 0.03	35 ± 1.5
Jaggar, 2002 (137)	Pig	Pial arteries	NA	RT	0.7 ± 0.08	1.44 ± 0.01		
Zhao, 2007 (301)	Rat	Mesenteric arteries	NA	RT	2.7 ± 0.31	1.27 ± 0.01	1.9 ± 1.154	46.5 ± 3.52
Zhao, 2008 (300)	Rat	Cerebral arteries	NA	RT	0.74 ± 0.12	1.7 ± 0.03		
Zheng, 2008 (302)	Mouse	Resistance pulmonary arteries	NA	RT	0.04 ± 0.01*	1.3 ± 0.2	0.85 ± 0.05	75 ± 3.3
Zheng, 2008 (302)	Mouse	Conduit pulmonary arteries	NA	RT	0.01 ± 0.009*	1.2 ± 0.1	1.0 ± 0.04	85 ± 6.7
Zheng, 2008 (302)	Mouse	Mesenteric arteries	NA	RT	0.2 ± 0.05*	1.8 ± 0.5	2.5 ± 0.1	190 ± 6.7

Table 2, continued.

		Study Details			*Calcium Spark Properties*			
Reference	**Spec.**	**Vessel Type**	**M.T.**	**Temp.**	**Freq. (Hz)**	**Amp. (F/Fo)**	**FWHM (μm)**	**FDHM (ms)**
Rueda, 2006 (234)	Rat	Cerebral arteries	NA	RT	0.01 ± 0.001*	1.75 ± 0.04	2.6 ± 0.1	55.5 ± 2.6
Yang, 2005 (290)	Rat	Pulmonary arteries	NA	RT	0.014 ± 0.003*	1.74 ± 0.03	1.65 ± 0.09	44.6 ± 3.2
Zhang, 2003 (299)	Rat	Pulmonary arteries	NA	RT	0.62 ± 0.08		1.57	35.6 ± 1.6
Gollasch, 1998 (95)	Rat	Cerebral arteries	NA	RT	1.30 ± 2.6	1.69 ± 0.02		46.7 ± 4.3
Pucovsky, 2006 (228)	Guinea pig	Mesenteric arteries	NA	RT	0.34 ± 0.07	2.99 ± 0.05		

* reported in sparks/μm^2, ∞ units are μm^2, Spec. = species used in study, MT = myogenic tone, Freq. = frequency (Hz), Amp. = amplitude (F/Fo), FWHM = full-width half-maximum (μm), FDHM = full-duration half-maximum (ms). RT = room temperature

Table 3. Ca^{2+} spark properties in intact, unpressurized vessels

	Study Details				*Calcium Spark Properties*			
Reference	**Spec.**	**Vessel Type**	**M.T.**	**Temp.**	**Freq. (Hz)**	**Amp. (F/Fo)**	**FWHM (μm)**	**FDHM (ms)**
Cheranov, 2006 (48)	Rat	Cerebral arteries	No ♮	RT	1.53 ±	1.36 ± 0.01		
Xi, 2009 (288)	Pig	Cerebral arterioles	No ♮	35 °C	0.12 ± 0.02	1.56 ±0.01		
Jeffries, 2009 (142)	Pig	Retinal arterioles	No	RT	0.27 ± 0.03	1.47 ± 0.02		27 ± 3
Curtis, 2004 (55)	Rat	Retinal arterioles	No	37 °C	0.56 ± 0.06	1.81 ± 0.04	1.25 ± 0.05	23.6 ± 1.15
Curtis, 2008 (56)	Rat	Retinal arterioles	No	37 °C	0.75 ± 0.09	1.93 ± 0.10	1.59 ± 0.20	20.6 ± 2.4
Gollasch, 1998 (97)	Rat	Cerebral arteries	No	RT	1.30 ± 2.6	1.69 ± 0.02		46.7 ± 4.3
Jaggar, 1998 (139)	Rat	Cerebral arteries	No	RT	0.24 ± 0.15			60.7 ± 10.5

♮ Experiments done in 30 mM K^+ to mimic myogenic tone, Spec. = species used in study, MT = myogenic tone, Freq. = frequency (Hz), Amp. = amplitude (F/Fo), FWHM = full-width half-maximum (μm), FDHM = full-duration half-maximum (ms), RT = room temperature

Table 4. Ca^{2+} spark properties in intact, pressurized vessels

	Study Details				*Calcium Spark Properties*			
Reference	**Spec.**	**Vessel Type**	**M.T.**	**Temp.**	**Freq. (Hz)**	**Amp. (F/Fo)**	**FWHM (μm)**	**FDHM (ms)**
Lamont, 2004 (160)	Rat	Mesenteric arteries	No	RT	0.018 ± 0.001*			
Heppner, 2002 (119)	Rat	Cerebral arteries	Yes	37 °C	0.94 ± 0.09			
Mandala, 2007 (180)	Rat	Cerebral arteries	Yes	37 °C	1.47 ± 0.051			
Miriel, 1999 (195)	Rat	Mesenteric arteries	Yes	37 °C		3.9 ± 0.9	2.29 ± 0.07	37.4 ± 11.3

* reported in sparks/μm/second, Spec. = species used in study, MT = myogenic tone, Freq. = frequency (Hz), Amp. = amplitude (F/Fo), FWHM = full-width half-maximum (μm), FDHM = full-duration half-maximum (ms), RT = room temperature.

Role of RyR isoforms. Because all three RyR isoforms may be expressed in vascular smooth muscle (76), it is possible that the proportional distribution of the RyR isoforms may provide an explanation for differences in Ca^{2+} spark occurrence and properties. There is some evidence in the literature that the different isoforms do impact Ca^{2+} sparks in these cells: RyR1 and RyR2 appear essential for the formation of Ca^{2+} sparks, while the role of RyR3 is more controversial (76). Studies using cells from neonatal RyR1 (-/-) and RyR1 (+/-) mice suggest that RyR1 is essential for the formation of calcium sparks (168). In rat portal vein, antisense blockade of isoform expression showed that RyR1 and RyR2 are essential for the formation of Ca^{2+} sparks, while RyR3 does not have an impact on their formation, but may alter global Ca^{2+} levels and ultimately impact the regulation of myogenic tone in those vessels (54, 196). In contrast, studies using RyR3 (-/-) mice suggest that RyR3 may actually inhibit Ca^{2+} sparks, as their frequency increases in animals lacking functional RyR3 (172).

Role of protein kinases.

In addition to the role of RyR isoforms in determining the properties of Ca^{2+} sparks, protein kinase signaling pathways can also act on RyR to alter Ca^{2+} sparks. PKC activation is known to contribute to myogenic tone (121, 212), and it has also been shown that activation of this pathway can decrease the occurrence of sparks in some cells (29, 170). The cAMP-PKA pathway has two targets in smooth muscle cells that can alter sparks: RyR (53, 253) and

phospholamban (246, 280), whose phosphorylation by PKA leads to disinhibition of the SR Ca^{2+} ATPase and increased Ca^{2+} in the SR, which then increases spark activity. Like PKA, NO-dependent signaling and cGMP-dependent PKG may also increase Ca^{2+} activity by increasing SR Ca^{2+} and sensitizing RyR to Ca^{2+}-dependent activation (29, 138).

2. Inositol1,4,5-triphosphate Receptors (IP_3R)

2.1. Structure.

Like RyR, inositol 1,4,5-trisphosphate receptors (IP_3R) are large, tetrameric Ca^{2+} release channels located on the endoplasmic reticulum of all animal tissues (87). They are somewhat similar in structure to RyRs, but have a much more compact design that may explain some of the functional differences between the receptors (149, 258). Each IP_3R monomer has a mass of approximately 310 kDa and contains one binding site for the IP_3 molecule (87). Because RyR have been studied in greater detail than IP_3R, a large amount of structural information on IP_3R has been extrapolated from RyR structure (258). Like the RyR, the large size of IP_3R makes it difficult to resolve the exact structure of the receptors and therefore, the details remain to be definitively defined (258). IP_3R have a pinwheel-like shape, with the head of the pinwheel consisting of a very large, square cytoplasmic domain containing the majority of the IP_3R monomers and

channel domain (57). The center of the pinwheel contains the channel domains, which join to the rest of the cytosolic portion of the channel by slender linkages that may be involved in conformational changes in the receptor (87, 112). The three-dimensional structure of IP_3R can be seen in (Figure 3).

Two conformations have been identified for IP_3R- the windmill and the square, which occur based on the absence or presence of luminal Ca^{2+}, respectively (112), and one study has suggested that other compounds may also cause conformational changes in the receptor (149). The channel's ligand, IP_3, also plays an important role in conformational changes, as IP_3 binding to the receptor may expose a stimulatory Ca^{2+} binding site on the receptor and also lead to occlusion of an inhibitory site (4). However, further evidence for these changes has been difficult to obtain, as the locations of these Ca^{2+} binding sites on the proteins has yet to be clearly defined (258). Similarly, the pore structure and exact location of the IP_3 binding site on IP_3R remain unclear. While all studies agree that the IP_3 binding site is on the cytoplasmic region of the channel (258), some show it in the peripheral region (112, 242), while others suggest a more central location (57).

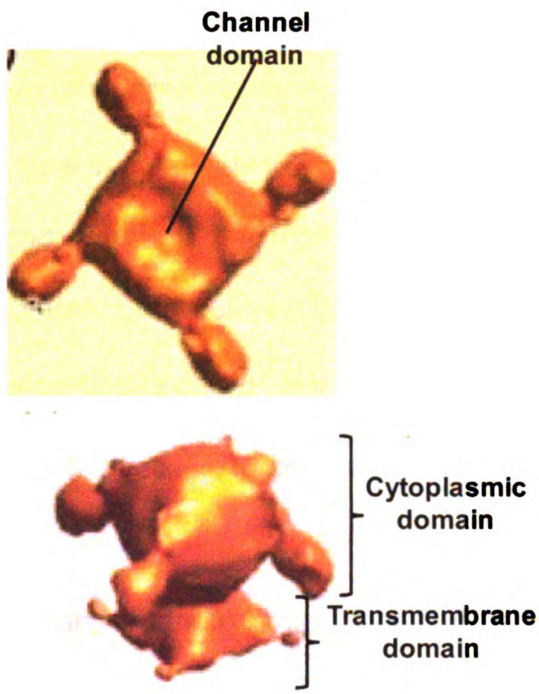

Figure 3. Three-dimensional structure of inositol 1,4,5 triphosphate receptors

The top picture shows a top-down view of an IP_3 receptor, with the center channel and clamp domains highlighted. The bottom image shows a side view of the receptor with the large cytoplamic domain and the smaller transmembrane domain labeled accordingly. Adapted from Taylor et al, 2004 (259).

2.2. Isoforms and Expression.

Similar to RyR, IP_3R exist in three isoforms (IP_3R1-IP_3R3), which are the products of distinct genes in mammals (87). These isoforms have ~70% homology in amino acid sequence, and the pore and ligand-binding regions are very highly conserved across the isoforms (87). Invertebrates and some central nervous system tissues express only IP_3R1, but the majority of body tissues, including vascular smooth muscle, express multiple IP_3R isoforms (87, 148).

Several studies have examined the expression of IP_3R isoforms in smooth muscle cells. Early studies in the vas deferens and in aortic smooth muscle cells showed relatively high amounts of IP_3R1 (207). Tasker et al. (256), demonstrated that the other isoforms are important in smooth muscle developmentally, and their expression decreases over time as the expression of IP_3R1 increases. Later studies by the same group also found that IP_3R2 and IP_3R3 are expressed in higher amounts in proliferating smooth muscle cells, suggesting specialized functions of the various IP_3R isoforms (257). Grayson et al. (100), compared the relative contribution of each isoform in basilar, mesenteric and thoracic arteries and found that IP_3R1 made a relative contribution of about 75% of all IP_3Rs in each of the vessel types. All three vessels also had greater expression of IP_3R3 than IP_3R2, and thoracic arteries had considerably less total IP_3R than basilar or mesenteric artery. In contrast to

smooth muscle cells, cardiac (218) and skeletal (64) muscle cells express IP_3R2 at levels much higher than IP_3R1 or IP_3R3, although total IP_3R expression in these cells is much lower than that of smooth muscle (270). This larger proportion of IP_3R2 could have great functional implications in cardiac and skeletal muscle because IP_3R2 has a higher Ca^{2+} sensitivity than either IP_3R1 or IP_3R3 (87).

2.3. Splice Variants.

Alternative splicing of the genes for IP_3R1-3 leads to an increase in the diversity of IP_3Rs in some tissue types. There are three main regions of the IP_3R genes in which alternative splicing takes place- SI, SII and SIII, with most studies focusing on the SII variants (59, 87). The functional consequences of these splice variants has not been studied in detail, and little is known about their presence or significance in smooth muscle, as the majority of studies have been conducted in neuronal tissues, where only IP_3R1 are expressed (87). In the brain, the SII variants may lead to changes in channel phosphorylation that cause allosteric modification of the receptors and alterations on Ca^{2+} signaling (251). The SII region of the IP3R gene only exists in the IP_3R1 isoform, making it difficult to predict the effects of variants in tissues such as vascular smooth muscle where all three IP_3Rs are expressed (87).

2.4. Regulation.

Inositol 1,4,5 trisphosphate. As the name suggests, the IP_3 molecule is a critical modulator of IP_3R. In vascular smooth muscle, IP_3 is generated and activates its receptor via a specific signaling mechanism. Binding of vasoconstrictor ligands to their G-protein coupled receptors on the plasma membrane lead to activation of Gα(q) subunit, which then directly activates phospholipase C (PLCβ) inside the cell. Once activated, PLCβ cleaves phosphatidylinositol 1,4 bisphosphate (PIP_2), producing diacylglycerol (DAG) and the IP_3 that is then free to bind to IP_3R on the endoplasmic reticulum (19). IP_3 and Ca^{2+} are both critical regulators of channel activity (and must be present for activation to occur), but their mechanisms of regulation of IP_3R function are very different (87). Overall, IP_3 affects IP_3R activity by altering the sensitivity of the channel to Ca^{2+} inhibition, meaning a decreased concentration of IP_3 makes IP_3R more sensitive to Ca^{2+}-dependent channel inhibition, while a higher concentration of IP_3 decreases the sensitivity of the channel to Ca^{2+} inhibition (131, 179). Unfortunately, the details of the mechanism are unclear and are especially understudied, *in vivo* (87).

Calcium. Aside from IP_3 , Ca^{2+} is the most important regulator of IP_3R function. Ca^{2+} is not capable of activating the receptor in the absence of IP_3. Much like

RyR, the sensitivity of IP_3R to IP_3 is determined by the concentration of Ca^{2+} in the cytosol (66). Across all three isoforms, IP_3R activity correlates to cytosolic Ca^{2+} concentration, forming a bell-shaped curve, meaning that Ca^{2+} can be either excitatory or inhibitory at these receptors (263). Because the structure of IP_3R have not been definitively resolved, the exact number and location of Ca^{2+} binding sites is not clear (66). The stimulatory binding sites are likely located on the receptor itself, and Ca^{2+} binding appears to be essential for channel opening, as removing Ca^{2+} impairs channel opening (86). It also has been shown that at nanomolar Ca^{2+}, IP_3 binding to the receptor is increased via a stabilization of the IP_3 binding site containing an IP_3 molecule (258). The inhibitory Ca^{2+} binding site may be located either on the receptor itself, or on an accessory protein (66). Devogelaere et al. (66), suggested in their review of the IP_3R ligand-binding domain, that a low-affinity Ca^{2+} binding site would account for Ca^{2+}-dependent inhibition, but no studies have confirmed the presence of this site, and the mechanism of inhibition is still undefined.

Calmodulin. Calmodulin importantly regulates the function of IP_3R due to its ability to bind to and alter the activity of the receptors. The calmodulin binding site has been definitively defined, *in vitro*, on the coupling domain of the IP_3R1 receptor (177). The nature of the interaction of calmodulin with IP_3R1 and IP_3R2 appears similar to that of the Ca^{2+}-dependent inhibition seen in RyR: Ca^{2+}

binding to calmodulin causes a conformational change in the molecule, which alters its interaction with IP_3R and decreases channel activity (233). However, IP_3R3 does not bind calmodulin, and is therefore not subject to the Ca^{2+}-dependent inhibition of the receptor via calmodulin seen in the other two isoforms (40). The exact relationship between calmodulin and IP_3R, *in vivo*, is still unknown. Almost all of the studies to date have been binding studies conducted *in vitro*, and concrete evidence of complex formation such as coimmunoprecipitation of calmodulin and IP_3R does not exist (87).

Phosphorylation. IP_3R function can be regulated by phosphorylation by the activity of many different kinases. However, the vast majority of these studies have been conducted in vitro and in non-smooth muscle cell types, making the correlation to vascular smooth muscle less clear (66). Protein kinase A (PKA) and protein kinase G (PKG) have two identical phosphorylation sites on IP_3R1, and increases in cyclic AMP (cAMP) lead to the phosphorylation of these sites by PKA (83), while increases in cyclic GMP (cGMP) lead to phosphorylation by PKG (250). Once these sites are phosphorylated, the majority of studies report an increase in Ca^{2+} release from IP_3R (87), although the presence of splice variants, especially in the SII region can lead to PKG insensitivity (87). Similar to RyR, IP_3R can also be phosphorylated by both PKA and CamKII, which each have consensus sites on the receptor, and although there is limited evidence that

these modifications decrease IP_3R activity, the functional consequences are essentially unknown (84).

Protein Partners. There are many proteins within smooth muscle cells which are capable of interacting with IP_3R to alter their activity (87). IRBIT (IP_3 binding protein released with inositol 1,4,5 triphosphate) is a protein that, when phosphorylated, interacts with the N-terminus of IP_3R (9). Recently, it was determined that IRBIT binding reduces the sensitivity of IP_3R to IP_3, and that knockdown of IRBIT caused an increase in Ca^{2+} release from IP_3R (8). RACK1, a scaffold protein linking PKC to its substrates, also interacts with IP_3 receptors by binding to two separate sites on the IP_3R N-terminus (215). RACK1 binding increases the sensitivity of IP_3R to IP_3 and increases Ca^{2+} release from the SR, and this potentiation of activity is further increased in cells with overexpression of RACK1 (215). Like RyR, the immunophillin FKBP12 may also be an important regulator of IP_3R activity, but the exact nature of their interaction is more controversial than with RyR (87). It has been proposed that FKBP12 alters the interaction between PKC and IP_3R to augment Ca^{2+} release from the receptors (214). The adapter proteins ankyrin and Homer each interact with IP_3R and impact its function (87). Ankyrin, which couples its protein targets to the cytoskeleton, binds to IP_3R near the pore sequence and inhibits Ca^{2+} release by decreasing the sensitivity of the channel to IP_3 (117). Homer has been indirectly

linked to the activity of IP_3R- although a direct modification of IP_3R by Homer has not been demonstrated, IP_3R possess a consensus sequence for Homer binding (264), and disruption of Homer's cross-links to TRPC1 channels decreases the activity of IP_3R (294).

2.5. Pharmacology.

Similar to RyR, there are several substances that can be used as tools to pharmacologically modulate the activity of IP_3R. While IP_3 is not cell permeant, analogs with additional side groups such as Bt-IP_3 (287) that can enter vascular smooth muscle cells have been synthesized and used to study IP_3R function in intact cells and tissues. There are currently no isoform-specific IP_3R-targeting drugs, and future research in this area would help improve our understanding of the functional role that the different types of IP_3R play in various cell types.

Table 5. Common pharmacological modulators of IP_3 receptors

Compound	Concentration	Ca^{2+} Release	Effect on IP_3R
IP_3	μM	(+)	increased P_o; decreased Ca^{2+} inhibition (87)
Adenophostin B	nM	(+)	increased P_o; cooperative binding increases effect (163)
Xestospongins	nM- μM	(-)	unclear; may block pore or uncouple IP_3 binding from Ca^{2+} release (163)
Heparin	μM	(-)	completely inhibits IP_3 binding (87)
2-APB	μM	(-)	decreased P_o with no affect on IP_3 binding (163)
mAb18A10	2-50 μg/ml	(-)	monoclonal antibody blocks IP_3 binding (199)

(+) = increased Ca^{2+} release

(-) = decreased Ca^{2+} release

P_o = probability of channel opening

2.6. Calcium Waves.

Calcium waves, which are transient, global oscillations in intracellular Ca^{2+} within a cell, are a critical Ca^{2+} signaling mechanism in smooth muscle and other cells. Calcium release from the SR plays a major role in these Ca^{2+} waves in multiple types of vascular smooth muscle including cerebral (107), mesenteric (216), and pulmonary (223) arteries. Because IP_3R are very sensitive to intracellular Ca^{2+} and IP_3 concentrations, it is not surprising that oscillating levels of these two second messengers leads to nearly identical patterns of oscillation in the activity of IP_3R (166). The regulation of IP_3R by multiple mechanisms also means that there are multiple ways in which IP_3R can be involved in the generation of Ca^{2+} waves. IP_3R are sensitive to both positive and negative feedback based on Ca^{2+} concentration (19). Each global Ca^{2+} wave can be triggered by a local increase in Ca^{2+} that activates one or more nearby IP_3R, leading to increased cytosolic Ca^{2+} and activation of adjacent IP_3R via CICR. Once the global Ca^{2+} concentration increases to a specific level, the IP_3R close due to the negative feedback inhibition by Ca^{2+}. This allows sequestration of Ca^{2+} back into stores and the termination of the Ca^{2+} wave (127). Studies in non-smooth muscle cells also have suggested that feedback regulation by Ca^{2+} of PLC can lead to oscillations in the levels of IP_3, contributing to calcium waves (116). Similarly, protein kinase C (PKC), whose activator diacyl glycerol (DAG) is produced

alongside IP_3, may act as a negative feedback regulator of IP_3 formation (109) and contribute to Ca^{2+} waves.

3. Myogenic Tone.

Myogenic tone is a hallmark feature of many types of vascular smooth muscle that is observed in almost all small blood vessels with a diameter less than 150 μm (63). This state of partial constriction is essential for physiological function because it allows blood vessels to either constrict or dilate from their steady-state diameters in response to various stimuli, which ultimately regulates blood flow to tissues throughout the body (124). This constant, steady-state myogenic tone is distinct from the myogenic response, in which vessels constrict in response to an increase in intraluminal pressure, although many similar mechanisms apply to both phenomena (63). Intracellular Ca^{2+} concentration is the most significant determinant of myogenic tone, and many extracellular stimuli such as pressure, stretch, hormones, neurotransmitters and endothelial factors contribute to the regulation of intracellular Ca^{2+} concentration (63, 124, 133). Regardless of the origin, vascular smooth muscle cells need to integrate each of these vasoconstrictor or vasodilator signals, and ion channels are importantly used to convert each of these extracellular stimuli into the intracellular changes in Ca^{2+} and membrane potential (133).

Mechanism of contraction

Smooth muscle cells do not have the striated arrangement of actin and myosin seen in skeletal muscle. They have proportionally more actin than skeletal muscle, and their thin filaments attach to dense bodies within the cell that that ultimately allow for contraction of the cell. Smooth muscle cell contraction can be initiated by mechanical, electrical, or chemical stimuli. The magnitude of contraction depends on two factors: the intracellular Ca^{2+} concentration and the degree of phosphorylation and crossbridge cycling between actin and myosin. Regardless of the initial stimulus, Ca^{2+} that enters into smooth muscle cells binds to calmodulin, which then activates Myosin Light Chain Kinase (MLCK). MLCK phosphorylates Myosin Light Chain (MLC), allowing for the formation of actin-myosin crossbridges, which cycle due to myosin ATPase activity and cause the shortening and force genertaion of the smooth muscle cell. This ATPase activity is much slower than that of skeletal muscle, leading to a slower power stroke velocity. Other kinases in smooth muscle cells, such as PKC and Rho Kinase contribute to contraction through phosphorylation and inhibition of Myosin Light Chain Phosphatase (MLCP). MLCP facilitates relaxation of smooth muscle cells through dephosphorylation of MLC. Relaxation of smooth muscle cells occurs through loss of Ca^{2+} stimulus via decreased influx through plasma membrane channels or by increased reuptake into intracellular stores. This decrease in Ca^{2+} lowers the rate of MLC phosphorylation and promotes relaxation of the smooth muscle cells (125, 261, 273).

Signaling pathways

Changes in intraluminal pressure are very important in the signaling pathways underlying myogenic tone because the mechanical events related to a change in intraluminal pressure activate signaling pathways, which then modulate Ca^{2+} availability and contraction (31, 201). This ability to constrict in response to pressure changes is inherent to the smooth muscle cells: studies using endothelial denudation (63) and pharmacological inhibition of nerve activity (115) both lacked an effect on myogenic tone. In arterioles, several studies have shown that increases in pressure lead to graded membrane depolarization and increased myogenic tone (61). Similar studies looking at the effects of membrane stretch have linked stretch–induced contraction and membrane depolarization (210, 244). Despite the evidence linking pressure and stretch to changes in membrane potential and myogenic tone, the specific mechanisms are undefined. It is clear, however, that both global and local Ca^{2+} signaling pathways within smooth muscle cells are very important (61). Globally, increased intraluminal pressure increases Ca^{2+} in rat cremaster arterioles (307) and cerebral arteries (152). The contribution of VGCC is significant, as they are responsible for a large proportion of depolarization-mediated Ca^{2+} entry in vascular SMC (204). The mechanisms linking VGCC activity to changes in pressure are not completely clear, but there are three basic possibilities, which may all play a role (63). First, VGCC may open due to depolarization caused by an upstream stimulus (likely membrane stretch) (60, 244). Second, actions on

the VGCC such as phosphorylation in response to agonists could change the threshold of activation or inactivation to increase channel opening probability (2, 15). Third, a mechanical stimulus could have a direct effect on VGCC gating (162, 189). The current evidence suggests that VGCC activation is secondary to membrane depolarization, which occurs due to the activity of nonselective cation channels and mechanosensitive channels (60, 244, 286). Transient Receptor Potential (TRP) channels, in particular, have been implicated in mechanosensation in vascular smooth muscle cells (61). Some TRP channels are Ca^{2+}-permeable, while others are Na^{+}-selective or nonselective cation channels. Welsh et al. (281) and Earley et al. (74, 75) used antisense knockdowns of TRPC6 and TRPM4, respectively, to demonstrate that the channels are linked in series in an important pathway regulating tone. TRPC6 is the mechanosensor, and it's Ca^{2+} influx leads to the activation of TRPM4, which then depolarizes the membrane. The authors also suggested a role for PKC-mediated sensitization of TRPM4 to increase tone.

The activity of G protein-coupled receptors (GPCR) and their downstream signaling pathways are also important to the modulation of myogenic tone. Mechanical stimulation of the smooth muscle membrane by pressure or stretch has been proposed to activate GPCR, which are coupled to Phospholipase C (PLC) (141, 213). Numerous studies support a significant role for PLC in the mechanisms underlying myogenic tone (10, 141, 213). Also, membrane depolarizationmay activate/modulate GPCR and/or PLC (178). Increased PLC

activity leads to an increase in the production of IP_3 and DAG. IP_3 goes on to activate IP_3R and facilitate the production of Ca^{2+} waves, discussed below. DAG activates PKC, which has been shown to increase tone by enhancing the activity of nonspecific cation channels, causing membrane depolarization (248). PKC is also involved in Ca^{2+} sensitization (94, 292) in smooth muscle, and a number of studies have implicated PKC in pressure-induced myogenic tone (121, 186, 212).

Role of Ca^{2+} sparks and waves

As described previously, Ca^{2+} sparks are the result of local Ca^{2+} release from ryanodine receptors in the SR and are reported to play an integral role in the modulation of tone (28). Several investigators have characterized this negative-feedback role of RyR in vascular smooth muscle (155, 195, 202, 231). Depolarization-induced Ca^{2+} influx into smooth muscle cells activates RyR, which produce Ca^{2+} sparks. The resulting local increase in Ca^{2+} activates nearby BK_{Ca}, whose K^+ efflux hyperpolarizes the membrane, causing closure of VGCC and a decrease or stabilization of tone. Vasodilators can also affect this pathway to relax vascular smooth muscle, as PKA and PKG have both been reported to increase spark frequency (221). In contrast, Wellman et al. (279) demonstrated in human cerebral arteries that the activity of RyR and BK_{Ca} channels are not tightly correlated. Also in contrast to the negative feedback role of Ca^{2+} sparks are studies by Yang et al. (291) showing a lack of Ca^{2+} sparks in first-order rat cremaster arterioles. These differences suggest heterogeneity

between species, vascular bed, or vessel type in the role that RyR sparks play in the regulation of myogenic tone.

Ca^{2+} waves, both synchronous and asynchronous, have been reported in many types of vascular smooth muscle , but their role in the modulation of myogenic tone is still not clear (61). Both synchronous and asynchronous waves are the result of IP_3-mediated Ca^{2+} release from the SR, but few studies have addressed the effects of pressure on Ca^{2+} waves. Jaggar (136) showed in cerebral arteries that increasing pressure from 10 to 60 mm Hg leads to a doubling in Ca^{2+} wave frequency. The waves were also inhibited by ryanodine, suggesting the involvement of RyR and SR stores. However, even though Ca^{2+} waves were inhibited, ryanodine actually increased tone, suggesting that waves may not be a major determinant of tone in this system. In contrast to these findings, Zacharia et al. (296) saw a decrease in asynchronous waves as myogenic tone increased in mouse mesenteric arteries, presumably because VGCC activation and Ca^{2+} influx led to inactivation of IP_3R. More studies are needed in order to determine the specific role of IP_3R and Ca^{2+} waves in the regulation of myogenic tone.

CHAPTER 2: MATERIALS AND METHODS

1. Animals

All animal protocols were conducted within the guidelines of the Institutional Animal Care and Use Committee at Michigan State University and followed the *Guide for the Care and Use of Laboratory Animals* of the National Research Council (USA) (1). Male golden Syrian hamsters, 6-10 weeks of age and weighing 75-150 g were obtained from Harlan Laboratories. Male C57BL/6 mice, 6-10 weeks of age weighing 20-30g were obtained from Jackson Labs. Upon arrival, both hamsters and mice were group housed in a temperature and humidity controlled room with a 12-hour light/dark cycle, and all animals had free access to food and water. All animals were allowed to acclimate to these conditions after arrival for 7 days before they were used in any experiments.

2. Euthanasia

All animals were euthanized in the laboratory by carbon dioxide (CO_2) asphyxiation followed by cervical dislocation. Lack of response to a painful stimulus was verified before proceeding with tissue dissection.

3. Isolation of blood vessels

Following euthanasia, hamster or mouse testes were removed and placed in 4°C Ca^{2+}-free physiological salt solution ($0Ca^{2+}$ PSS) containing in mM: NaCl 137, KCl 5.6, $MgCl_2$ 1, HEPES 10, glucose 10, pH 7.4, 295 mOsm). The cremaster muscle was dissected from the testicle and then pinned flat to a Sylgard pad positioned in a recirculating/cooled bath containing 0 Ca^{2+} PSS and 10μM each of sodium nitroprusside and diltiazem. Second-order cremaster arterioles were isolated by hand dissection using a stereomicroscope as previously described (38, 135). Cremaster feed arteries were dissected, *in situ*, by surgically exposing the iliac arteries and carefully isolating small artery branches that were upstream from the first-order arterioles in the cremaster muscle microcirculation. Visualization of both the cremaster feed artery and arterioles is shown in **Figure 4**.

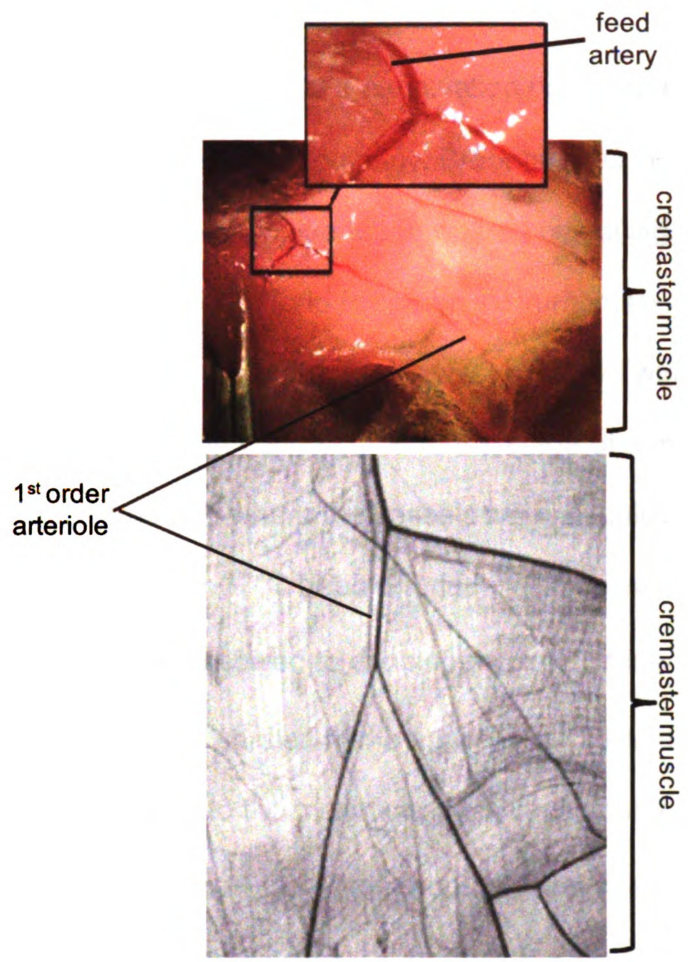

Figure 4. Visualization of cremaster feed arteries and arterioles

Top panel: Cremaster feed arteries are small branches off the iliac artery that are located proximal to the first-order cremaster arterioles. The inset box shows a magnified image of the cremaster feed artery. Bottom panel shows a cremaster muscle that was been pinned flat and transilluminated. First-order cremaster arterioles are indicated in both the top and bottom panels. Bottom panel modified from Jackson et al. (135).

4. Vessel cannulation

Arterioles or feed arteries were moved to a cannulation rig using a 50-100 μl Wiretrol pipette (Drummond Scientific Company, Broomal, PA). Each vessel was then cannulated onto two glass micropipettes (prepared by pulling, breaking and fire-polishing glass capillary tubes (World Precision Instruments)), and secured to the pipettes using 11-0 ophthalmic suture (Ashaway Line and Twine Mfg. Co., Ashaway, RI). The chamber then was secured to the stage of a microscope (Leica DMIL, Wetzlar, Germany), where the vessels were visualized and heated to 34°C (cremaster arterioles) or 37°C (feed arteries). The vessels were then pressurized to 80 cm H_2O, and allowed to develop myogenic tone, as previously described (38, 134). All vessels studied had a minimum of 20% resting myogenic tone when compared to the maximum passive diameter of the vessel obtained in 0 Ca^{2+} PSS at 80 cm H_2O. Throughout all experiments, cannulated vessels were constantly superfused with physiological salt solution (PSS: 140 mM NaCl, 5 mM KCl, 1.8 mM $CaCl_2$, 1 mM $MgCl_2$, 10 mM HEPES, 10 mM glucose, pH 7.4) alone or containing a drug.

5. Diameter measurement

The diameters of all vessels not loaded with Fluo 4 dye were measured throughout the experiment using Diamtrak software (T.O. Neild, Adelaide, Australia) (200). Diamtrak was set to record the diameter of the vessels, and the plane of focus was set such that the inner diameter of all vessels was constantly tracked. Following each experiment, the diameters were extracted from the

Diamtrak files using the DT Review portion of the Diamtrak software. In Fluo 4-loaded arterioles, steady-state diameters were measured separately from Ca^{2+} measurements. A different procedure was used in the Fluo 4-loaded vessels: Immediately prior to Ca^{2+} measurements, the vessels were briefly transilluminated with dim, 586 nm light, the microscope was focused on the vessel wall at midplane and and recordings of the transilluminated vessels made using Piper software and stored on a personal computer for later analysis. The microscope then was returned to the plane of focus for Ca^{2+} measurements. After the experiments were concluded, the internal vessel diameters then were measured using the Image J (3) using the acquired transilluminated images.

6. Calcium imaging:

The smooth muscle cells of cannulated vessels were loaded with the intensiometric Ca^{2+} indicator, Fluo-4 by bath incubation. The dye solution contained 5 μM Fluo 4-AM dye (Invitrogen, Carlsbad, CA) in 0.5% dimethyl sulfoxide (DMSO) and 0.1% bovine serum albumin (USB Corp., Cleveland, OH) in PSS (mouse vessels) or 0 Ca^{2+} PSS (hamster vessels), and it was applied to the vessels for 2 hours at room temperature, followed by a 30 minute superfusion with PSS to wash Fluo-4 from the bath, and allow for dye de-esterification and gradual temperature increase. All vessels were imaged using a long working-distance 40x water-immersion objective (N.A. 0.8, working distance 3 mm; Leica, Wetzlar, Germany). The z-resolution with this objective in PSS was 2.186 μm. Fluo 4 fluorescence at 526 nm was acquired at 30 frames per second using a

spinning-disc confocal system (CSU-10B, Solamere, Salt Lake City, UT) with 488 nm laser illumination (Solamere, Salt Lake City, UT) and an intensified CCD camera (XR Mega-10, Stanford Photonics, Palo Alto, CA). Each recording period consisted of 500 frames (16.67 seconds at 30 fps). Images were recorded using Piper software (Stanford Photonics, Palo Alto, CA) and analyzed using SparkAn (courtesy of Drs. M.T. Nelson and A.D. Bonev, University of Vermont) and Image J (3) software. The occurrence of both Ca^{2+} sparks and Ca^{2+} waves were counted manually by visualizing each smooth muscle cell within a vessel separately using a masking procedure, and scoring whether any Ca^{2+} sparks and/or waves appeared during the recording period (500 frames over 16.6 seconds). These occurrences were then verified using SparkAn as increases in fluorescence that were at least 15% above basal levels for sparks and 20% above baseline for waves. SparkAn was also used to calculate the average frequency, amplitude (F/Fo) and Full Duration Half Maximum (FDHM) of Ca^{2+} events recorded from a single cell. In Sparkan, an ROI (10 x 10 pixels) was placed on each cell that displayed at least one Ca^{2+} event during the recording period. The frequency, amplitude and FDHM therefore provides the average rate of spark or wave occurrence, peak amplitude and duration of Ca^{2+} events, respectively, per cell within a vessel. To calculate the spatial spread (Full Width Half Maximum, FWHM) of each Ca^{2+} spark and wave using Image J, a hand-drawn ROI first was used to calculate the pre-spark/wave basal Ca^{2+} of each smooth muscle cell. Next, FWHM was calculated by comparing the basal

intensity of each cell to plot profiles for the peak fluorescence of each spark or wave. Plot profiles were generated by drawing a longitudinal line through the center of each cell in which a spark or wave was recorded. The cross-sectional length of each smooth muscle cell within the appropriate confocal slice was also measured using Image J. Calcium transients in smooth muscle cells induced by caffeine (10 mM) were assessed using Fura 2 as described previously (38, 134) with simultaneous measurement of internal diameter as described above.

7. Measurement of Ca^{2+} wave synchronicity

To determine whether Ca^{2+} waves in HCA and HFA were synchronous, SparkAn was used to produce a graph of Ca^{2+} activity in every cell by placing a 10 x 10 pixel ROI on each cell that exhibited at least one wave within a vessel. The data from each ROI then was combined by averaging the ROI's across each time point to produce an overall representative trace of global Ca^{2+} activity in the whole vessel during the recording period. This averaged tracing was then analyzed to determine the presence of any peaks with a fluorescence greater than 1.2 F/Fo.

8. Vessel dissociation

Mouse cremaster feed arteries or cremaster arterioles were dissected as described above, and subjected to a dissociation protocol as previously described (135), with some modifications. All possible vessels from one animal

were pooled into 1ml of dissociation solution (0 Ca^{2+} PSS containing: 10 μM sodium nitroprusside, 10 μM diltiazem, 1% bovine serum albumen (BSA), and 100 μM $CaCl_2$). Vessels were then incubated for 35 minutes in a 37°C solution containing 26 Units/mL papain and 1 mg/ml dithioerythritol. The vessels were then incubated for 19 minutes in a 37°C solution containing 1.95 Units/ml collagenase, 0.15 mg/ml elastase and 1mg/ml soybean trypsin inhibitor. Next, the solution was pipetted off, and the 4 ml cold dissociation solution was carefully added and allowed to sit at room temperature for 10 minutes. This solution was then carefully removed without disturbing the vessels at the bottom and replaced with 1 ml Ca^{2+}-free PSS. The vessels were then triturated 1-3 times to release the smooth muscle and endothelial cells. This solution was transferred to a siliconized centrifuge tube to prevent cell adhesion.

9. RNA Isolation and Quantitation

Control tissues (heart, brain, diaphragm and intestinal smooth muscle) were hand dissected and immediately submerged in RNAlater (Ambion, Austin, TX). Tissues were removed from RNAlater, processed using RNeasy tissue kits (Qiagen, Germantown, MD) per manufacturer's protocol and resultant RNA quantitated with a Nanodrop 1000 (Thermo Scientific, Wilmington, DE).

Feed arteries and cremaster arterioles were enzymatically dissociated to obtain single smooth muscle cells, as described previously (135). Smooth muscle cells from the small intestine were isolated as described previously (111), with slight

modification. After 35 min incubation of tissue with enzyme containing dissociation buffer, supernatant was removed and replaced with 4 ml cold enzyme-free dissociation solution, incubated for 10 min at room temperature, supernatant aspirated, and sample resuspended in 1 ml enzyme-free cold dissociation solution. Resultant cells were separated by trituration using a 1 ml pipette. Cells were viewed with bright field microscopy for collection as previously described (111) using 70 μm diameter, heat-polished glass pipettes. Only long, relaxed cells were collected and all vascular smooth muscle samples contained 50 cells. Bath solution samples were collected as controls.

10. Real-time qPCR (RT-qPCR)

For heart, brain, diaphragm and intestinal smooth muscle, RNA isolates were reverse transcribed (RT) (2 μg per reaction) using a High Capacity RNA to cDNA kit (Applied Biosystems, Foster City, CA, # 4387406), per manufacturer's protocol. Resultant cDNA was quantitated with a Nanodrop 1000. RT-qPCR 20 μL reactions were prepared with Applied Biosystems TaqMan Gene Expression Master Mix (# 4369016), inventoried Gene Expression Assays RYR1 (Mm01175172_g1), RYR2 (Mm00465877_m1), RYR3 (Mm01328421_m1), α-smooth muscle actin (Mm01204962_gH) and run for 40 cycles on an ABI 7500 Thermocycler, per manufacturer's instruction. All reactions were run in triplicate including no reverse transcription (NRT) controls. Samples of 50 smooth muscle cells or an equivalent volume of bath solution (control) were prepared for RT-qPCR using the Cells-to-PreAmp C_T kit (Applied Biosystems, Foster City, CA, #

4387299) per manufacturer's instructions. RT-qPCR 20 µL reactions were prepared and run as described above. Relative abundance of target RNA was normalized to α -smooth muscle actin RNA which showed no differences among samples. PCR efficiency (E) was $10^{(-1/slope)}$ with slope estimated from serial dilutions of cDNA from each of the control tissues. Because of the low level of expression of transcripts in the arterial and arteriolar smooth muscle samples, serial dilutions of cDNA from intestinal smooth muscle was used to compute PCR efficiencies for these samples. Relative abundance of target RNA was calculated from $(E_{\alpha\text{-actin}}{}^{CT})/(E_{target}{}^{CT})$, where PCR crossing points (C_T) were determined using ABI 7500 software (v2.02).

11. RyR immunofluorescence

For single cell immunofluorescence (IHF), feed arteries or arterioles were dissected and dissociated as described above. As soon as the dissociation was complete, the cell suspensions were spun onto glass microscope slides using a Shandon Cytospin 4 Centrifuge for 3 minutes at 750 rpm. The samples on the slides then were fixed with 4% paraformaldehyde for 20 minutes followed by 3 washes in phosphate-buffered saline (PBS), with a 15 minute incubation in PBS between each wash. For whole-vessel IHF, individual feed arteries or cremaster arterioles were cannulated and pressurized as described above. They were fixed in 4% paraformaldehyde for 20 minutes while still cannulated and pressurized. After 3 washes in PBS, vessels were removed from the cannula and pinned to 35 mm Sylgard-containing culture dishes. Both the single cells and whole vessels

then were subjected to the same IHF protocol. Incubation in all solutions took place at 4 ºC, and primary and secondary antibodies were diluted in PBS + 0.1% Triton X-100 to permeabilize the cells. Samples were incubated in 10% normal goat serum for 60 minutes then washed as described above and placed overnight in the primary antibody against RyR1/2 (mouse monoclonal, Sigma). Samples were washed with PBS, placed into 10% normal goat serum for another 60 minutes, washed again in PBS, incubated 90 minutes in AlexaFluor 488 secondary antibody (Molecular Probes). After a final wash in PBS, slides were mounted using ProLong Gold with DAPI (Invitrogen) to stain the cell nuclei, and coverslips were sealed into place using clear nail polish.

All slides were imaged at the Center for Advanced Microscopy at Michigan State University on an Olymous FluoView FV1000 confocal laser scanning microscope. Slides were imaged with an Olympus PLAPON 60x oil immersion objective, with numerical aperture 1.42. Whole vessels were imaged with a 2x optical zoom and 2 µm z-slices, and single cells were images with a 4x optical zoom and 0.5 µm z-slices. Every image set was taken with identical PMT, gain and offset settings.

RyR expression patterns for single cell and whole-vessels were quantified using Image J. A line was drawn through a single cell or whole vessel (avoiding the nucleus), and a plot profile of the intensity of RyR staining along the line was generated. The data points from this line then were used to determine the

coefficient of variation (standard deviation divided by mean intensity) for MFA and MCA as an index of the non-uniformity of staining.

12. Chemicals

Ryanodine was obtained from Ascent Scientific (Bristol, UK), and xestospongin D and 2-APB, from Calbiochem (San Diego, CA). Fluo-4 was obtained from Invitrogen (Carlsbad, CA). All other drugs and chemicals were obtained from Sigma-Aldrich (St. Louis, MO) unless noted otherwise in the text. Caffeine and tetraethyl ammonium were dissolved directly into PSS. All other drugs were dissolved in DMSO and then diluted to their final concentrations in PSS. DMSO alone was without effect in cannulated vessels.

13. Data analysis and statistics

Data are shown as means ± 95% confidence intervals for the occurrence of Ca^{2+} sparks and waves, or means ± SE for all other data. Statistical significance was determined using Student's t test or ANOVA followed by a post hoc Tukey's test. All statistical comparisons were performed at the 95% confidence level.

CHAPTER 3: Heterogeneous function of ryanodine receptors, but not IP_3 receptors in hamster cremaster muscle feed arteries and arterioles

Rationale:

The sarcoplasmic reticulum of vascular smooth muscle cells contains at least two types of Ca^{2+}-release channels: ryanodine receptors (RyR) and inositol 1,4,5 trisphosphate receptors (IP_3R) (284). Ryanodine receptors underlie Ca^{2+}sparks, (46) and they also may participate in more global intracellular Ca^{2+} events through Ca^{2+}-induced Ca^{2+}-release (CICR) (284). Calcium release during G-protein coupled receptor activation is mediated by IP_3R, and these Ca^{2+} release channels also underlie Ca^{2+} waves (284). In some systems, both RyR and IP_3R contribute to Ca^{2+} signals (20, 284). What remains unclear is the role played by these channels in microvascular smooth muscle and the regulation of myogenic tone.

Ryanodine receptor-mediated Ca^{2+} sparks have been observed in retinal arterioles (36, 55, 56, 265). In contrast, recent studies of cells isolated from first-order rat cremaster arterioles failed to detect Ca^{2+} sparks (291). In addition, further studies of ureter arteriolar smooth muscle cells (30) found no role for RyR in these microvessels. While most studies of smooth muscle from larger vessels suggest that Ca^{2+} sparks activate sarcolemmal large conductance, Ca^{2+}-activated K^+ channels (BK_{Ca}) participating in the negative feedback regulation of

membrane potential and vascular tone (284), studies of renal arterioles suggest that RyR participate in the positive feedback regulation of vascular tone through CICR in this microcirculation (11, 80, 81). Thus, there appear to be substantial regional differences in the function of RyR in the microcirculation.

Similarly, the role played by IP_3R in the regulation of myogenic tone in the microcirculation is largely unknown. Recent studies of ureter arterioles suggest that IP_3R play a dominant role in Ca^{2+} signaling in these vessels during agonist-induced constriction (30). However, the arterioles in these studies were unpressurized, hence the function of IP_3R during pressure-induced myogenic tone was not addressed. In rat first-order cremaster arterioles, the IP_3R antagonist, 2-aminoethoxydiphenylborate (2-APB), has been reported to inhibit myogenic tone (222) (consistent with a major role for IP_3R) or have little effect (157). The lack of Ca^{2+} waves observed in small, Fluo 4-loaded pressurized mesenteric arteries with substantial myogenic tone (195) would appear to argue against a major role for IP_3R in basal myogenic tone in these vessels. Thus, the function of IP_3R in arteriolar and resistance artery smooth muscle and their role in myogenic tone remains unclear.

The purpose of the present study was to characterize the subsarcolemmal Ca^{2+} signals in smooth muscle cells of small skeletal muscle arterioles compared to those observed in upstream feed arteries, and to test the hypothesis that RyR

and IP_3R contribute to Ca^{2+} signals and myogenic tone in both vessel types. We found that RyR participate in both Ca^{2+} sparks and Ca^{2+} waves in feed artery smooth muscle cells, and contribute to the negative feedback regulation of myogenic tone in these small arteries. In contrast, RyR appeared silent in smooth muscle cells of cremaster arterioles contributing neither to Ca^{2+} sparks, Ca^{2+} waves nor myogenic tone. On the other hand, we observed that IP_3R and upstream phospholipase C importantly contributed to Ca^{2+} waves, global Ca^{2+} levels and myogenic tone in smooth muscle cells of both feed arteries and arterioles. Our findings emphasize the differences in function between RyR and IP_3R in feed arteries and demonstrate heterogeneity in the function of RyR in feed arteries compared to their downstream arterioles.

Results:

Role of RyR in feed arteries:

We observed both Ca^{2+} sparks and Ca^{2+} waves in Fluo 4-loaded feed arteries studied at physiological temperature and pressure (**Figures 5 and 6, Table 6**). The two Ca^{2+} signals were differentiated based on their spatial spread within the cells: Ca^{2+} sparks were localized to small microdomains within a smooth muscle cell, while Ca^{2+} waves involved a more global increase in Ca^{2+} (**Figures 5, Table 6**). Spatial properties of both sparks and waves were quantified using Image J. The length of smooth muscle cross sections in confocal slices were measured in Fluo-4-loaded vessels and compared to the full-width, half maxima (FWHM) of

each Ca^{2+} event. The average length of smooth muscle cell optical cross sections was 77.1 ± 1.0 μm (n = 45 cells from 5 vessels) in feed arteries. Calcium sparks had a FWHM that was considerably smaller than the cross-section length (6.5 ± 0.1%, n = 45 cells from 5 vessels), while Ca^{2+} waves had FWHM that were much closer to the entire length (66.4 ± 2.7%, n = 42 cells from 5 vessels). Calcium sparks differed significantly in frequency, amplitude, and duration (Full-duration, half-maximum; FDHM) compared to waves (**Table 6**). Calcium sparks were observed in 39 ± 14% of feed artery smooth muscle cells, and Ca^{2+} waves were observed in 26 ± 14% of cells (n = 5 arteries, $p < 0.05$, **Figure 6**) A representative trace of both a Ca^{2+} spark and a Ca^{2+} wave are shown in **Figure 7.** We also looked at the synchronicity of the Ca^{2+} waves and found that the waves were asynchronous. While many waves occur per cell during the recording period, an average (global) measurement of the Fluo-4 signal showed no peaks with an F/Fo greater than 1.2 (**Figure 8**), indicating that the waves occurred asynchronously.

Table 6. Properties of Ca^{2+} signals in cremaster feed arteries and arterioles

Vessel type	Ca^{2+} signal	Cross-section length (μm)	FWHM (μm)	Frequency (Hz)	Amplitude (F/F_o)	FDHM (s)
Feed arteries	sparks	77.13 ± 1.00	5.08 ± 0.71	0.14 ± 0.01	1.56 ± 0.03	0.37 ± 0.07
Feed arteries	waves	71.18 ± 1.07	47.83 ± 2.40	0.38 ± 0.25 *	1.81 ± 0.33 *	0.80 ± 0.30 *
Arterioles	waves	36.8 ± 0.64 †	21.0 ± 0.39 †	0.40 ± 0.02 *	1.72 ± 0.04 *	0.91 ± 0.08 *

FWHM = full-width, half-maximum, FDHM = full-duration, half-maximum, Values are means ± SE, * = $p < 0.05$ compared to feed artery Ca^{2+} sparks, † = $p < 0.05$ compared to feed artery. See text for details.

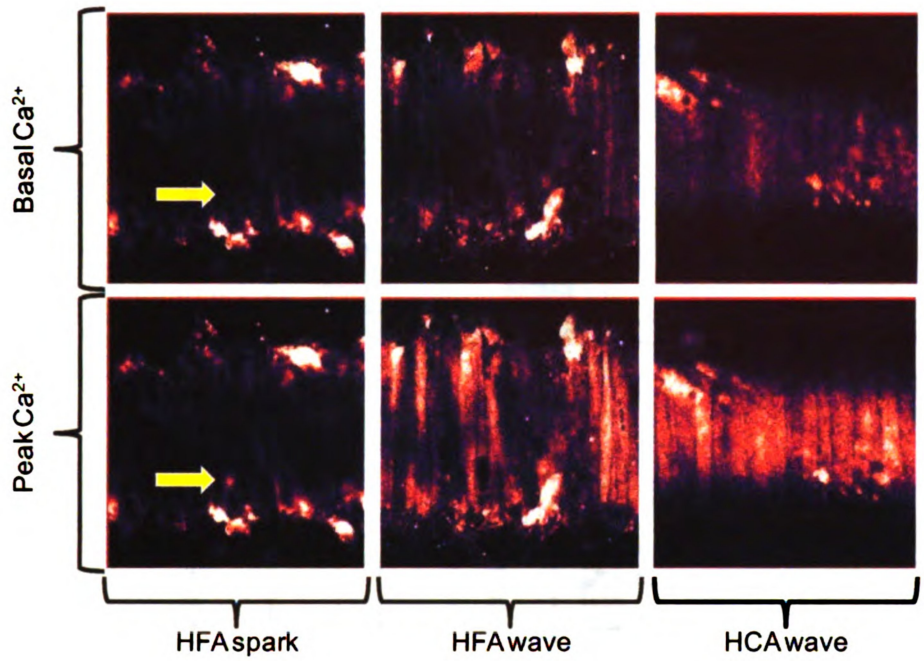

Figure 5. Representative fluorescent images of Ca^{2+} sparks and waves in cremaster feed arteries and arterioles

Shown are confocal images of Fluo 4-loaded hamster feed arteries (HFA) and hamster cremaster arterioles (HCA), as indicated. The upper panels show basal Ca^{2+} levels, and the bottom panels show peak Ca^{2+} levels for: (left to right) a feed artery spark (position indicated by the arrow), feed artery waves and cremaster arteriole waves. Sparks occur in a small, restricted area of smooth muscle cells, while waves occur in a much larger area of the cells.

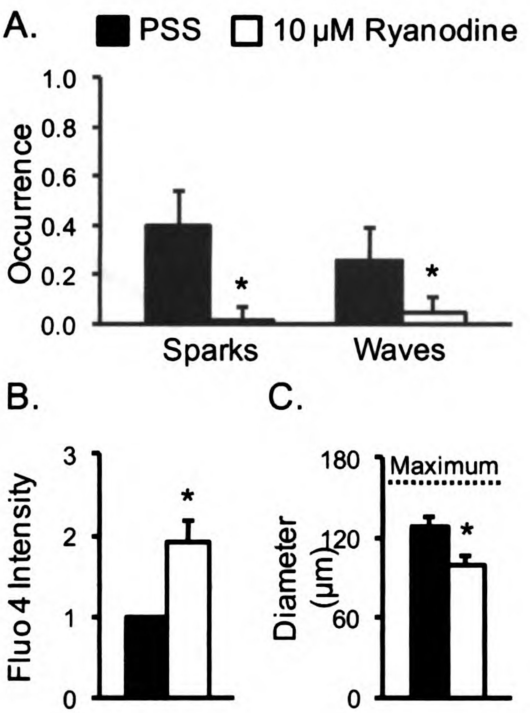

Figure 6. Ryanodine receptors contribute to Ca^{2+} sparks, Ca^{2+} waves, and myogenic tone in cremaster feed arteries.

Data are: means ± 95% confidence intervals for (A) occurrence of Ca^{2+} sparks and waves; means ± SE for (B) Global Fluo 4 signal, an index of global intracellular Ca^{2+}; and (C) diameter, in Fluo 4-loaded cremaster feed arteries at 80 cm H_2O in the absence (PSS) and presence of ryanodine (10μM) as indicated. * = significantly different from value in PSS, $p < 0.05$. Maximum diameter of arteries is shown by dashed line in panel C.

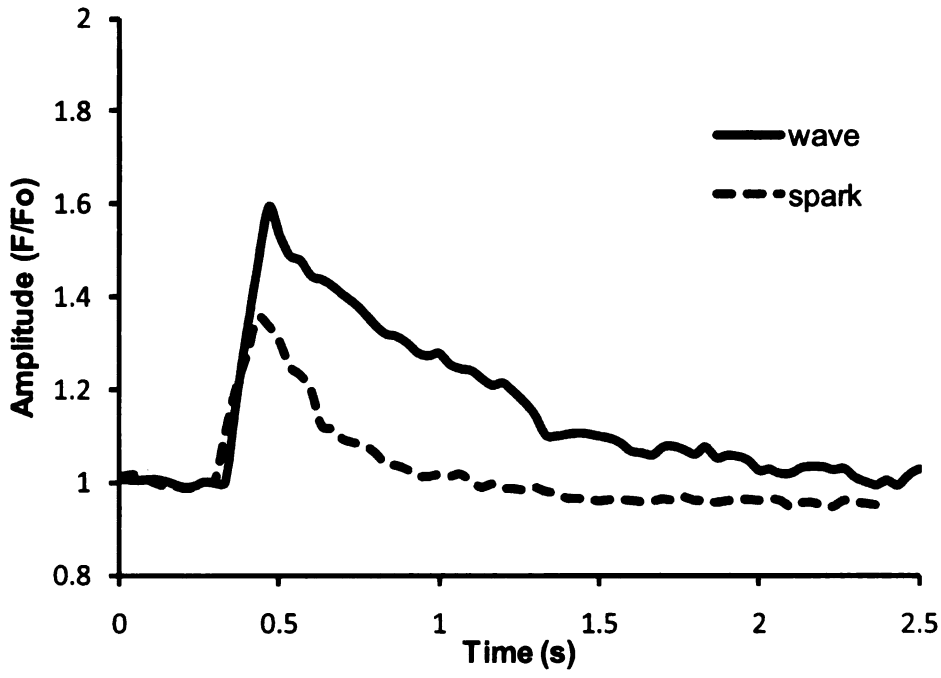

Figure 7. Representative SparkAn tracing for a Ca^{2+} spark and wave in hamster feed artery.

The graph depicts the change in amplitude over time of one representative spark (dashed line) and one wave (solid line), as measured by a 10 x 10 pixel ROI in the SparkAn program. The spark occurs over a shorter period of time and has a much smaller amplitude than the calcium wave.

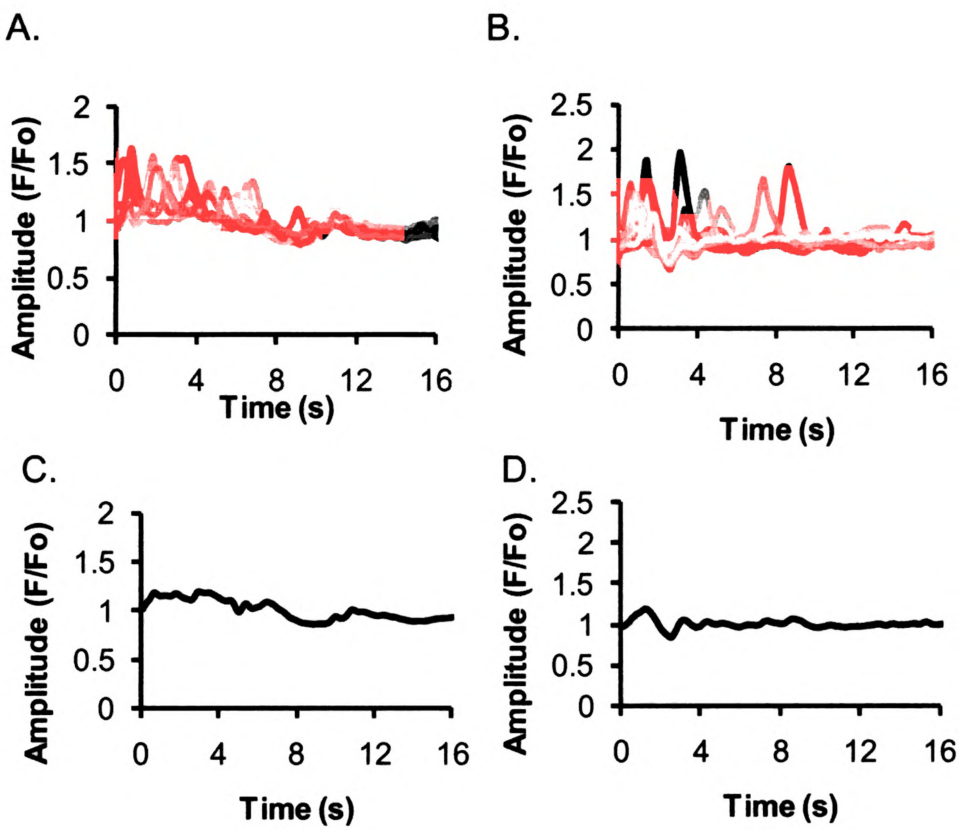

Figure 8. Calcium waves in hamster cremaster feed arteries and arterioles are asynchronous.

(A) and (B) depict representative SparkAn amplitude vs. time tracings for each cell that displayed at least one Ca^{2+} wave during the recording period for HFA and HCA, respectively, and many waves with amplitude greater than 1.2 F/Fo were recorded for both vessel types. (C) and (D) show graphs averaging all of the individual tracings above for HFA and HCA, respectively. In these average traces, no peaks with amplitude greater than 1.2 F/Fo were generated.

Superfusion of feed arteries with the RyR antagonist, ryanodine (10 μM), decreased the proportion of smooth muscle cells that displayed Ca^{2+} sparks and Ca^{2+} waves to 2 ± 5% and 5 ± 6%, respectively (n = 5 vessels, $p < 0.05$ compared to control) (**Figure 6A**). Application of ryanodine also led to significant vasoconstriction (**Figure 6B**) that was associated with a significant increase in global Fluo-4 intensity, suggesting an increase in intracellular Ca^{2+} (**Figure 6C**).

The ryanodine-induced increase in global Ca^{2+} and the associated vasoconstriction are consistent with the negative feedback role that has been reported for RyR in other systems (284). To further test this hypothesis, we compared the vasomotor effects of ryanodine with those of the BK_{Ca} channel blocker, tetraethyl ammonium (TEA), at a concentration of TEA (1 mM) that we have previously shown to selectively inhibit BK_{Ca} channels in hamster vascular smooth muscle (33, 34). Alone, both ryanodine (10 μM) and TEA (1 mM) caused significant constriction of feed arteries (**Figure 9**). However, in the presence of TEA (1 mM), ryanodine (10 μM) failed to produce vasoconstriction, consistent with numerous previous studies (284) implicating coupling of RyR function to the function of BK_{Ca} channels. The lack of effect of ryanodine in the presence of TEA was not due to the lack of ability of the smooth muscle to contract, because in the presence of both TEA and ryanodine, the L-type Ca^{2+} channel agonist, Bay K 8644 still was able to produce constriction of the same magnitude as that

induced by ryanodine alone (**Figure 9**). Thus, in feed arteries, ryanodine receptors appear play an important role in the negative feedback regulation of myogenic tone.

To verify these observations and rule out any nonspecific effects of TEA, we also compared the effects of ryanodine to those of paxilline, a more selective BK_{Ca} inhibitor. Paxilline (100 nM) and TEA caused similar constrictions in HFA, and ryanodine did not constrict HFA in the presence of paxilline. Paxilline-induced constriction of HFA was also inhibited in the presence of ryanodine (**Figure 10**, n = 3, $p < 0.05$). These data confirm the previous observation that ryanodine receptors participate in the regulation of tone in HFA. The data also suggest that TEA is specific for BK_{Ca} channels in these smooth muscle cells, as reported previously (33, 34)

Lack of a role for RyR in arterioles:

In contrast to our findings in feed arteries and prior studies in other larger vessels, Ca^{2+} sparks were not observed in the smooth muscle cells of Fluo 4-loaded cremaster arterioles (2 sparks observed in 1015 cells from 49 vessels). Calcium waves, however, were routinely observed: 48 ± 9% of cells in arterioles at physiological pressure and temperature displayed Ca^{2+} waves (**Figure 6**). The frequency, amplitude and FDHM of Ca^{2+} waves were similar to those observed in feed arteries (**Table 6**). The FWHM of the Ca^{2+} waves in arteriolar

smooth muscle cells was less than that of the feed arteries (21.0 ± 0.39 μm, n = 40 cells from 5 vessels; 57.7 ± 1.5% of slice length; $p < 0.05$), even with the smaller average cross section lengths of confocal slices in the arterioles (36.8 ± 0.64 μm) (**Table 6**). These events, however, were much larger than Ca^{2+} sparks observed in the feed arteries (**Table 6**).

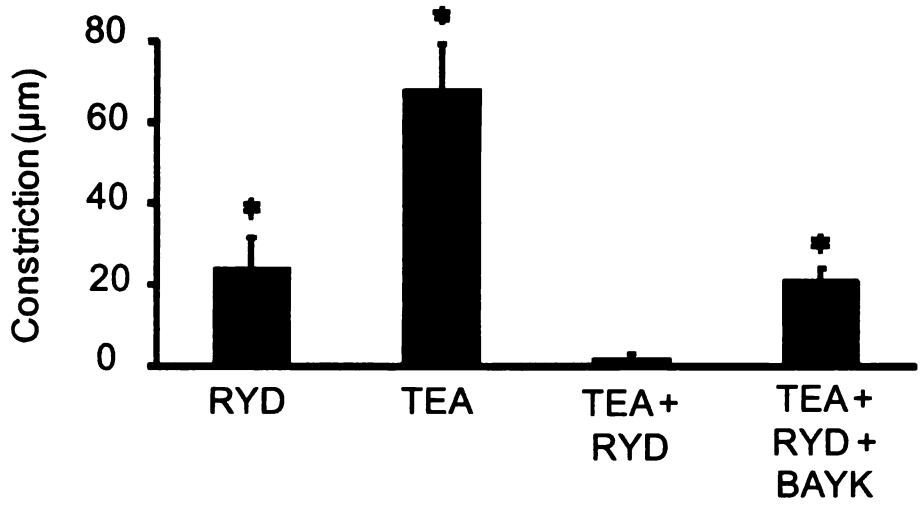

Figure 9. Blockade of BK_{Ca} channels inhibits ryanodine-induced constriction of feed arteries.

Data are mean constrictions ± SE (µm, n = 4) induced by ryanodine (Ryd, 10 µM), the BK_{Ca} channel blocker tetraethyl ammonium (TEA, 1 mM), Ryd in the presence of TEA, or the L-type Ca^{2+} channel agonist, Bay K 8644 (Bay K, 5 nM) in the presence of Ryd + TEA as indicated. Resting diameters of the feed arteries were 133 ± 8 µm and maximum diameters were 183 ± 11 µm upon removal of extracellular Ca^{2+}. * = significantly different from 0, $p < 0.05$.

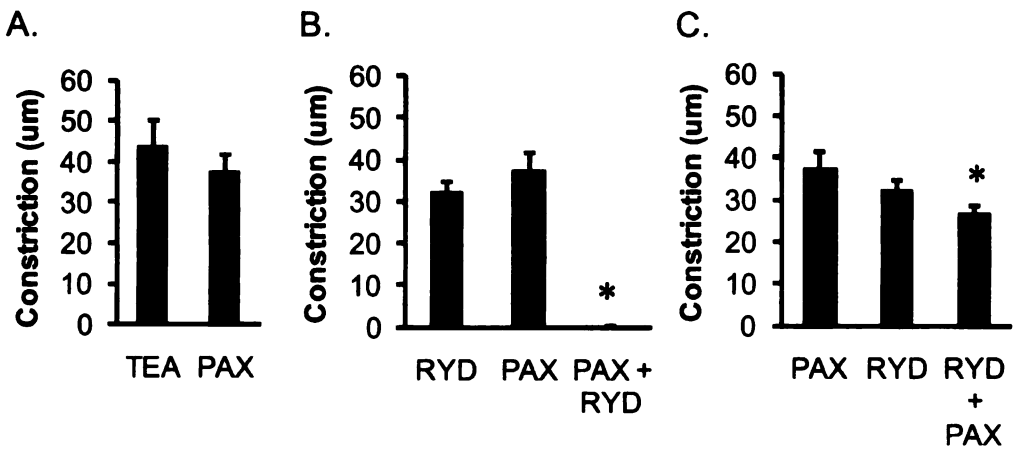

Figure 10. Ryanodine receptors and BK_{Ca} are functionally coupled in hamster feed arteries

Data are mean constrictions ± SE (μm, n = 4). (A) TEA (1 mM) and paxilline (PAX; 100 nM) cause similar constrictions in HFA. (B) PAX-induced blockade of BK_{Ca} inhibits ryanodine-induced constriction. * = significantly different from RYD alone. (C) In the presence of ryanodine, PAX-induced constriction is inhibited. Resting diameters of the feed arteries were 159 ± 7 μm and maximum diameters were 226 ± 1 μm upon removal of extracellular Ca^{2+}. * = significicantly different from PAX alone.

Consistent with the absence of Ca^{2+} sparks in smooth muscle cells of cremaster arterioles, we found that ryanodine (10 μM) had no significant effect on Ca^{2+} signals in these microvessels: in the presence of ryanodine, Ca^{2+} waves were still observed in 47 ± 9% of cells ($n = 10$, $p > 0.05$), and this RyR-antagonist had no effect on their amplitude or frequency (**Figure 11A**). Ryanodine also was without significant effect on global intracellular Ca^{2+} (**Figure 11B**) or arteriolar diameter (**Figure 11C**). To rule out the possibility that the concentration of ryanodine used was insufficient, we repeated the experiments outlined above using a higher concentration (50 μM) of this alkaloid and obtained similar results: ryanodine (50 μM) had no effect on Ca^{2+} wave parameters, global Ca^{2+} or diameter (**Figure 12**, $n = 7$, $p > 0.05$ for each).

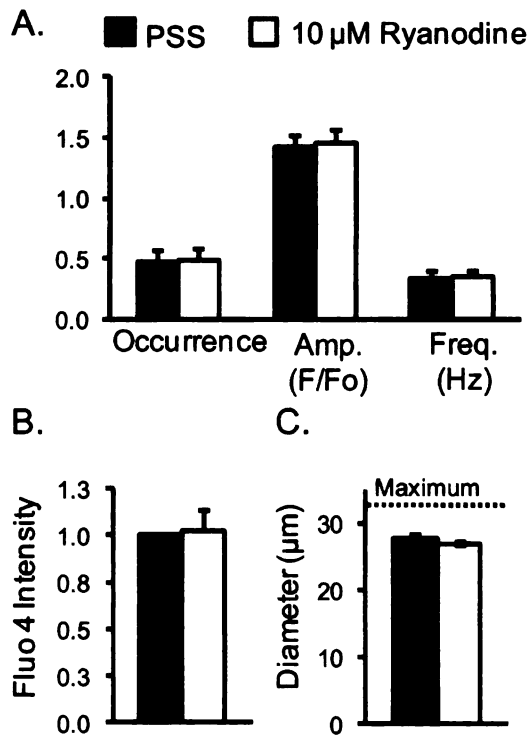

Figure 11. Ryanodine receptors do not contribute to Ca^{2+} signals or myogenic tone in hamster cremaster arterioles

In Fluo 4-loaded cannulated arterioles at 80 cm H_2O, Ca^{2+} waves, but not Ca^{2+} sparks, were routinely observed. Data are: means ± 95% confidence intervals for (A) occurrence of Ca^{2+} waves; means ± SE for amplitude (Amp.) and frequency (Freq.) of Ca^{2+} waves ($n = 6$, $p > 0.05$); (B) Global Fluo 4 signal, an index of global intracellular Ca^{2+} ($n = 6$, $p > 0.05$); and (C) diameter ($n = 8$, $p > 0.05$) in the absence (PSS) or presence of ryanodine (10 μM) as indicated.

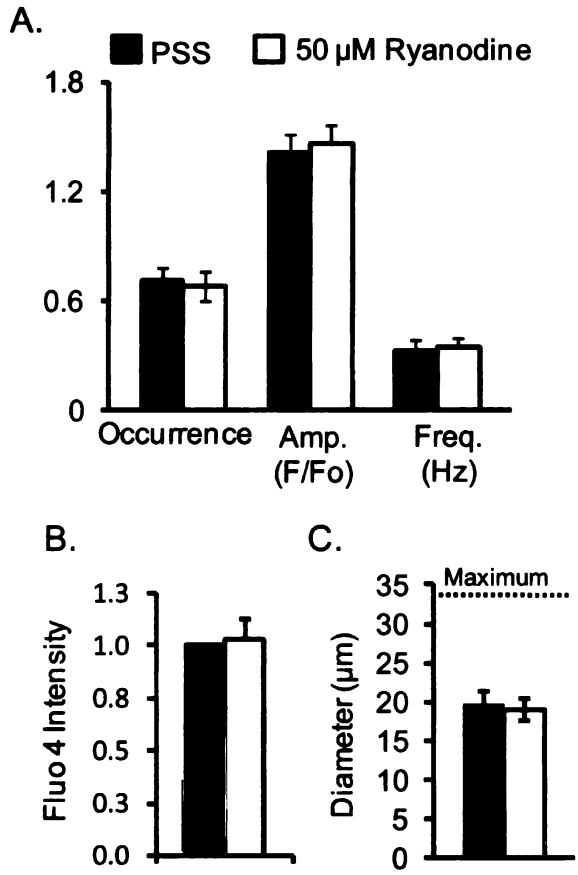

Figure 12. Increased concentration of ryanodine has no effect on Ca^{2+} waves, global Ca^{2+} or diameter in hamster cremaster arterioles

In Fluo 4-loaded cannulated arterioles at 80 cm H_2O, Ca^{2+} waves, but not Ca^{2+} sparks, were routinely observed. Data are: means ± 95% confidence intervals for (A) occurrence of Ca^{2+} waves; means ± SE for amplitude (Amp.) and frequency (Freq.) of Ca^{2+} waves ($n = 6$, $p > 0.05$); (B) Global Fluo 4 signal, an

index of global intracellular Ca^{2+} ($n = 6$, $p > 0.05$); and (C) diameter ($n = 8$, $p > 0.05$) in the absence (PSS) or presence of ryanodine (50 μM) as indicated.

Ryanodine (10 μM) also had no significant effect on TEA-induced constriction of the arterioles (**Figure 13**). As in the feed arteries, we verified the specificity of TEA in HCA by looking at the effects of ryanodine and paxilline on myogenic tone. As in HFA, TEA and paxilline produced similar constrictions in HCA, ryanodine did not constrict arterioles or alter paxilline-induced constriction (**Figure 14**, $n = 3$, $p < 0.05$).

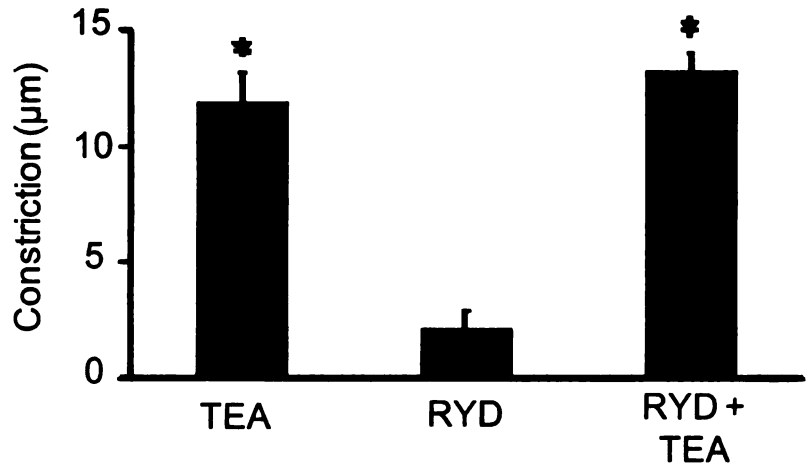

Figure 13. Ryanodine does not alter TEA-induced constriction of arterioles

Data are mean constrictions ± SE (μm, n = 5) induced by the BK_{Ca} channel blocker, tetraethyl ammonium (TEA, 1 mM), the RyR antagonist, ryanodine (Ryd, 10 μM), or TEA in the presence of Ryd as indicated. Resting diameters of the arterioles were 24 ± 2 μm and the vessels dilated to 33 ± 3 μm upon removal of extracellular Ca^{2+}. * = significantly different from 0, $p < 0.05$.

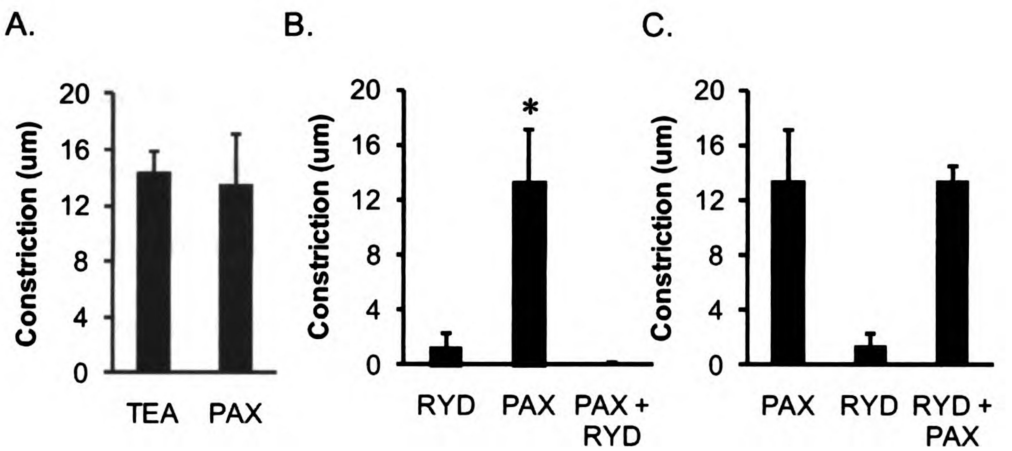

Figure 14. Ryanodine has no effect on paxilline-induced constriction of arterioles.

Data are mean constrictions ± SE (μm, n = 4). (A) TEA (1 mM) and paxilline (PAX; 100 nM) cause similar constrictions in HCA ($p > 0.05$). (B) Ryanodine has no significant effect on arteriolar diameter in the absence or presence of PAX (p . 0.05), whereas PAX constricts arterioles. * = significantly different from 0, $p < 0.05$. (C) the ryanodine receptor antagonist, ryanodine (10 μM) does not inhibit PAX-induced constriction of HCA ($p > 0.05$ compared to PAX alone).

The higher concentration of ryanodine (50 μM) also had no effect on responses induced by the BK_{Ca} channel blocker, TEA (1 mM) ($n = 5$, $p < 0.05$). Thus, in contrast to our findings in feed arteries, RyR appeared to be silent in arteriolar smooth muscle cells, contributing to neither Ca^{2+} signals nor myogenic tone in arterioles under the conditions of our experiments.

Functional evidence for expression of RyR in arterioles and efficacy of ryanodine: Because ryanodine had no effect in the arterioles, we examined the functional expression of RyR using the RyR agonist, caffeine (284) (10 mM, **Figure 15-17**), and the ability of ryanodine to block the effects of caffeine as a test of the efficacy of ryanodine (**Figure 16**). Similar to Potocnik and Hill (123), we found that caffeine had biphasic effects on both intracellular Ca^{2+} and vessel diameter in arterioles pressurized to 80 cm H_2O that were difficult to interpret (**Figure 15**). However, vessels pressurized to 20 cm H_2O, with little myogenic tone, consistently responded to caffeine (10 mM) with a typical, transient increase in intracellular Ca^{2+} that was associated with a transient constriction (**Figure 17**, $n = 7$, $p < 0.05$). In separate experiments, we found that ryanodine (10 μM) abolished the caffeine-induced constriction (**Figure 17**), confirming that ryanodine effectively blocks RyR in the arterioles. As above, ryanodine, alone, did not affect arteriolar diameter, and diameter was not changed when caffeine was added in the presence of this RyR antagonist ($n = 7$, $p > 0.05$,).

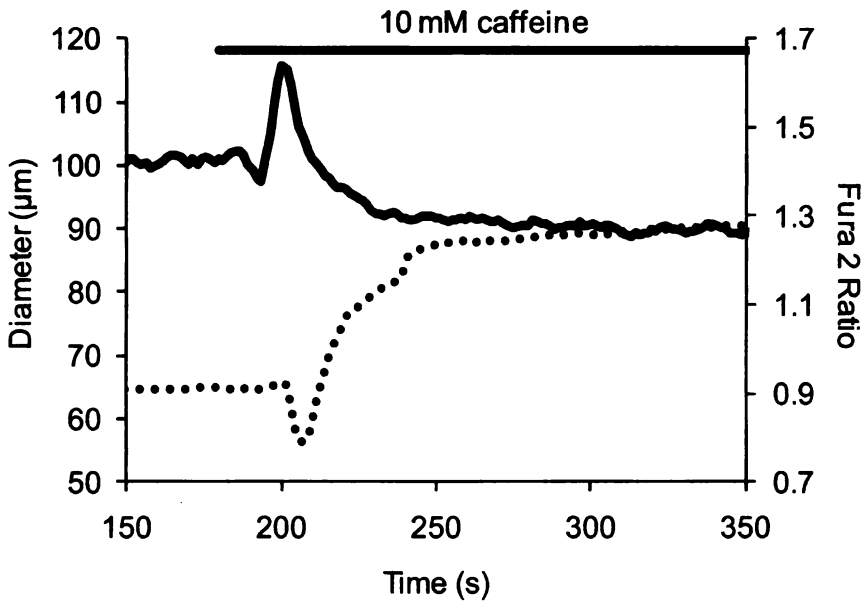

Figure 15. Effect of caffeine in arterioles at 80 cm H_2O

Representative trace of a Fura 2-loaded HCA in the presence of caffeine. The RyR agonist, caffeine (10 mM) causes a transient constriction followed by a sustained dilation of HCA (dashed line). The diameter effects are immediately preceded by a transient increase and sustained decrease in Fura 2 ratio (solid line).

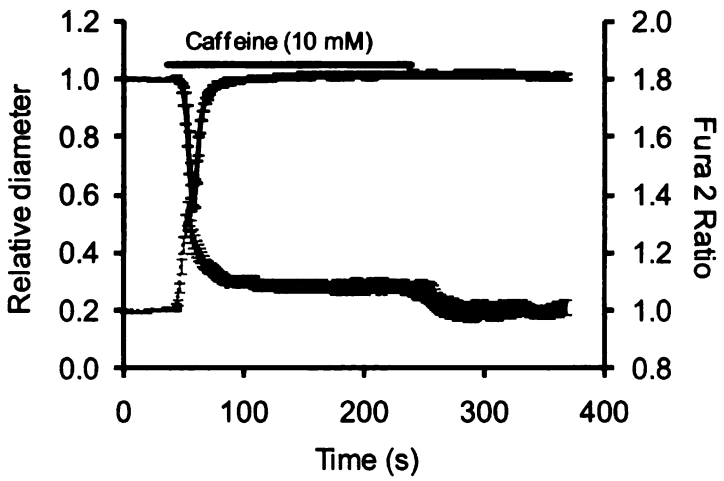

Figure 16. Functional evidence for ryanodine receptors in cremaster arterioles

Shown are means ± SE (n = 7) for arteriolar internal diameter normalized to the resting diameter of the vessels (Top tracing - black) and intracellular Ca^{2+} measured as the ratio of emission intensity for 340 nm/380 nm illumination (Bottom tracing – gray) for cannulated cremaster arterioles at 20 cm H_2O. Heavy solid line represents the time of exposure to 10 mM caffeine as indicated.

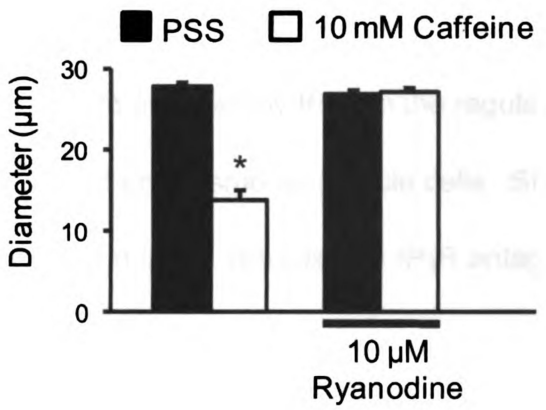

Figure 17. Caffeine-induced constriction of arterioles is blocked by ryanodine

Data are mean diameters ± SE (n = 7) of arterioles pressurized to 20 cm H_2O before (PSS) and at the peak of the constriction induced by caffeine (10 mM), in the absence or presence of ryanodine (10 µM) as indicated. * = significantly different from diameter in PSS, $p < 0.05$.

Role of IP_3 receptors and phospholipase C in feed arteries:

We next investigated the role played by IP_3R in the regulation of Ca^{2+} signals and myogenic tone in feed artery smooth muscle cells. Similar to the effects of ryanodine on Ca^{2+} waves in these vessels, the IP_3R antagonist, xestospongin D (5 μM) nearly abolished the occurrence of Ca^{2+} waves and significantly decreased the amplitude and frequency of what few waves remained (**Figure 18A**). Similar results were obtained using 2-APB (100 μM) another IP_3R antagonist (**Figure 18E**). Consistent with a role for IP_3 and IP_3R in the mechanisms underlying Ca^{2+} waves, we found that an inhibitor of phospholipase C (PLC), U73122 (10 μM), also greatly attenuated the occurrence, amplitude and frequency of Ca^{2+} waves in feed artery smooth muscle cells (**Figure 19**). The inactive analog of this compound (U73343, 10 μM) was without effect (data not shown, $p > 0.05$). However, in distinct contrast to the effects of ryanodine on Ca^{2+} sparks, neither the IP_3R antagonists (xestospongin D or 2-APB) nor the PLC inhibitor (U73122) had any effect on the occurrence, amplitude or frequency of Ca^{2+} sparks in feed artery smooth muscle cells (**Figure 18B**, **Figure 18F** and **Figure 19B**). Furthermore, in contrast to the effects of ryanodine on global Ca^{2+} and diameter in feed arteries, xestospongin D, 2-APB or U73122 each reduced global Ca^{2+} signals and dilated the feed arteries (**Figure 18C-D**, **Figure 18G-H** and **Figure 19C-D**). The dramatic effects of the IP_3R antagonists in feed arteries

indicates that unlike RyR, IP_3R are not involved in the negative feedback regulation of myogenic tone in these small arteries.

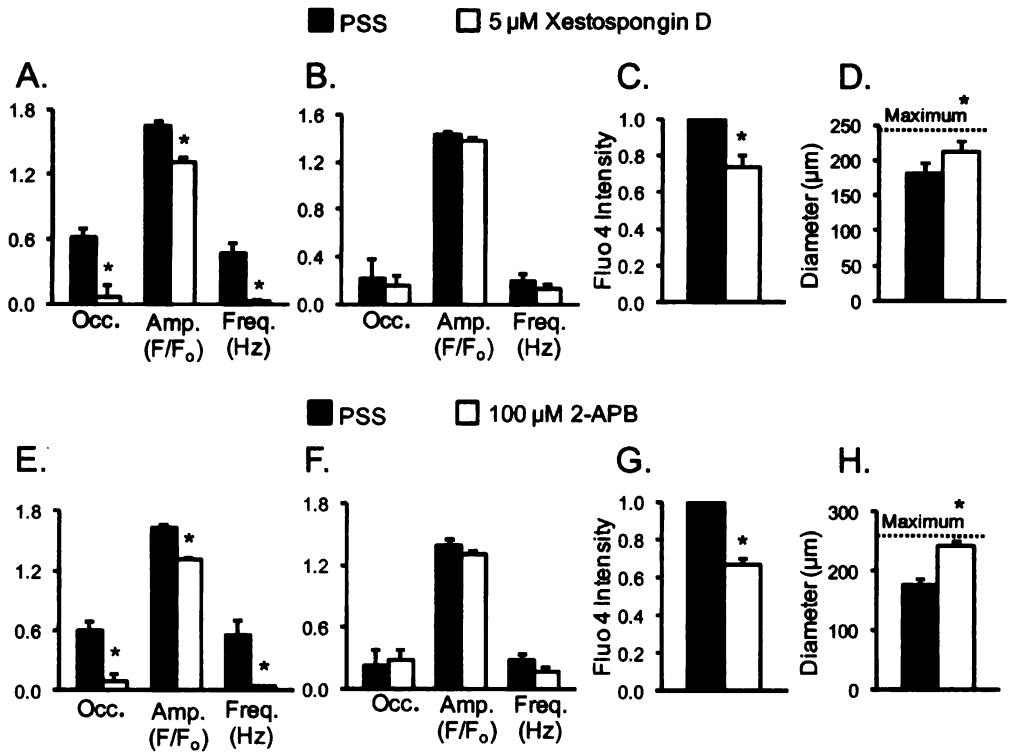

Figure 18. IP_3 receptors contribute to Ca^{2+} waves and myogenic tone, but not Ca^{2+} sparks in cremaster feed arteries

Data are: (A) means ± 95% confidence intervals for occurrence (Occ.) of Ca^{2+} waves; means ± SE for amplitude (Amp.), and frequency (Freq.) of Ca^{2+} waves; (B) occurrence, amplitude and frequency of Ca^{2+} sparks as in (A); (C) Global Fluo 4 intensity, an index of global intracellular Ca^{2+}; and (D) diameter, in the absence (PSS) and presence of the IP_3 receptor antagonist, xestospongin D (5 µM) as indicated. Panels E-H as in A-D but in the absence or presence of 2-aminoethoxydiphenyl borate (2-APB, 100 µM). * = significantly different from value in PSS, $p < 0.05$.

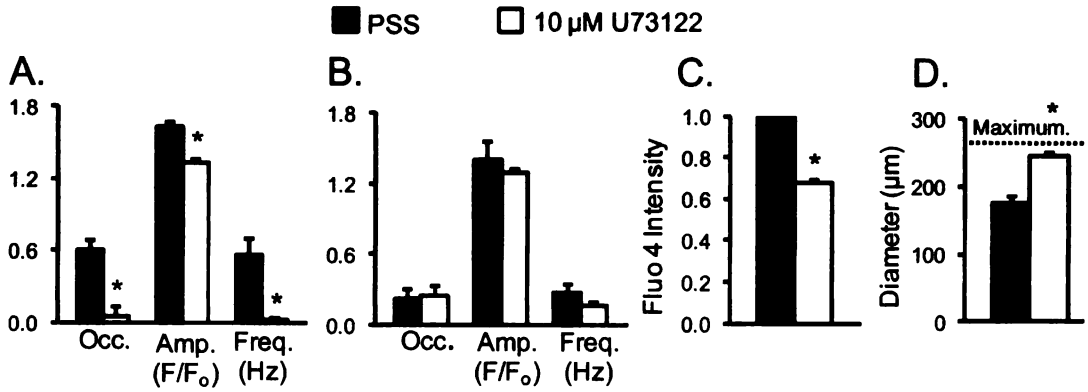

Figure 19. Phospholipase C contributes to Ca^{2+} waves and myogenic tone, but not Ca^{2+} sparks in cremaster feed arteries

Data are: (A) means ± 95% confidence intervals for occurrence (Occ.) of Ca^{2+} waves; means ± SE for amplitude (Amp.), and frequency (Freq.) of Ca^{2+} waves; (B) occurrence, amplitude and frequency of Ca^{2+} sparks as in (A); (C) Global Fluo 4 intensity, an index of global intracellular Ca^{2+}; and (D) diameter, in the absence (PSS) and presence of the phospholipase C inhibitor, U78122 (10 µM) as indicated. * = significantly different from value in PSS, $p < 0.05$.

Role of IP_3 receptors in arteriolar smooth muscle

Similar to our observations in feed arteries, we found that antagonists of IP_3R (xestospongin D or 2-APB) and an inhibitor of PLC (U73122) abolished the occurrence of Ca^{2+} waves in HCA and significantly decreased the amplitude and frequency of any remaining waves (**Figure 20A**, **Figure 20D** and **Figure 21A**). As was observed in feed arteries, these antagonists also dilated the arterioles and reduced global Ca^{2+} levels (**Figure 20B-C**, **Figure 21B-C**). To rule out nonspecific effects of U73122, we also tested the effects of the constriction induced by the VGCC agonist, BayK 8644 (5 nM). Alone, 5 nM Bay K constricted arterioles 20.9 +/- 2.6 um. The constriction was unchanged in the presence of 10 μM U73122 (25.6 +/- 2.1 n = 3, $p > 0.05$). Thus, U73122 did not inhibit the ability of the smooth muscle to contract.

Role of intraluminal pressure on Ca^{2+} events in hamster cremaster feed arteres and arterioles.

To rule out the possibility that 80 cm H_2O may not be a physiologically equivalent pressure between HCA and HFA, we documented the active and passive diameters of the vessels in PSS and 0 Ca^{2+}-PSS at 20, 40, 80 and 120 cm H_2O (**Figure 22**) Each pressure produced a similar amount of myogenic tone between HCA and HFA, and 80 cm H_2O generated the largest amount of myogenic tone in both vessel types (**Figure 22**). We then repeated the experiments in Fluo 4-loaded HCA and HFA to determine the effect of the same

pressures on the occurrence, amplitude and frequency of Ca^{2+} waves and sparks (**Figure 23-25**). In both HFA (**Figure 23**) and HCA (**Figure 24**), increased pressure increased the occurrence (proportion of cells which display at least one wave per recording period), and frequency of waves, while Ca^{2+} amplitude was unaffected by changes in intraluminal pressure. For Ca^{2+} sparks measured in HFA, occurrence, amplitude and frequency were all unchanged by the pressure changes (**Figure 25**).

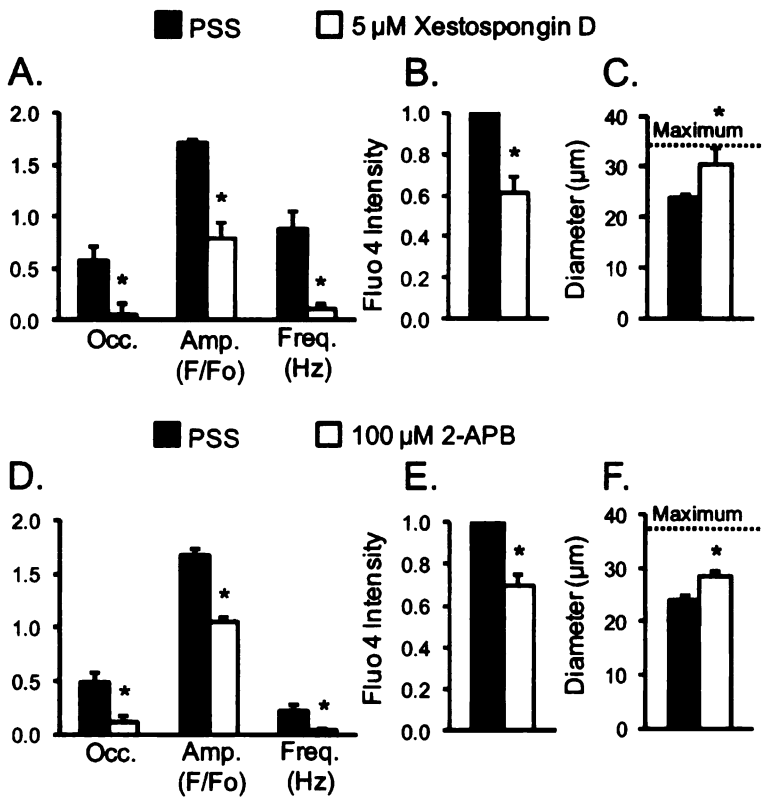

Figure 20. IP_3 receptors contribute to Ca^{2+} waves and myogenic tone in cremaster arterioles

Data are: (A) means ± 95% confidence intervals for occurrence (Occ.) of Ca^{2+} waves; means ± SE for amplitude (Amp.), and frequency (Freq.) of Ca^{2+} waves; (C) Global Fluo 4 intensity, an index of global intracellular Ca^{2+}; and (D) diameter, in the absence (PSS) and presence of the IP_3 receptor antagonist, xestospongin D (5 μM) as indicated. Panels D-F as in A-C but in the absence or presence of 2-aminoethoxydiphenyl borate (2-APB, 100 μM). * = significantly different from value in PSS, $p < 0.05$.

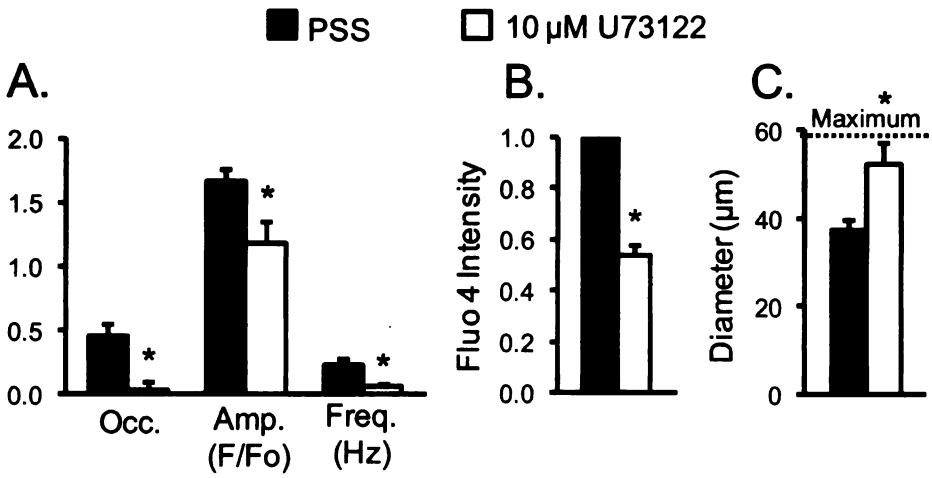

Figure 21. Phospholipase C contributes to Ca^{2+} waves and myogenic tone in cremaster arterioles.

Data are means ± 95% confidence intervals for: (A) occurrence (Occ.), means ± SE for amplitude amplitude (Amp.), and frequency (Freq.) of Ca^{2+} waves; (B) Global Fluo 4 intensity, an index of global intracellular Ca^{2+}; and (C) diameter, in the absence (PSS) and presence of the phospholipase C inhibitor, U73122 (10 µM) as indicated. * = significantly different from value in PSS, $p < 0.05$.

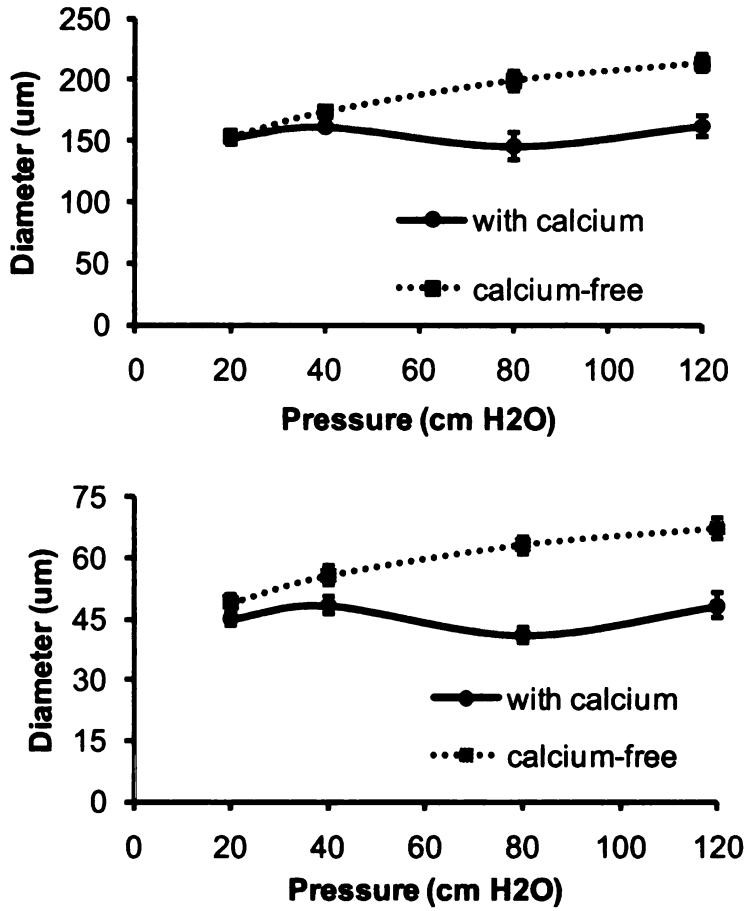

Figure 22. Effects of pressure on myogenic tone in cremaster feed arteries and arterioles.

Data are mean steady-state diameters ± SE (n = 3) for HFA (top panel) and HCA (bottom panel) pressurized to 20, 40, 80 and 120 cm H_2O in PSS with active tone (solid lines) and passive diameters in Ca^{2+}-free PSS (dashed lines).

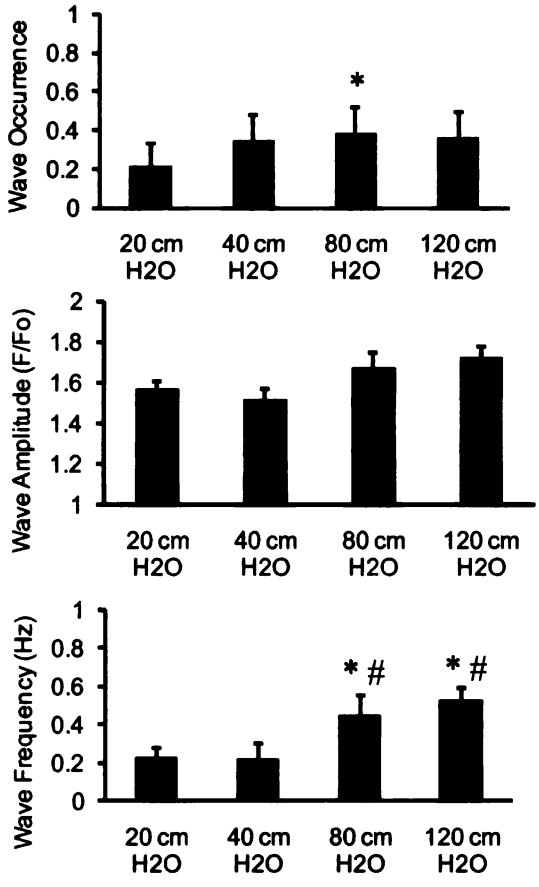

Figure 23. Effect of intraluminal pressure on Ca^{2+} wave properties in feed arteries.

(Top panel) Data are means ± 95% confidence intervals for the occurrence of Ca^{2+} waves in HFA; (Center panel) Data are means ± SE for Ca^{2+} wave amplitudes; (Bottom panel) Data are means ± SE for Ca^{2+} wave frequency. (n = 3 vessels). * = $p < 0.05$ compared to 20 cm H_2O. # = $p < 0.05$ compared to 40 cm H_2O.

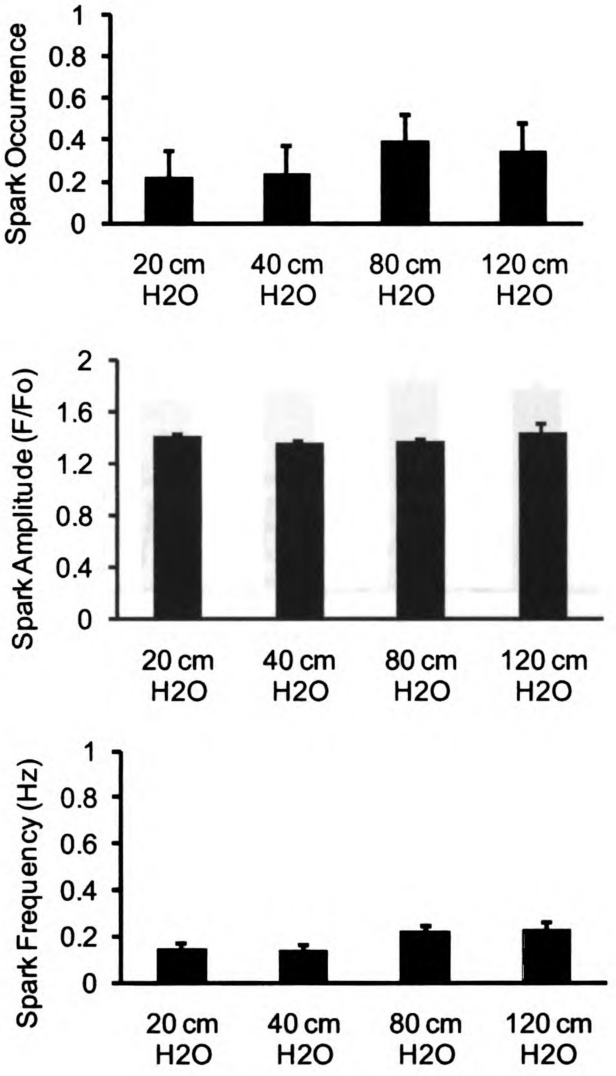

Figure 24. Effect of intraluminal pressure on Ca^{2+} spark properties in feed arteries

(Top panel) Data are means ± 95% confidence intervals for the occurrence of Ca^{2+} sparks in HFA; (Center panel) Data are means ± SE for Ca^{2+} spark amplitudes; (Bottom panel) Data are means ± SE for Ca^{2+} spark frequency. (n = 3 vessels, $p > 0.05$ for all values).

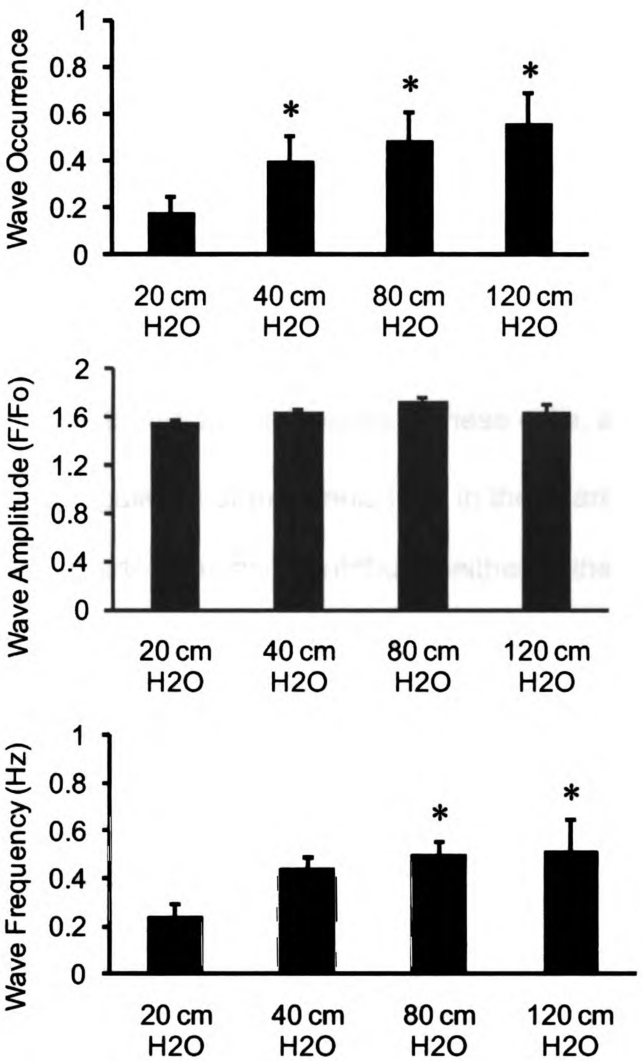

Figure 25. Effect of intraluminal pressure on Ca^{2+} wave properties in cremaster arterioles

(Top panel) Data are means ± 95% confidence intervals for the occurrence of Ca^{2+} waves; (Center panel) Data are means ± SE for Ca^{2+} wave amplitudes; (Bottom panel) Data are means ± SE for Ca^{2+} wave frequency. (n = 3 vessels). * = $p < 0.05$ compared to 20 cm H_2O.

Discussion:

Our studies highlight that significant differences exist in the role played by RyR in regulating both subsarcolemmal Ca^{2+}signals and myogenic tone in feed arteries and their downstream arterioles, and show that RyR and IP_3R serve different roles in regulating myogenic tone. While RyR underlie Ca^{2+} sparks in feed artery smooth muscle cells, contribute to Ca^{2+} waves in these cells, and participate in the negative feedback regulation of myogenic tone in these arteries, RyR appear to be silent in cremaster arterioles and contribute neither to the regulation of smooth muscle Ca^{2+} signals nor myogenic tone in these microvessels. In contrast, IP_3 receptors importantly contribute to Ca^{2+} waves and myogenic tone, likely through a positive feedback mechanism (see below), in both feed arteries and their downstream arterioles.

In feed arteries, we found that ryanodine (10 μM) inhibited Ca^{2+} sparks and Ca^{2+} waves, led to an elevation in global Ca^{2+} and produced vasoconstriction. These data are consistent with a number of prior studies and further support the hypothesis that RyR, likely through their functional coupling to BK_{Ca} channels, participate in the negative feedback regulation of myogenic tone in resistance arteries (96, 139, 155, 202). Consistent with this hypothesis, we found that ryanodine-induced constriction of feed arteries was eliminated in the presence of the BK_{Ca} channel blockers, TEA (1 mM) or paxilline (100 nM).

Our finding that ryanodine also inhibits Ca^{2+} waves supports prior studies in several smooth muscles (99, 118, 130) including retinal arteriolar smooth muscle cells (265) where RyR also contribute to Ca^{2+} waves, likely through CICR. Our studies differ from reports in renal afferent arterioles where ryanodine dilates the arterioles and reduces agonist-induced vasoconstriction (11). These data support our contention that there is significant regional heterogeneity in the function of RyR in vascular smooth muscle cells.

In contrast to our findings in the feed arteries, we were unable to detect Ca^{2+} sparks in cremaster arterioles using identical methods. Supporting these observations, we found that the RyR antagonist, ryanodine (10-50 μM), had no effect on Ca^{2+} wave dynamics, global intracellular Ca^{2+}, myogenic tone or constriction induced by the BK_{Ca} channel blockers, TEA (1 mM) or paxilline (100 nM) in pressurized second-order cremaster arterioles. These data suggest that RyR do not participate in Ca^{2+} signaling underlying myogenic tone in second-order skeletal muscle arterioles, at least under the conditions of our experiments. Our findings are in agreement with recent studies on smooth muscle cells isolated from first-order rat cremasteric arterioles by Yang et al. (291), who also failed to detect Ca^{2+} sparks in their experiments, and recent observations in precapillary arterioles in ureter and vas deferens (30). However, in contrast to the study by Yang et al. (291), who found that ryanodine significantly constricted first-order rat cremaster arterioles studied via pressure myography, we found that

ryanodine had no significant effect on diameter or intracellular Ca^{2+} signals in second-order hamster cremaster arterioles. This difference between arteriolar branch-order may mean that first-order arterioles are transitional between feed arteries, where we found that ryanodine inhibited Ca^{2+} sparks and waves and produced robust vasoconstriction, and second-order arterioles, where RyR appeared to be silent. We do not think that our data can be explained by a complete lack of RyR or a lack of efficacy of ryanodine in the arterioles. Caffeine produced robust Ca^{2+} transients in arteriolar smooth muscle cells demonstrating the functional presence of RyR. Furthermore, we were able to block the effects of caffeine with ryanodine verifying that the concentration used of this alkaloid effectively inhibited RyR. In addition, a high concentration of ryanodine (50 μM) also was found to have no effect on Ca^{2+} signals or diameter in the arterioles. Thus, our data suggest that RyR play little role in the regulation of basal myogenic tone in second-order arterioles, in contrast to the negative feedback role reported in arterial smooth muscle (138, 155, 202, 295). Our findings are also in contrast to observations made in retinal arterioles, where RyR-based Ca^{2+} sparks previously have been reported (55, 56) and appear to contribute to global calcium signaling (265). Ryanodine receptors also appear to contribute to positive-feedback CICR in renal pre-glomerular arterioles (80, 81). Taken with our results, these data from retinal and renal arterioles support the hypothesis that there are substantial regional differences in the function of RyR in arteriolar smooth muscle cells, as well as differences in RyR function between arterioles and upstream feed arteries.

The lack of effect of ryanodine on Ca^{2+} signals, myogenic tone, and TEA- or paxilline-induced constriction in second-order arterioles also suggests that the source of Ca^{2+} responsible for regulation of BK_{Ca} channels in these vessels is likely different than what has been reported in arterial smooth muscle, where Ca^{2+} sparks importantly control BK_{Ca} channel function and smooth muscle excitability (96, 138, 155, 202). Studies in neurons (18, 101, 252) and coronary smooth muscle (103) have suggested that Ca^{2+} influx through voltage-gated Ca^{2+} channels also may regulate BK_{Ca} channels. Our preliminary studies in cremaster arterioles are consistent with this hypothesis (24). Further studies will be required to test this hypothesis.

Our studies do not illuminate the mechanisms responsible for the differences in function of RyR between vessels. However, prior studies in other smooth muscles have suggested that the pattern of RyR isoform expression can significantly alter the function of RyR (54, 144, 145, 172, 302). Ryanodine receptor isoforms 1 and/or 2 appear essential for Ca^{2+}-spark formation (54, 144), whereas RYR3 (172), or a spliced variant of this isoform (146) may be inhibitory. Preliminary studies in mouse cremaster feed arteries and their downstream arterioles are consistent with our functional studies performed in hamster vessels, and indicate differences in expression of RyR isoforms that could

underlie the functional differences between arteries and arterioles (161). Additional studies will be required to critically test this hypothesis.

We found that smooth muscle cells in pressurized small arteries and their downstream arterioles, which develop similar levels of myogenic tone, consistently displayed Ca^{2+} waves in the absence of added agonist. Our observations are different from those obtained in rat small mesenteric arteries (195) where only 7% of cells generated Ca^{2+} waves during myogenic tone, and recent studies from rat mesenteric and vas deferens arterioles and arteries where Ca^{2+} oscillations were not observed in unpressurized vessels in the absence of vasoconstrictor agonists (30). These data support the notion that there are significant regional differences in mechanisms regulating and underlying Ca^{2+} signaling and myogenic tone. To control for pressure-related differences in the regulation of Ca^{2+} signals, we looked for differences in the properties of HFA and HCA Ca^{2+} signals over a range of different intraluminal pressures and found that the primary pressure used (80 cm H_2O) appears to be physiologically equivalent in these vessels and does not likely play a role in the differences we observed. Similarly, we looked at the synchronicity of Ca^{2+} signals in HFA and HCA. Calcium waves were asynchronous in both vessel types, and therefore the pattern of rhythmicity of the Ca^{2+} signals does not underlie the differences observed between HFA and HCA.

We found that a phospholipase C inhibitor (U73122, 10 μM) and two structurally different IP_3 receptor antagonists (xestospongin D, 5 μM or 2-APB, 100 μM) nearly abolished the occurrence of Ca^{2+} waves, reduced global intracellular Ca^{2+} and inhibited myogenic tone in feed arteries and cremaster arterioles. These data support a large body of evidence implicating phospholipase C in the genesis of myogenic tone (10, 50, 132, 140, 141, 213) and extend a recent report in vas deferens arterioles suggesting a central role for IP_3 receptors in the regulation of agonist-induced arteriolar tone (30). Recent studies suggest that U73122 may act to deplete intracellular Ca^{2+} stores (176). We do not think that such an effect can explain the inhibitory effect of U73122 that we observed on Ca^{2+} waves because this phospholipase C inhibitor had no effect on RyR-based Ca^{2+} sparks in feed arteries. In smooth muscle, RyR and IP_3R appear to access the same pool of Ca^{2+} (190), thus lack of effect of U73122 on Ca^{2+} sparks argues against this agent working by depletion of intracellular Ca^{2+} stores.

Calcium influx through voltage-gated Ca^{2+} channels and other ion channels importantly contributes to myogenic tone (63, 124). Our finding of a major role for the phospholipase C - IP_3 - IP_3R pathway in the regulation of global Ca^{2+} and myogenic tone suggests that IP_3R may play a positive feedback role, likely amplifying Ca^{2+} signals from other sources and contributing to the Ca^{2+}-dependent component of myogenic tone in small arteries and arterioles. In small

arteries, while RyR may contribute to this amplification (as we found that ryanodine inhibited not only Ca^{2+} sparks, but also Ca^{2+} waves in hamster feed arteries), the major function of RyR in the feed arteries appears to be in the negative feedback regulation of myogenic tone, as discussed above. Thus, RyR and IP_3R serve distinct, contrasting roles in the regulation of myogenic tone in feed arteries, whereas only the positive feedback function of IP_3R appeared functional in cremaster arterioles.

Overall, these studies demonstrate that there are important differences in the regulation of both smooth muscle cell Ca^{2+} signals and myogenic tone between feed arteries and their downstream arterioles. The well-documented negative-feedback role played by RyR in the regulation of myogenic tone does not appear to hold true in second order cremaster arterioles. In contrast, PLC and IP_3R appear to function similarly in cremaster feed artery and arteriolar smooth muscle cells. The differences we observed between feed arteries and downstream arterioles caution the extrapolation of data gathered in arteries to arterioles and vice versa, even in closely related vasculatures. These differences in mechanisms also point to potential, novel therapeutic targets to modulate the tone of arterioles, for example, independent from upstream resistance arteries. Such microvessel-specific therapeutic targeting would allow modulation of tissue blood flow and within-organ blood flow distribution potentially without substantial effects on systemic blood pressure and side-effects, like orthostatic hypotension,

which often result from drugs that non-specifically target both resistance arteries and arterioles.

CHAPTER 4: Expression and localization of RyR and IP_3R isoforms underlie differences in their role in Ca^{2+} oscillations and myogenic tone

Rationale

In Chapter 3, we showed that there are important functional differences in the role played by RyR in hamster cremaster feed arteries and their downstream arterioles in Ca^{2+} signaling and myogenic tone. While RyR are important regulators of Ca^{2+} signaling and tone in HFA, they appear to be silent in HCA, despite the presence of functional receptors. We propose here that expression and distribution of ryanodine receptors (RyR) may underlie their variable roles in different types of vascular smooth muscle.

Ryanodine receptors exist in 3 different isoforms (RyR1-3), all of which can be expressed in vascular smooth muscle (54, 113, 206). Several studies have looked at the gene expression of RyR isoforms in blood vessels (54, 113, 172, 206, 290, 302). Zheng et al. (302) and Yang et al (290) found expression of all 3 subtypes in mouse pulmonary and mesenteric arteries, but Yang showed RyR2 expression 15-20 times greater than the other subtypes, suggesting its importance in RyR Ca^{2+} release in pulmonary artery smooth muscle. Coussin et al (54) and Lohn et al. (172) also showed expression of all 3 isoforms in rat portal vein, and mouse cerebral artery, respectively, but determined functionally that only RyR1 and RyR2 are important to the production of Ca^{2+} sparks, which

importantly activate BK_{Ca} channels to regulate tone in those vessels (202). Lohn also suggested that RyR3 may actually be inhibitory to Ca^{2+} sparks (172). The RyR subtype distribution in microvascular smooth muscle remains unstudied.

The purpose of the present study was to (1) define the role of RyR in cremaster feed arteries (MFA) and cremaster arterioles (MCA) in C57BL/6 mice in the regulation of Ca^{2+} signaling and myogenic tone in comparison to HFA and HCA and (2) to test the hypothesis that it is the expression of RyR isoform genes and the location of those proteins within the cell that determines the functional role of RyR in vascular smooth muscle cells.

Results:

Role of RyR in mouse cremaster feed arteries and arterioles

Isolated cannulated mouse feed arteries (MFA) loaded with Fluo 4 dye displayed both Ca^{2+} sparks and Ca^{2+} waves (**Figure 26**), similar to our findings in HFA from Chapter 3. Sparks occurred in 39 ± 2% of cells within each vessel, and they had average amplitude of 1.62 ± 0.15 F/Fo and average frequency of 0.20 ± 0.08 Hz. Waves occurred in 41 ± 2% of cells, and they had an average amplitude and frequency of 1.85 ± 0.17 F/Fo and 0.52 ± 0.11 Hz, respectively (**Figure 26A-B, Table 7**). In the presence of the RyR antagoninst ryanodine (10 μM), the occurrence, amplitude and frequency of both Ca^{2+} sparks and Ca^{2+} waves were significantly decreased ($p < 0.05$, $n = 5$) (**Figure 26A-B**). Ryanodine also led to

a significant increase in intracellular Ca^{2+} and vascoconstriction in MFA (**Figure 26C-D**). These data suggest that, as in HFA and other resistance arteries, RyR participate in the regulation of subsarcolemmal Ca^{2+} signals and myogenic tone in MFA.

Table 7. Properties of Ca^{2+} sparks and waves in mouse cremaster feed arteries and arterioles

Vessel type	Ca^{2+} signal	Cross-section length (μm)	FWHM (μm)	Frequency (Hz)	Amplitude (F/F_o)	FDHM (s)
Feed arteries	sparks	55.62 ± 2.01	3.10 ± 0.25	0.20 ± 0.08	1.62 ± 0.15	0.33 ± 0.07
Feed arteries	waves	52.07 ± 1.84	33.73 ± 2.06*	0.52 ± 0.11*	1.85 ± 0.17*	0.83 ± 0.13*
Arterioles	waves	22.25 ± 1.33 †	16.7 ± 1.59 †	0.38 ± 0.03*	1.93 ± 0.02*	0.74 ± 0.11*

FWHM = full-width, half-maximum, FDHM = full-duration, half-maximum, Values are means ± SE, * = $p < 0.05$ compared to feed artery Ca^{2+} sparks, † = $p < 0.05$ compared to feed artery.

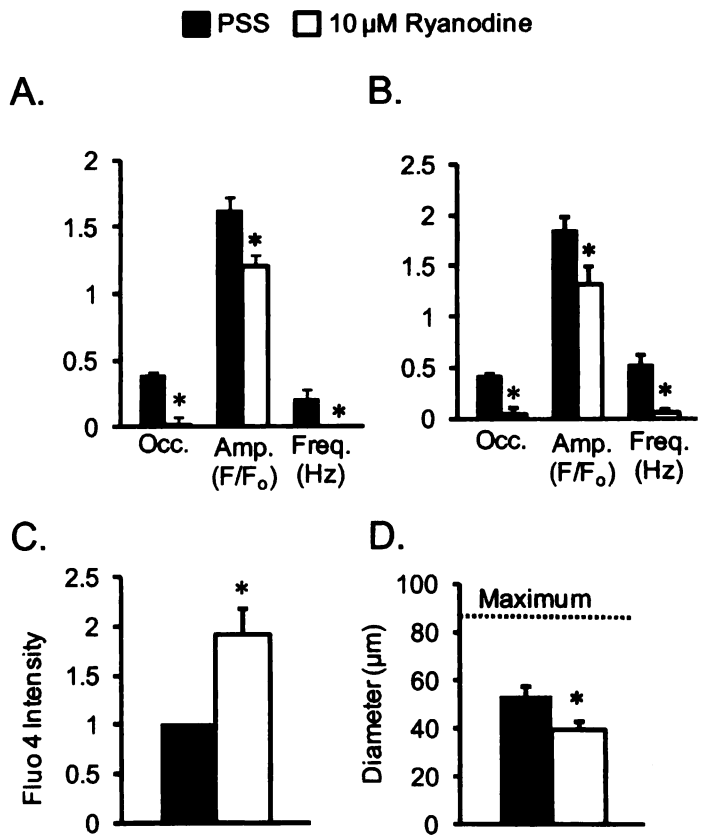

Figure 26. Ryanodine receptors modulate Ca^{2+} signals and myogenic tone in mouse feed arteries

Data are: (A) means ± 95% confidence intervals for occurrence (Occ.) of Ca^{2+} sparks, and means ± SE for amplitude (Amp.), and frequency (Freq.) of Ca^{2+} waves; (B) occurrence, amplitude and frequency of Ca^{2+} waves as in (A); (C) means ± SE for global Fluo 4 intensity, an index of global intracellular Ca^{2+}; and (D) diameter, in the absence (PSS) and presence of the RyR antagonist, ryanodine (10 μM) as indicated. * = significantly different from value in PSS, $p < 0.05$, $n = 5$.

Like HCA, but in contrast to HFA and MFA, mouse cremaster arteriolar (MCA) smooth muscle exhibited Ca^{2+} waves, but not Ca^{2+} sparks. Sparks did not occur in MCA (0 of 59 cells from 3 arterioles), and waves had occurrences of 46 ± 7%, amplitudes of 1.93 ± 0.02 F/Fo and a frequency of 0.38 ± 0.03 Hz (**Figure 27A).** As we observed in HCA, ryanodine (10 μM), had no effect on the occurrence, amplitude or frequency of Ca^{2+} waves (**Figure 27A**, $p > 0.05$, $n = 3$ arterioles). Ryanodine also did not constrict MCA (**Figure 27C**), or alter global intracellular Ca^{2+} within the vascular smooth muscle layer of MCA (**Figure 27B**). These data suggest that RyR are not involved in the regulation of Ca^{2+} signals or myogenic tone in MCA We also verified the proposed coupling of RyR and BK_{Ca} channels in MFA, and their lack of coupling in MCA. Identical to our results in HFA and HCA, in the presence of TEA (1 mM), ryanodine-induced constricition was inhibited ($n = 5$, $p < 0.05$), whereas ryanodine (10 μM) had no effect on TEA-induced constriction in MCA ($n = 5$, $p > 0.05$).

Role of IP_3R in mouse cremaster feed arteries and arterioles

Next, we used IP_3R inhibitors to pharmacologically determine the role of IP_3R in both MFA and MCA. In cannulated, Fluo 4-loaded MFA, the IP_3R antagonist xestospongin D (5 μM) significantly decreased the occurrence, amplitude and frequency of Ca^{2+} waves, but it did not alter the occurrence or properties of Ca^{2+} sparks in those smooth muscle cells (**Figure 28A-B**). Consistent with its effects

on Ca^{2+} waves, xestospongin decreased intracellular Ca^{2+} (**Figure 28C**) and significantly dilated HFA (**Figure 28D**). Repetition of these experiments with 2-APB, another IP_3R antagonist, yielded similar results: inhibition of the occurrence of Ca^{2+} waves and attenuation of their frequency and amplitude with no effect on Ca^{2+} sparks (**Figure 29**). Thus, it appears that, similar to HFA, IP_3R play an important role in the occurrence of Ca^{2+} waves and myogenic tone, but not Ca^{2+} sparks.

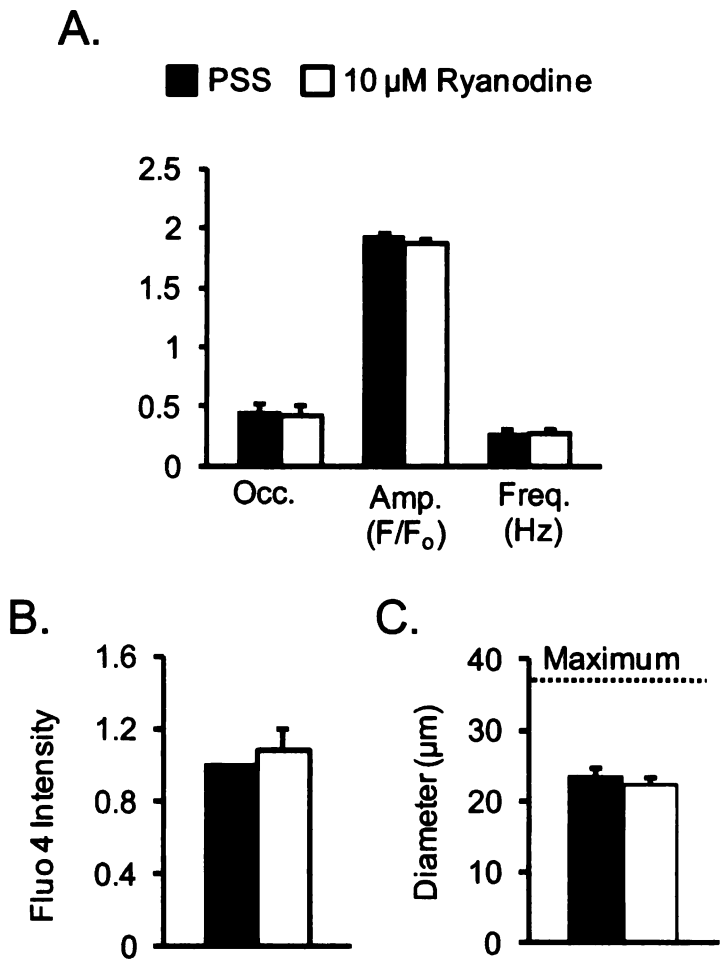

Figure 27. Ryanodine receptors do not modulate Ca^{2+} oscillations and myogenic tone in mouse cremaster arterioles

Data are: (A) means ± 95% confidence intervals for occurrence (Occ.) of Ca^{2+} sparks, and means ± SE for amplitude (Amp.), and frequency (Freq.) of Ca^{2+} waves; (B) means ± SE for global Fluo 4 intensity, an index of global intracellular Ca^{2+}; and (C) diameter, in the absence (PSS) and presence of the RyR antagonist, ryanodine (10 µM) as indicated. * = significantly different from value in PSS, $p < 0.05$, $n = 3$ arterioles.

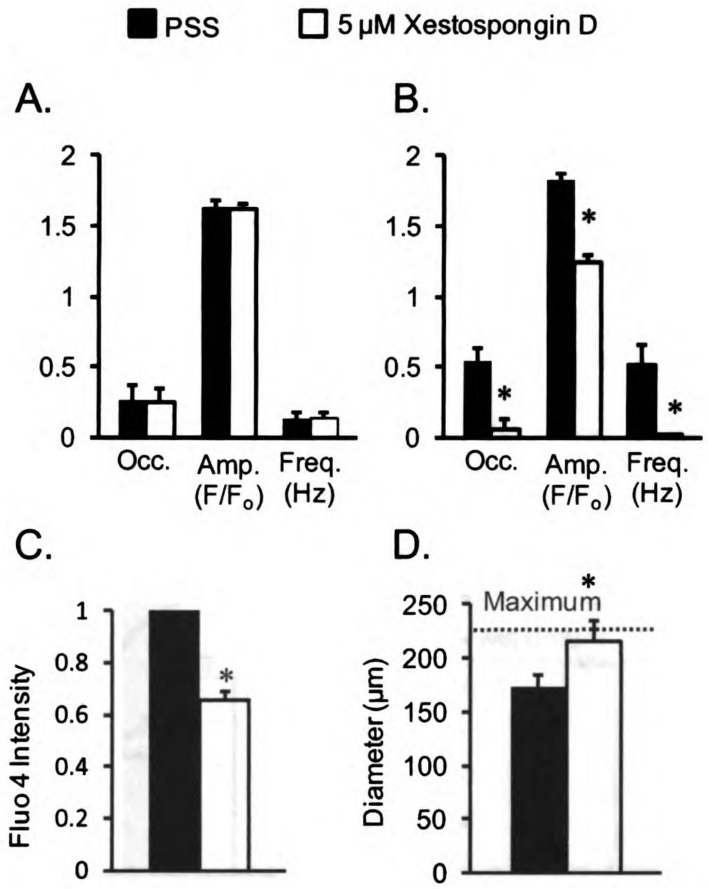

Figure 28. IP_3 receptors regulate Ca^{2+} waves and myogenic tone, but not Ca^{2+} sparks in mouse feed arteries.

Data are: (A) means ± 95% confidence intervals for occurrence (Occ.) of Ca^{2+} sparks, and means ± SE for amplitude (Amp.), and frequency (Freq.) of Ca^{2+} waves; (B) occurrence, amplitude and frequency of Ca^{2+} waves as in (A); (C) means ± SE for global Fluo 4 intensity, an index of global intracellular Ca^{2+}; and (D) diameter, in the absence (PSS) and presence of the RyR antagonist, ryanodine (10 µM) as indicated. * = significantly different from value in PSS, $p < 0.05$, $n = 3$.

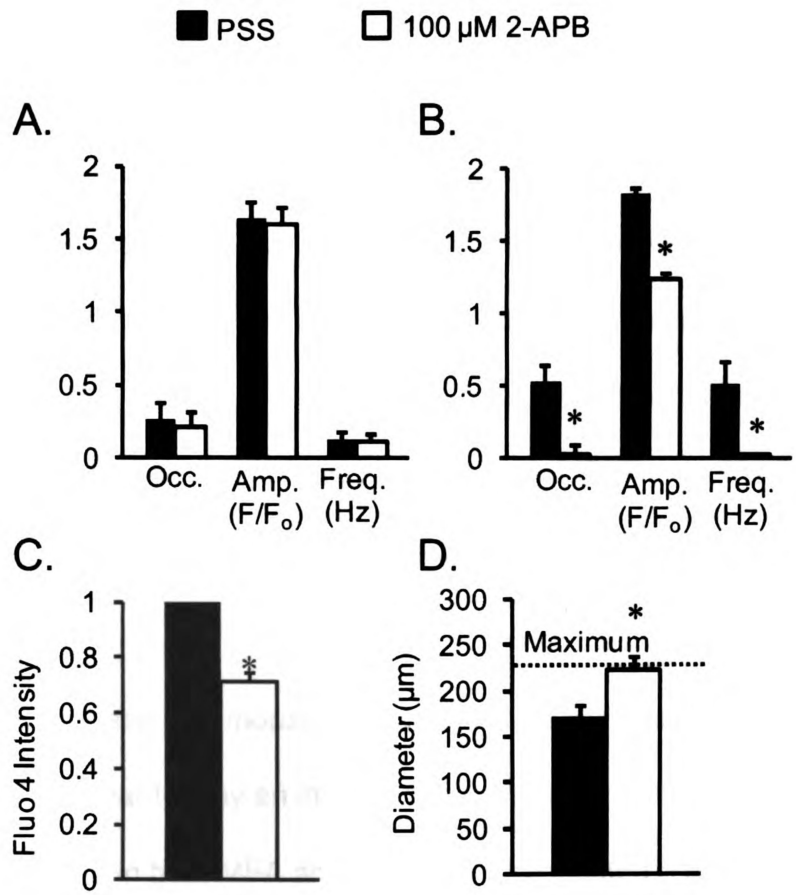

Figure 29. 2-APB inhibits Ca^{2+} waves but not Ca^{2+} sparks in mouse feed arteries

Data are: (A) means ± 95% confidence intervals for occurrence (Occ.) of Ca^{2+} sparks, and means ± SE for amplitude (Amp.), and frequency (Freq.) of Ca^{2+} waves; (B) occurrence, amplitude and frequency of Ca^{2+} waves as in (A); (C) means ± SE for global Fluo 4 intensity, an index of global intracellular Ca^{2+}; and (D) diameter, in the absence (PSS) and presence of the RyR antagonist, ryanodine (10 µM) as indicated. * = significantly different from value in PSS, $p < 0.05$, $n = 3$.

Although MCA do not produce Ca^{2+} sparks, the effect of xestospongin D on Ca^{2+} waves in these vessels is the same as what we observed for HFA, MFA and HCA. Application of xestospongin (5 μM) to cannulated, Fluo 4-loaded MCA decreased the occurrence, amplitude and frequency of waves in those vessels (**Figure 30A**). It also decreased global Ca^{2+} and caused significant vasodilation of the arterioles (**Figure 30B-C**). As with MFA, we repeated the experiments using 2-APB and saw similar results, suggesting that IP_3R modulate both Ca^{2+} waves and myogenic tone in MCA (**Figure 31**).

Role of phospholipase C in mouse cremaster feed arteries and arterioles

Because IP_3R appear to play an important role in the regulation of Ca^{2+} waves and myogenic tone in both MFA and MCA, we investigated a potential role for the upstream phospholipase C (PLC) in these signaling pathways. In cannulated, Fluo 4-loaded MFA, the PLC inhibitor U73122 (10 μM) affected myogenic tone and Ca^{2+} oscillations the same as blocking IP_3R directly with xestospongin or 2-APB. U73122 did not alter the occurrence or properties of Ca^{2+} sparks (**Figure 32A**), but did significantly decrease the occurrence, amplitude and frequency of Ca^{2+} waves (**Figure 32B**) as well as reducing global Ca^{2+} and inhibiting myogenic tone (**Figure 32C-D**) in the MFA. U73122 had similar effects in MCA: it decreased the occurrence, amplitude an frequency of Ca^{2+} waves, decreased global Ca^{2+} and dilated the arterioles (**Figure 33**). These data suggest that PLC-

related activation of IP_3R is important in the regulation of Ca^{2+} waves and myogenic tone.

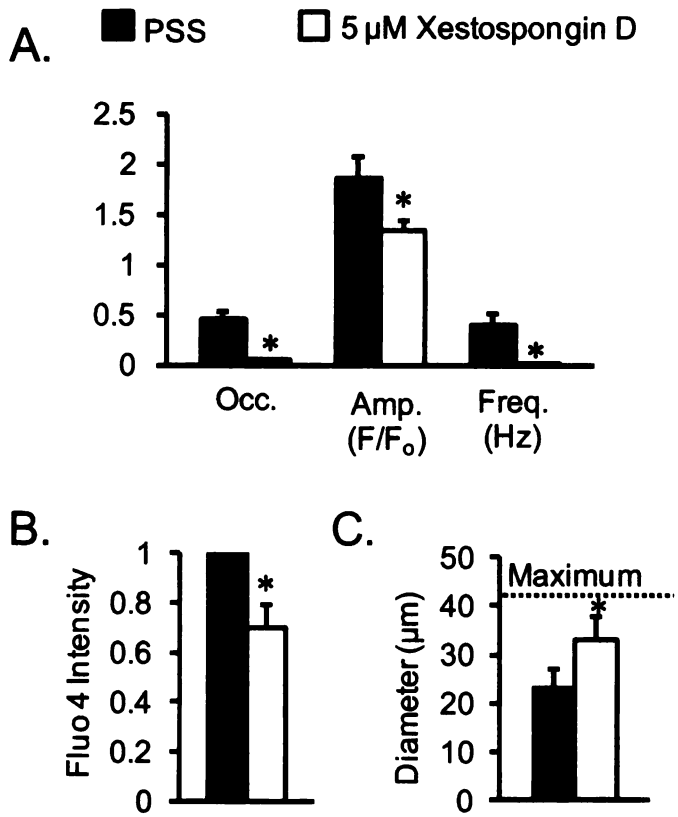

Figure 30. IP_3 receptors regulate Ca^{2+} waves and myogenic tone in mouse cremaster arterioles.

Data are: (A) means ± 95% confidence intervals for occurrence (Occ.) of Ca^{2+} waves, and means ± SE for amplitude (Amp.), and frequency (Freq.) of Ca^{2+} waves; (B) means ± SE for global Fluo 4 intensity, an index of global intracellular Ca^{2+}; and (C) diameter, in the absence (PSS) and presence of the RyR antagonist, ryanodine (10 μM) as indicated. * = significantly different from value in PSS, $p < 0.05$, $n = 3$ arterioles.

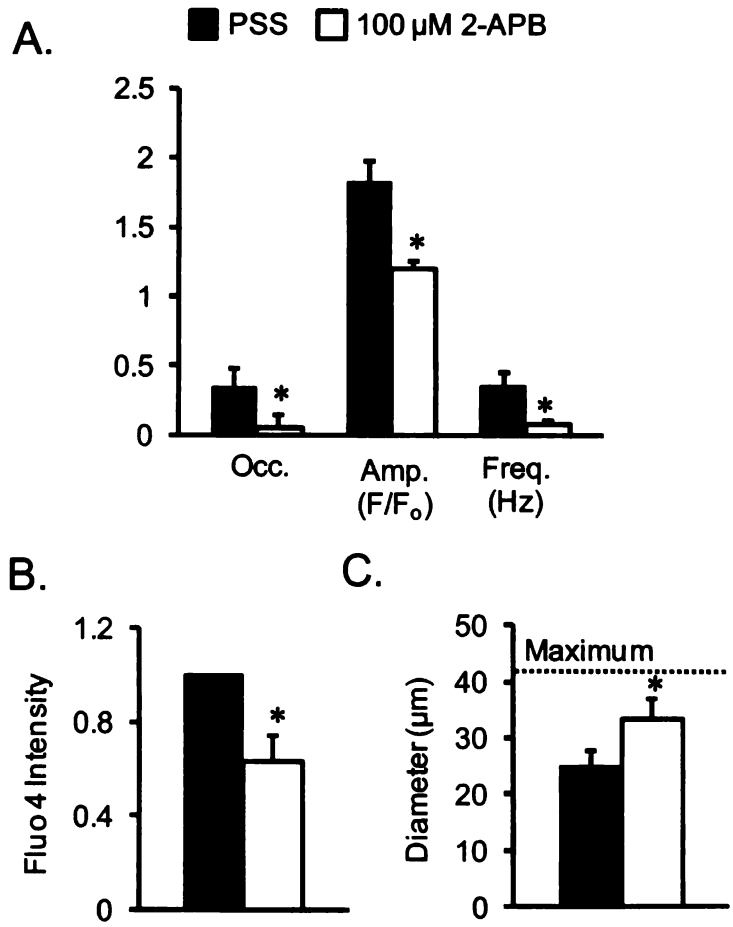

Figure 31. 2-APB inhibits Ca^{2+} waves and myogenic tone in mouse cremaster arterioles

Data are: (A) means ± 95% confidence intervals for occurrence (Occ.) of Ca^{2+} waves, and means ± SE for amplitude (Amp.), and frequency (Freq.) of Ca^{2+} waves; (B) means ± SE for global Fluo 4 intensity, an index of global intracellular Ca^{2+}; and (C) diameter, in the absence (PSS) and presence of the IP_3R antagonist, 2-APB (100 µM) as indicated. * = significantly different from value in PSS, $p < 0.05$, $n = 3$ arterioles.

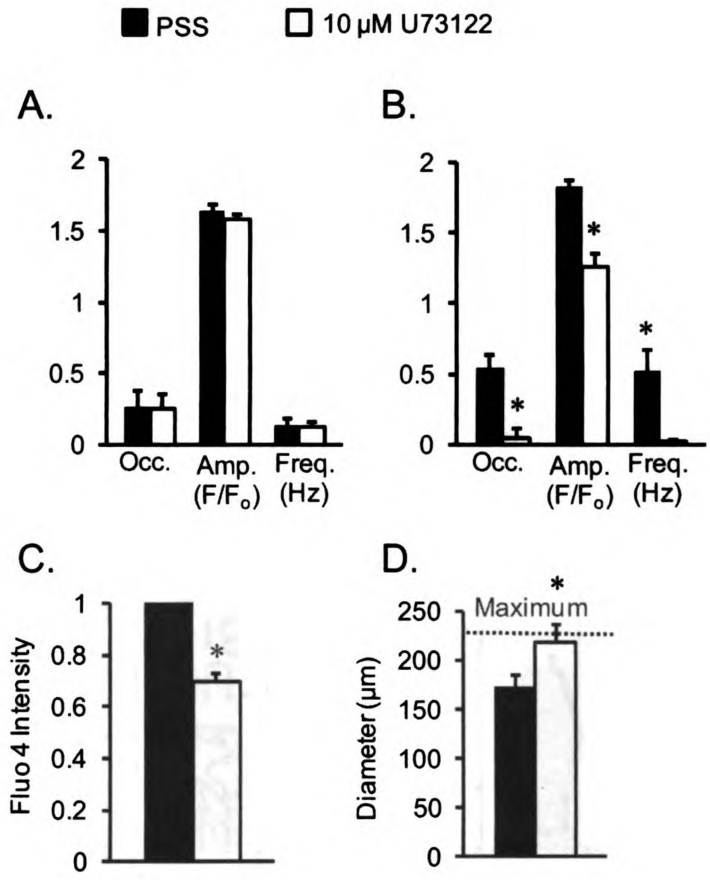

Figure 32. Phospholipsae C regulates waves and myogenic tone in mouse feed arteries

Data are: (A) means ± 95% confidence intervals for occurrence (Occ.) of Ca^{2+} sparks, and means ± SE for amplitude (Amp.), and frequency (Freq.) of Ca^{2+} waves; (B) occurrence, amplitude and frequency of Ca^{2+} waves as in (A); (C) means ± SE for global Fluo 4 intensity, an index of global intracellular Ca^{2+}; and (D) diameter, in the absence (PSS) and presence of the RyR antagonist, ryanodine (10 µM) as indicated. * = significantly different from value in PSS, $p < 0.05$, $n = 3$.

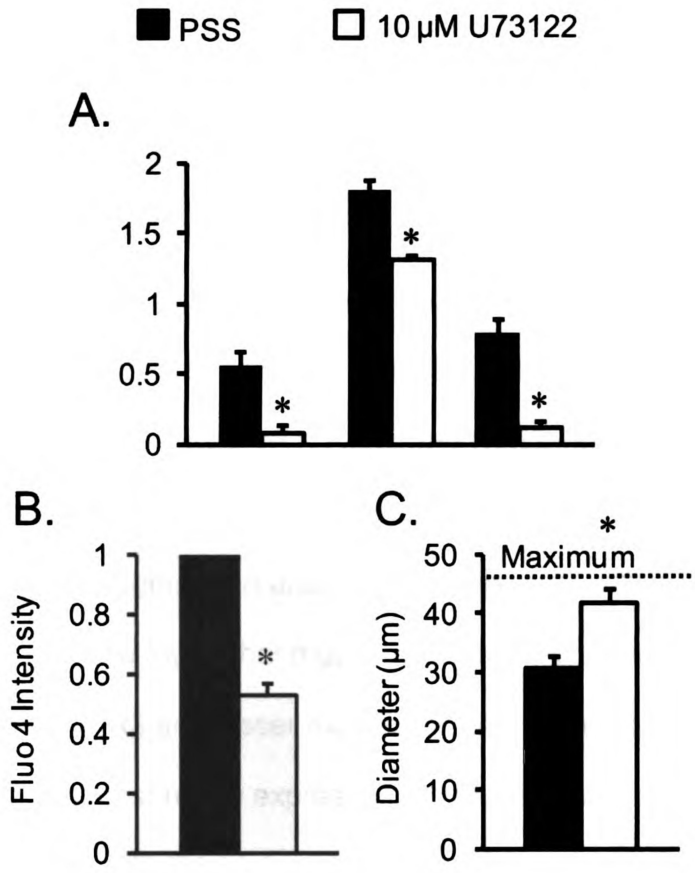

Figure 33. Phospholipase C regulates Ca^{2+} waves and myogenic tone in mouse cremaster arterioles

Data are: (A) means ± 95% confidence intervals for occurrence (Occ.) of Ca^{2+} waves, and means ± SE for amplitude (Amp.), and frequency (Freq.) of Ca^{2+} waves; (B) means ± SE for global Fluo 4 intensity, an index of global intracellular Ca^{2+}; and (C) diameter, in the absence (PSS) and presence of the RyR antagonist, ryanodine (10 µM) as indicated. * = significantly different from value in PSS, $p < 0.05$, $n = 3$ arterioles.

Expression of RyR isoform mRNA in smooth muscle cells of mouse cremaster feed arteries and arterioles

Because there are important functional differences in the role of RyR between MFA and MCA, we used quantitative real-time PCR to determine the expression of the different RyR isoforms in the smooth muscle cells of these two vessels. We used validated primers for RyR1, RyR2 and RyR3. In preliminary experiments, we verified that the purchased primers identified RyR isoforms in control tissues (diaphragm, heart and brain). Consistent with numerous studies in the literature (85), we found that mouse diaphragm expressed a high level of RyR1, followed by RyR3 and lesser expression of RyR2 (data not shown). In contrast, RyR2 was most highly expressed in mouse heart, followed by RyR3 with little expression of RyR1 (data not shown). Mouse brain expressed all three isoforms (data not shown). These results confirmed the manufacturer's stated specificity of the primers used.

Using samples of 50 smooth muscle cells enzymatically isolated from mouse feed arteries or cremaster arterioles we found no detectable expression of RyR1 (**Figure 34**, n = 8 per group): no signal was detected in preamplified samples even after 40 rounds of PCR. Both RyR2 and RyR3 expression was observed in feed artery and arteriolar smooth muscle cells. In feed artery cells, RyR2 was detected ($C_T < 40$) in 8 of 8 samples, whereas 7 of 8 samples were positive for RyR2 in cremaster cells. Message for the RyR3 isoform was detected in 7 of 8

samples from both feed arteries and arterioles. However, the level of expression of these isoforms displayed significant regional heterogeneity. We found that feed artery smooth muscle cells expressed 2.14 ± 0.33 – fold more RyR2 than did smooth muscle cells from cremaster arterioles (**Figure 34**, $n = 7$, $p < 0.05$). Conversely, feed artery smooth muscle cells expressed only 0.65 ± 0.09-fold as much RyR3 as did cremaster arteriole smooth muscle cells (**Figure 34,** $n = 6$, $p < 0.05$). The ratio of RyR2/RyR3 expression was 3.66 ± 0.40 – fold greater in feed artery cells than in cremaster arteriole smooth muscle cells ($n = 6$, $p < 0.05$). These data suggest that differences in the expression of RyR isoforms between MFA and MCA may underlie the functional differences we observed in the regulation of Ca^{2+} signaling and myogenic tone.

Expression and localization of RyR isoform protein in intact feed arteries and arterioles

Because we found significant differences in the expression of RyR isoform mRNA, we next looked at potential differences in expression and localization of these channels at the protein level using immunoflurescence of intact, pressure-fixed MFA and MCA. Using a confocal laser scanning microscope to look at 2 µm slices through the smooth muscle layer of the vessels we found significant differences in the staining patterns for RyR in MFA compared to MCA. While, the feed arteries had bright, clustered staining (**Figure 35**), arterioles exhibited a dim, diffuse and nonspecific staining (**Figure 36**). A reference line drawn across the smooth muscle cells in Image J was used to generate a plot profile of the

intensity of RyR staining. The coefficients of variation of staining across these lines was significantly different between the vessel types, with MFA smooth muscle cells displaying significantly more variation in staining than MCA confirming the difference in RyR staining (**Figure 39**, $n = 4$, $p < 0.05$). These results support the visual impression that RyR staining in feed artery smooth muscle cells is more clustered and less uniform than staining in cremaster arteriolar smooth muscle cells

Expression and localization of RyR isoform protein in isolated smooth muscle cells from cremaster feed arteries and arterioles

To confirm the finding that there are differences in the staining for RyR between MFA and MCA, we completed another set of immunofluorescence studies looking at RyR expression in single smooth muscle cells isolated from MFA and MCA. These experiments yielded similar results: smooth muscle cells from MFA had bright, variegated staining (**Figure 37**), while cells from MCA had dimmer and more uniform staining patterns (**Figure 38**). Like the whole-vessel IHC studies, analysis of the coefficients of variation of RyR staining showed that isolated smooth muscle cells from MFA had significantly more variable staining than those from MCA (**Figure 39**, $n = 4$, $p < 0.05$), consistent with the variegated appearance of staining in MFA compared to MCA.

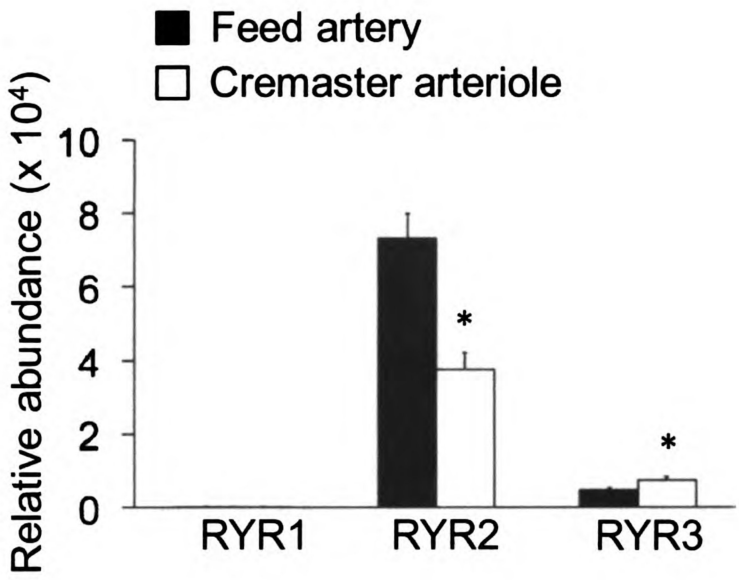

Figure 34. Heterogeneous expression of ryanodine receptor isoform mRNA between mouse cremaster feed artery and arteriolar smooth muscle cells

Data are means ± SE for the relative abundance of RyR isoform mRNA from MFA (black) and MCA (white). The values were calculated by comparing the RyR gene expression to α-smooth muscle actin, the calibrated reference gene. RyR1 was not detectable in either MFA, RyR2 expression was greater in MFA, and RyR3 expression was greater in MCA. (n = 6-8, * = $p < 0.05$ compared to MFA).

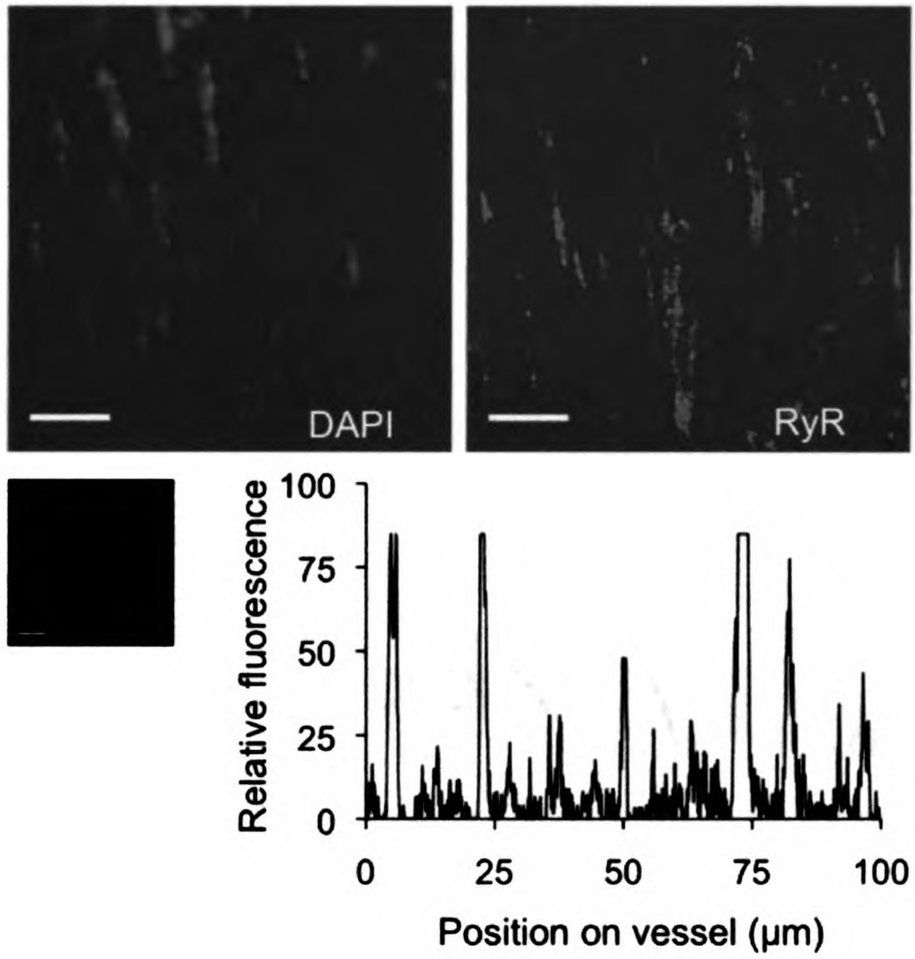

Figure 35. Expression and localization of ryanodine receptors in whole mouse cremaster feed arteries.

The top panels show representative immunohistochemical images of an intact MFA with staining for DAPI nuclear stain (left) and an anti-RyR1/2 antibody (right) within a 2 μm thick confocal slice of the smooth muscle layer. MFA smooth muscle show clustered, variegated staining for RyR. Scale bars are 20 μm. The bottom panels show the quantitation of variation in RyR staining across a reference line.

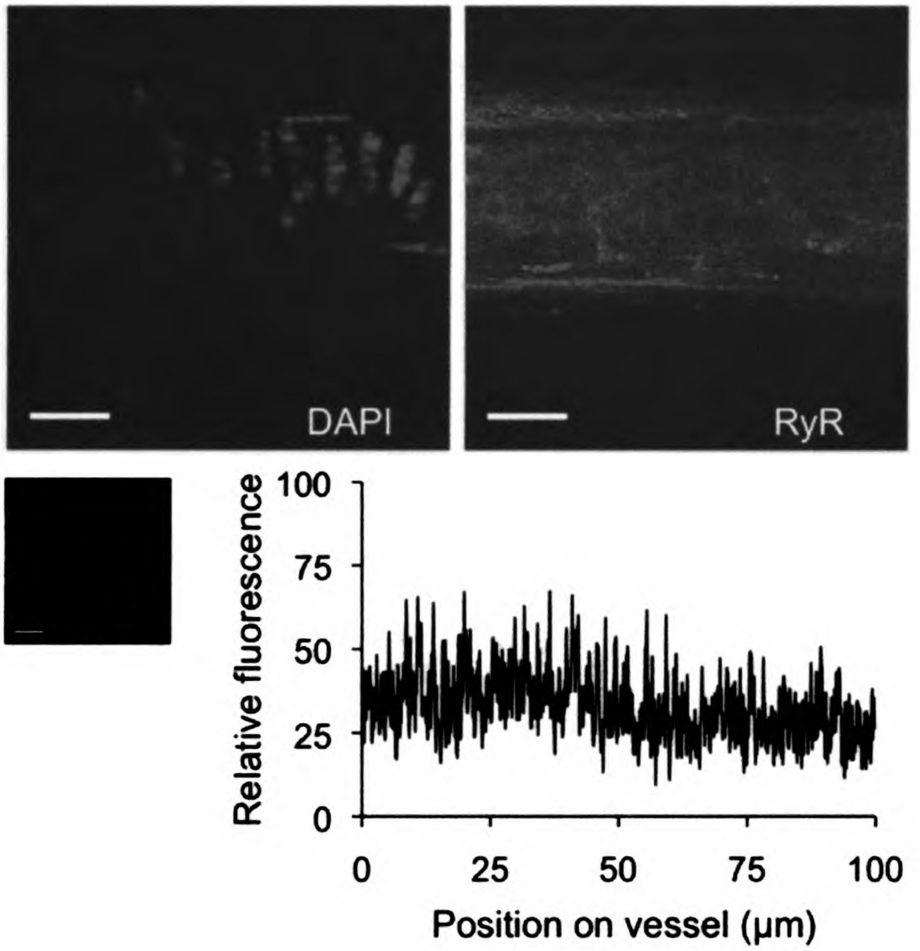

Figure 36. Expression and localization of ryanodine receptors in whole mouse cremaster arterioles.

The top panels show representative immunohistochemical images of an intact MCA with staining for DAPI nuclear stain (left) and an anti-RyR1/2 antibody (right) within a 2 μm thick confocal slice of the smooth muscle layer. MCA smooth muscle show diffuse, nonspecific staining for RyR. Scale bars are 20 μm. The bottom panels show the quantitation of variation in RyR staining across a reference line.

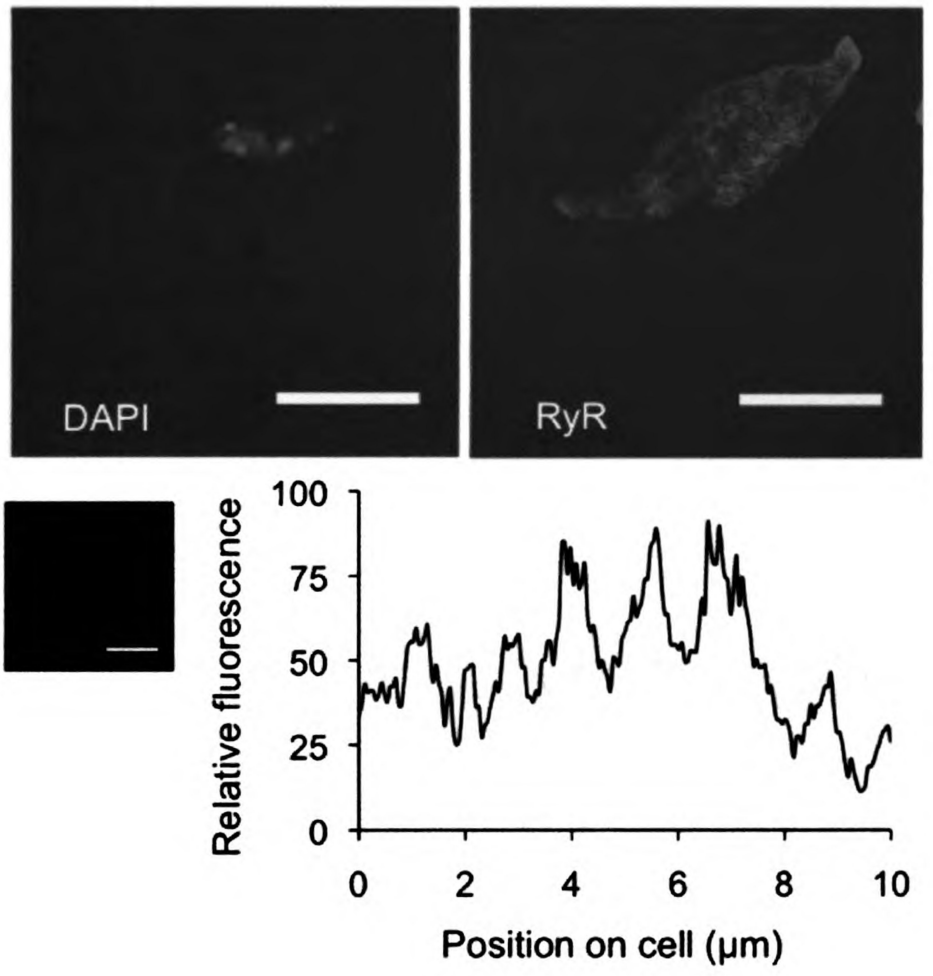

Figure 37. Expression and localization of ryanodine receptors in single mouse cremaster feed artery smooth muscle cells.

The top panels show representative immunohistochemical images of a single smooth muscle cell from MFA with staining for DAPI nuclear stain (left) and an anti-RyR1/2 antibody (right) within a 0.5 μm thick confocal slice of the smooth muscle layer. Like the whole vessels, single MFA smooth muscle cells displayed clustered, variegated staining for RyR. Scale bars are 10 μm. The bottom panels show the quantitation of variation in RyR staining across a reference line.

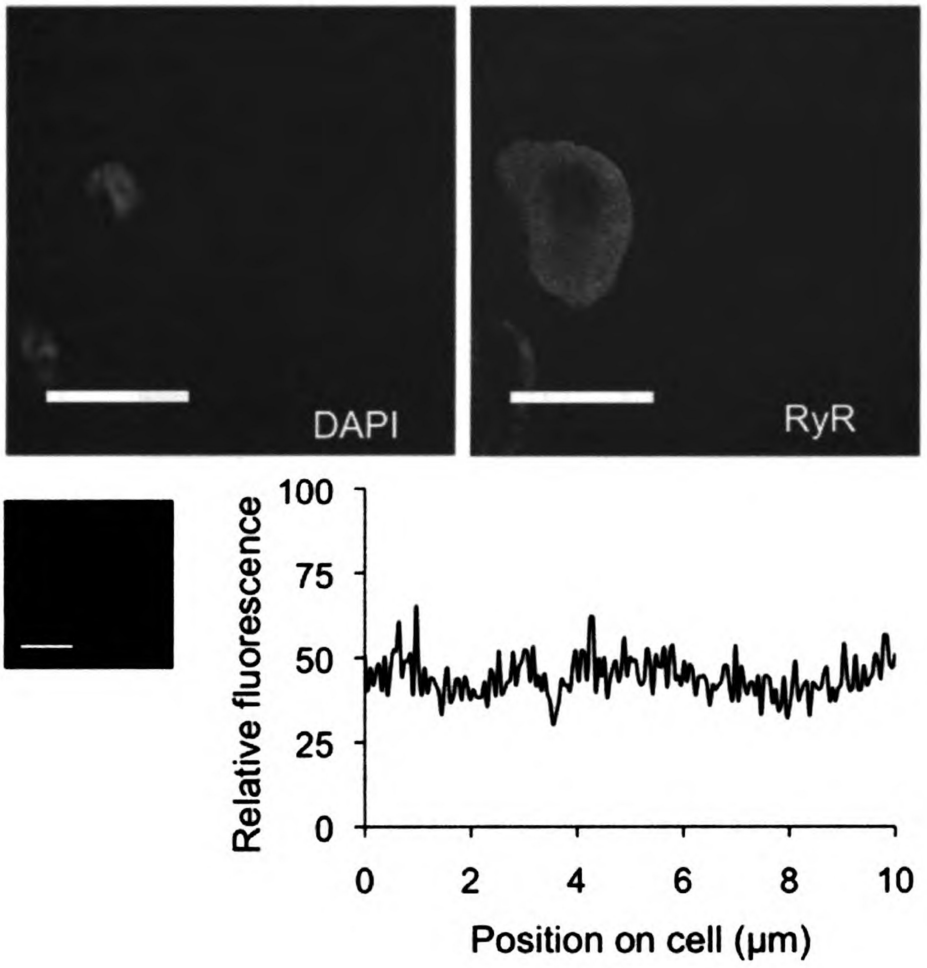

Figure 38. Expression and localization of ryanodine receptors in single mouse cremaster arteriolar smooth muscle cells.

The top panels show representative immunohistochemical images of a single smooth muscle cell from MCA with staining for DAPI nuclear stain (left) and an anti-RyR1/2 antibody (right) within a 0.5 μm thick confocal slice of the smooth muscle layer. Like the whole vessels, single MCA smooth muscle have diffuse, nonspecific staining for RyR. Scale bars are 10 μm. The bottom panels show the quantitation of variation in RyR staining across a reference line.

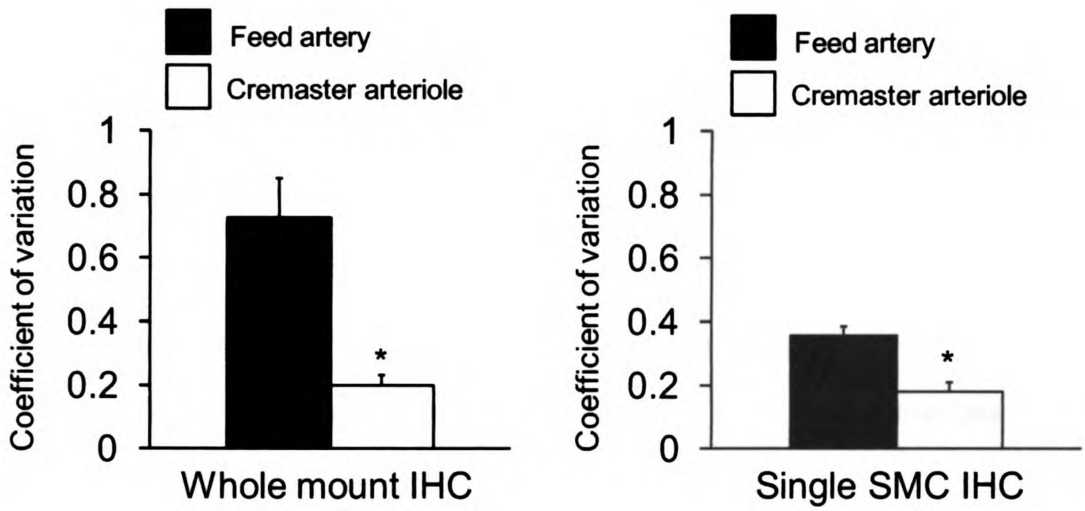

Figure 39. Different ryanodine receptor protein expression in mouse feed arteries and arterioles in both whole vessels and isolated smooth muscle cells

Data are means ± SE for the coefficients of variation of fluorescence from immunofluorescence RyR staining of whole MFA and MCA (left) and isolated smooth muscle cells from MFA and MCA (right). MFA (black) displayed significantly greater variation in staining for RyR compared to MCA ($n = 4$, $p < 0.05$).

Discussion

These studies highlight important differences in the role of RyR in MFA and MCA and provide insight into the molecular cause of those differences. In previous studies (25) and in Chapter 3, we have shown that in hamsters, there are significant differences in the regulation of Ca^{2+} signals and myogenic tone between HFA and HCA smooth muscle, particularly the role that subsarcolemmal RyR play in those cells. We hypothesized here that differences in the expression and/or localization of RyR isoforms may underlie the functional differences we observed. In contrast to the previous studies from our lab, these studies were done in mice in order to access more commercially available primers and antibodies. Therefore, our first goal in these studies was to determine the role of RyR and IP_3R in MFA and MCA and compare those data to the data from HFA and HCA. Based on the previous finding that RyR regulate Ca^{2+} oscillations and myogenic tone in HFA but not HCA, we hypothesized that these functional differences in the role of RyR would also be seen between MFA and MCA. Consistent with this hypothesis, we found that MFA displayed ryanodine-sensitive Ca^{2+} sparks and waves, while MCA only displayed Ca^{2+} waves, which were unaltered in the presence of ryanodine. These data suggest that RyR are involved in the regulation of Ca^{2+} sparks, Ca^{2+} waves and myogenic tone in MFA, but not MCA. As in our previous studies in hamster, it is IP_3R that importantly underlie Ca^{2+} waves and tone in MCA. Blocking IP_3R activity directly with xestospongin D or 2-APB or indirectly by inhibiting PLC with U73122

decrease Ca^{2+} waves and myogenic tone in both MFA and MCA. These data are consistent with our previous work in hamster arteries and arterioles and indicate that across species there are significant regional differences in the function of RyR. In cremaster feed arteries as has been reported in other arteries (96, 138, 155, 202), RyR activity appears to be functionally coupled to .BK_{Ca} channels and contribute to negative feedback regulation of vascular tone. In contrast, RyR appear to be silent in second-order cremaster arterioles and do not appear to contribute to the regulation of intracellular Ca^{2+} or myogenic tone, at least under the conditions of our experiments.

We also found that the morphology of sparks and waves was similar across species. There were no significant differences in the occurrence, amplitude or frequency of either sparks or waves compared to the equivalent vessels in hamsters (**Table 7** vs. **Table 6** from Chapter 3). The cross-sectional lengths of smooth muscle cells and FWHM of sparks and waves differed between species and vessel type, but this is attributable to the differences in size of the vessel types in the two species. These data in the mouse are especially novel because although many investigators have documented the properties of Ca^{2+} sparks in vascular smooth muscle, few have looked at their properties in a mouse model (see **Tables 2-4** for summary of the literature).

We also tested the hypothesis that regional differences in ryanodine receptor isoform expression underlies the contrasting roles that RyR play in small arteries

and arterioles. We found that smooth muscle cells from these vessels expressed only RyR2 and RyR3, that RyR2 was more highly expressed in artery vs. arteriole smooth muscle, that RyR3 was more highly expressed in arteriole vs. artery smooth muscle, and that the ratio of expression of RyR2/RyR3 was nearly 4-times higher in the smooth muscle cells from arteries compared with their down-stream arterioles. We think that these differences in RyR isoform expression may account for the functional differences that we observed. First, prior studies have suggested that RyR2 importantly contributes to calcium sparks in other smooth muscles (54, 144). Second, while controversial, studies have suggested that the RyR3 isoform (or one of its spliced variants) may inhibit spark formation (58, 146, 172). Thus, the higher ratio of RyR2/RyR3 that we observed in arteries vs. arterioles is consistent with our observation of sparks in arteries, but not in arterioles.

In contrast to a large number of studies of vascular smooth muscle cells from larger vessels (54, 165, 172, 206, 290, 302, 303), we found that RyR1 was not expressed by either small artery or arteriolar smooth muscle cells. We do not think that this is due to a technical limitation in our methods because we used validated primers and verified that these primers appropriately identified RyR1 expression in skeletal muscle and brain. We conclude that if RyR1 is expressed in smooth muscle cells from these vessels, then its expression must be at a level that is below the limits of detection, and far less than RyR2 and RyR3. It is important to note that most prior studies used whole vessel homogenates such

that message from cells other than vascular smooth muscle cells may have been amplified and contributed to message levels reported in those studies.

Differences in mRNA expression of the RyR isoforms may not correlate directly with the expression of the corresponding protein, and give no insight into the localization of those proteins within the cell. Therefore, we conducted a series of immunofluorescence experiments to better characterize RyR protein expression in MFA and MCA. Because we were unable to validate the specificity of all commercially-available, isoform-specific RyR antibodies, we used an RyR antibody that is specific for RyR1 and 2 which was validated in control tissues (heart, brain and diaphragm) by Western blotting. In both the whole-vessel and single-cell IHF, smooth muscle from MFA had clustered, variable staining for RyR, while MCA had diffuse, uniform staining. Given the lack of mRNA expression for RyR1 that we observed, these data suggest that RyR2 in MFA may form clusters in the SR that are required for generation of Ca^{2+} sparks (290). In contrast, staining in the MCA was very uniform and suggested no concentration in any intracellular structure. Further studies will be required to define the exact localization of RyR2 in MFA. However, the clustered staining pattern that we observed in MFA is consistent with Yang et al. (290) who observed discrete patches of RyR in pulmonary artery smooth muscle cells. The diffuse staining observed in MCA may be partially due to the low affinity that the anti-RyR antibody used for these studies has for RyR3, as the PCR showed higher amounts of RyR3 in the cremaster arterioles. It is also possible that there

is a spliced variant of RyR present in MCA that does not react properly with the anti-RyR antibody. Future studies examining the expression of spliced variants such as AS-8a which has a decreased capacity for Ca^{2+} release (146) might help to resolve some of these issues.

Our studies demonstrate that on both a functional and molecular level, there are important differences in the RyR of MFA and MCA. Few studies (54, 172) have looked at how differences in RyR gene expression correlate to differences in protein expression and how both sets of differences relate to functional changes. No studies have characterized these properties in the microvasculature, and a direct comparison between arterial and arteriolar RyR has also never been done. Functionally, we found that RyR are important regulators of subsarcolemmal Ca^{2+} signals and myogenic tone in MFA, but they do not appear to play an important role in either capacity in MCA. Instead, IP_3R appear to be the important regulators of SR Ca^{2+} release in MCA. These functional differences are likely the result of differences in the expression and/or distribution of RyR isoforms, as demonstrated on the gene- and protein expression levels. It is important to define the regulation of these different vascular beds because understanding differences such as those we showed between MFA and MCA can lead to the development of tissue- or vessel-specific treatments for conditions such as hypertension and diabetes that involve ion channel-related vasculopathies.

CHAPTER 5: SUMMARY AND CONCLUSIONS

The overall goal of this project was to elucidate the mechanisms by which SR Ca^{2+} release channels on the SR of cremaster arterioles and their upstream feed arteries regulate subsarcolemmal Ca^{2+} signals and myogenic tone. We knew from the literature that activation of BK_{Ca} channels by local Ca^{2+} sparks arising from RyR was part of an important negative feedback pathway regulating myogenic tone in the smooth muscle cells from many types of arteries (139, 155, 202). Consistent with these observations, we saw Ca^{2+} sparks, along with Ca^{2+} waves in cannulated, Fluo 4-loaded HFA. However, in the downstream HCA, we only saw the global Ca^{2+} waves, suggesting important differences between HFA and HCA. Further pharmacological experiments in cannulated vessels showed that RyR and BK_{Ca} channels are functionally coupled in HFA, but not HCA, despite the presence of functional RyR in HCA. Despite the obvious difference with Ca^{2+} sparks, the properties of Ca^{2+} waves are not different between HFA and HCA: they have similar morphology, asynchronicity and are equivalent at several intraluminal pressures.

Because RyR did not produce sparks and are not functionally coupled to BK_{Ca} channels in HCA, as in HFA and other arteries, we next used Ca^{2+} imaging

studies to investigate the role of RyR in subsarcolemmal Ca^{2+} signaling. In HFA, blocking RyR inhibited both Ca^{2+} sparks and waves, increased intracellular Ca^{2+} and caused vasoconstriction. Conversely, it had no effect in HCA, suggesting that RyR are silent in these smooth muscle cells. Based on these data, we hypothesized that it must be IP_3R importantly regulating Ca^{2+} signals and tone in HCA. In both HFA and HCA, blocking IP_3R or its upstream regulator, PLC decreased the occurrence of waves, global Ca^{2+} and tone. HFA Ca^{2+} sparks were unaltered. Thus, while both RyR and IP_3R contribute to Ca^{2+} oscillations and tone in HFA, only IP_3R appear important in HCA.

The next step in the project was to determine why RyR are silent in feed arteries but not cremaster arterioles. We hypothesized that differences in the expression and localization of RyR isoforms accounts for these functional differences. To test this, we performed a series of RT-qPCR experiments looking at gene expression of RyR1-3 in MFA and MCA. Surprisingly, neither MFA nor MCA expressed RyR1. Also, MFA expressed the greatest proportion of RyR2, while MCA expressed more RyR3. This finding is important because not only does it support the hypothesis, but it is also in agreement with the small literature that RyR3 may be inhibitory to Ca^{2+} sparks in vascular smooth muscle (172). We also used immunofluorescence and confocal microscopy in intact, pressure-fixed MFA and MCA as well as their isolated smooth muscle cells to determine the location and distribution of RyR. In both whole vessels and isolated cells, MFA

displayed bright, clustered staining for RyR, while MCA had dimmer, diffuse staining with significantly less variation. These data suggest that RyR are distributed differently within MFA and MCA. Taken together with the PCR data, they support the hypothesis that there are regional differences in the expression and distribution of RyR and that these differences may underlie the functional differences in Ca^{2+} signaling and regulation of myogenic tone that we have observed between feed arteries and their downstream arterioles.

Based on all of our studies, we have summarized the proposed roles and spatial organizations of RyR and IP_3R in both feed arteries and arterioles (**Figure 40**). Because microdomain increases in Ca^{2+} from Ca^{2+} sparks are able to activate BK_{Ca} channels in feed arteries, we propose that the SR in these smooth muscle cells is located in close proximity to the plasma membrane. However, because not all BK_{Ca} activity is due to the activity of RyR, we also propose that Ca^{2+} from VGCC located near BK_{Ca} also accounts for the activation of some BKCa channels. In contrast to the feed arteries, arteriolar RyR are silent, and the SR distance from the plasma membrane either does not play a role in the regulation of tone or it is large enough that Ca^{2+} sparks are not present because they would be unable to activate BK_{Ca} channels. Because RyR and BK_{Ca} are not coupled in arterioles, we propose that it is Ca^{2+} from VGCC that activate nearby BK_{Ca} in those smooth muscle cells. There are also important differences in the regulation of Ca^{2+} waves in both vessel types. Because both RyR and IP_3R

underlie Ca^{2+} waves in the feed arteries, it is likely that these channels are located nearby one another on the SR membrane and operate using a common source of Ca^{2+}. In arterioles, only the IP_3R are important for the production of feed arteries, despite the presence of functional RyR in those cells. The lack of a role for RyR could be due to the distance between RyR and IP3R in the SR membrane, or it could be because the IP_3R and RyR operate using separate Ca^{2+} pools within the SR.

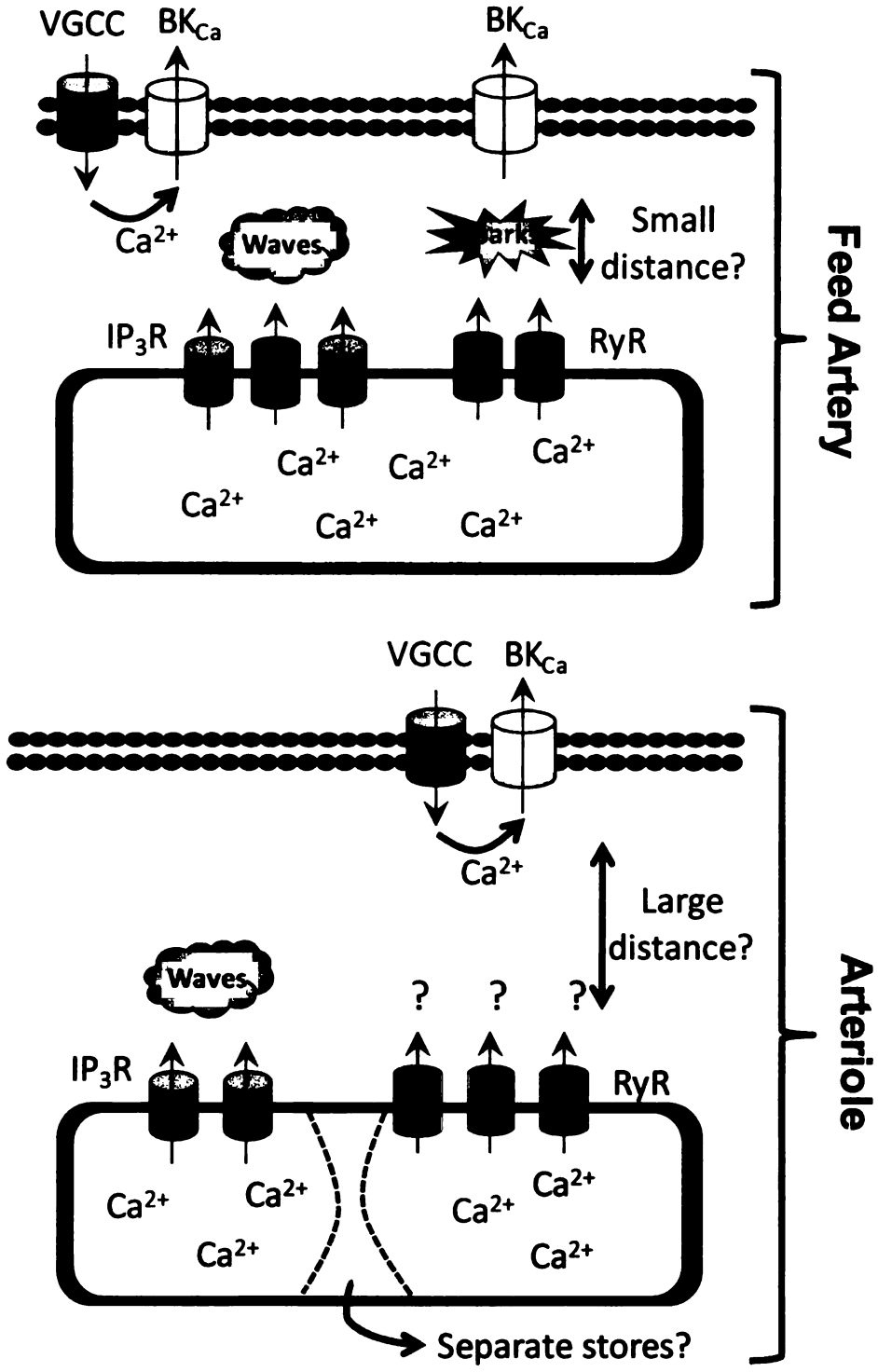

Figure 40. Proposed roles of ryanodine receptors and IP_3 receptors in cremaster feed arteries and arterioles.

We recognize that there are some limitations in these studies, many of which will guide the future directions of this project. By using a spinning disc confocal microscope at 30 fps for Ca^{2+} imaging, it is possible that we may have missed very brief Ca^{2+} events with durations shorter than 33 ms (the time required to capture one image). This might explain the lack of observation of Ca^{2+} sparks in HCA and MCA, and could partially explain why the average FDHM of Ca^{2+} sparks we recorded are longer in duration than the average value that has been reported by other investigators (see Tables 2-4). However, given the large number of cells imaged in all of the experiments performed, even short duration events should have appeared in at least a few images, which did not seem to be the case. Furthermore, the lack of effect of ryanodine (10-50 μM) on Ca^{2+} waves, global Ca^{2+} and diameter in both HCA and MCA imply that if such brief, non-detected events were present, they are functionally irrelevant. Nontheless, future studies should be performed using higher imaging rates to directly address this issue.

We also recognize that, although pharmacology is a powerful tool for looking at the role of ion channels in vascular smooth muscle function, the drugs used may have some nonspecific effects. Experiments were designed, in many cases, to rule out such effects. For example, we used two structurally different blockers of

IP_3R (xestospongin D and 2-APB) and observed similar effects, reducing concern that off target effects account for the results observed. However, studies have suggested that pharmacological agents that affect RyR or IP_3R may lead to depletion of Ca^{2+} from the SR (188) and thus indirectly inhibit Ca^{2+} signals originating from the SR. While we can exclude a role for SR Ca^{2+} depletion in the effects of U72122, xestospongin D and 2-APB in feed arteries because of their lack of effect on Ca^{2+} sparks, we cannot completely exclude a role for SR Ca^{2+} depletion from the effects of ryanodine in HFA and MFA. The presence of functional RyR in arteriolar smooth muscle (as assessed by caffeine-induced Ca^{2+} transients), and lack of effect of ryanodine on Ca^{2+} waves in HCA and MCA reduce concern for this off target effect. However, further studies should be performed to examine the state of Ca^{2+} stores in the absence and presence of all of the inhibitors used to directly test this alternative hypothesis. Studies in which intracellular stores are depleted of Ca^{2+} (using thapsigargin or cyclopiazonic acid) also should be performed to allow better understanding of the relative contribution that Ca^{2+} sparks and waves play in the regulation of myogenic tone. We also were limited in our IHF studies by the availability of commercial RyR antibodies. Future studies should be performed with antibodies specific to each individual RyR isoform so that the protein localization of each isoform can be better assessed. In addition, double label experiments need to be performed to verify, for example, that the RyR1/2 staining observed in MFA co-localizes with a marker of the SR (calnexin or SERCA2, for example) and to examine the

structure of the SR in feed arteries vs. arterioles. The expression and localization of IP_3R in feed arteries and arterioles also should be examined and correlated with RyR expression and localization.

This work highlights the need for a better understanding of microvascular smooth muscle physiology, as we cannot assume arterioles are regulated in the same way as larger vessels, even within the same tissue. Skeletal muscle makes up 40% of body mass (7), and arterioles are largely responsible for the regulation and distribution of blood flow to and within these tissues (17, 98, 182, 198). Thus, skeletal muscle arterioles also substantially contribute to blood pressure regulation and cardiovascular homeostasis. Myogenic tone is a hallmark feature of these small vessels, yet the exact mechanisms regulating tone and its underlying Ca^{2+} signals in the microcirculation are not clear, despite the knowledge that the importance of myogenic tone increases as vessels decrease in diameter (62). Studies in larger vessels (50, 63, 74, 192, 193, 203, 205, 213, 248, 281, 282, 305) demonstrate the wide variety of ion channels and processes contributing to Ca^{2+} signals and tone in arterial smooth muscle, and the existing body of literature in the microcirculation (10, 120, 122, 124) suggests similar diversity. Our work contributes to a better understanding of how SR Ca^{2+} release channels regulate tone both in the skeletal muscle microcirculation and its corresponding feed arteries.

A logical next step in this work would be to look at how the roles of RyR and IP_3R are affected in altered physiological states such as aging. For example, studies of RyR function in skeletal muscle have shown that Ca^{2+} spark formation is dramatically reduced in muscle from aged mice (277), which may be related to age-related decreases in the proportion of cardiac output that goes to the skeletal muscle (65, 226). If a similar process occurs in the vasculature, aging might cause a selective loss of RyR function in feed arteries, potentially contributing to aging-induced alterations in their function and contributing to altered regulation of blood pressure and blood flow that occur in the aging cardiovascular system. This idea is supported by data in humans showing that during exercise, older people have higher arterial blood pressures and likely increased vasoconstriction in muscles during periods of exercise (220, 225). Dysfunction in the regulations of myogenic tone has also been implicated in age-related changes in the cardiovascular system, although the mechanism is not clear (226). Myogenic tone in arterioles acts to prevent local hypertension in downstream capillaries, but the net effect of many tissues with increased tone is increased peripheral resistance in the upstream vasculature and therefore increased blood pressure. It is likely that the expression, activity and function of SR Ca^{2+} channels changes with increased blood pressure, as arterioles increase their myogenic activity and remodel to accommodate the increase in pressure. Now that we have defined the role of RyR (or lack thereof) in cremaster arterioles and their upstream feed arteries under normal conditions, we have the potential to look at RyR in many

altered physiological states, with the possibility to generate tissue- or vessel type-specific interventions.

REFERENCES

1. *Guide for the Care and Use of Laboratory Animals*: National Academic Press, 1996.

2. **Aaronson P and Jones A.** Ca dependence of Na influx during treatment of rabbit aorta with NE and high K solutions. *Am J Physiol* 254: C75-83, 1988.

3. **Abramoff MD, Magelhaes, P.J., Ram, S.J.** Image Processing with ImageJ. *Biophotonics International* 11: 36-42, 2004.

4. **Adkins C and Taylor C.** Lateral inhibition of inositol 1,4,5-trisphosphate receptors by cytosolic Ca(2+). *Curr Biol* 9: 1115-1118, 1999.

5. **Aghdasi B, Ye K, Resnick A, Huang A, Ha H, Guo X, Dawson T, Dawson V, and Snyder S.** FKBP12, the 12-kDa FK506-binding protein, is a physiologic regulator of the cell cycle. *Proc Natl Acad Sci U S A* 98: 2425-2430, 2001.

6. **Ahern G, Junankar P, and Dulhunty A.** Subconductance states in single-channel activity of skeletal muscle ryanodine receptors after removal of FKBP12. *Biophys J* 72: 146-162, 1997.

7. **Andersen P and Saltin B.** Maximal perfusion of skeletal muscle in man. *J Physiol* 366: 233-249, 1985.

8. **Ando H, Mizutani A, Kiefer H, Tsuzurugi D, Michikawa T, and Mikoshiba K.** IRBIT suppresses IP3 receptor activity by competing with IP3 for the common binding site on the IP3 receptor. *Mol Cell* 22: 795-806, 2006.

9. **Ando H, Mizutani A, Matsu-ura T, and Mikoshiba K.** IRBIT, a novel inositol 1,4,5-trisphosphate (IP3) receptor-binding protein, is released from the IP3 receptor upon IP3 binding to the receptor. *J Biol Chem* 278: 10602-10612, 2003.

10. **Bakker EN, Kerkhof CJ, and Sipkema P.** Signal transduction in spontaneous myogenic tone in isolated arterioles from rat skeletal muscle. *Cardiovasc Res* 41: 229-236, 1999.

11. **Balasubramanian L, Ahmed A, Lo CM, Sham JS, and Yip KP.** Integrin-mediated mechanotransduction in renal vascular smooth muscle cells: activation of calcium sparks. *Am J Physiol Regul Integr Comp Physiol* 293: R1586-1594, 2007.

12. **Bannister R, Grabner M, and Beam K.** The alpha(1S) III-IV loop influences 1,4-dihydropyridine receptor gating but is not directly involved in excitation-contraction coupling interactions with the type 1 ryanodine receptor. *J Biol Chem* 283: 23217-23223, 2008.

13. **Bayer K, Harbers K, and Schulman H.** alphaKAP is an anchoring protein for a novel CaM kinase II isoform in skeletal muscle. *EMBO J* 17: 5598-5605, 1998.

14. **Bayliss WM.** On the local reactions of the arterial wall to changes of internal pressure. *J Physiol* 28: 220-231, 1902.

15. **Benham C and Tsien R.** Noradrenaline modulation of calcium channels in single smooth muscle cells from rabbit ear artery. *J Physiol* 404: 767-784, 1988.

16. **Benkusky N, Farrell E, and Valdivia H.** Ryanodine receptor channelopathies. *Biochem Biophys Res Commun* 322: 1280-1285, 2004.

17. **Berg B, Cohen K, and Sarelius I.** Direct coupling between blood flow and metabolism at the capillary level in striated muscle. *Am J Physiol* 272: H2693-2700, 1997.

18. **Berkefeld H, Sailer CA, Bildl W, Rohde V, Thumfart JO, Eble S, Klugbauer N, Reisinger E, Bischofberger J, Oliver D, Knaus HG, Schulte U, and Fakler B.** BKCa-Cav channel complexes mediate rapid and localized Ca2+-activated K+ signaling. *Science* 314: 615-620, 2006.

19. **Berridge MJ.** Inositol trisphosphate and calcium signalling. *Nature* 361: 315-325, 1993.

20. **Berridge MJ.** Smooth muscle cell calcium activation mechanisms. *J Physiol* 586: 5047-5061, 2008.

21. **Beutner G, Sharma V, Giovannucci D, Yule D, and Sheu S.** Identification of a ryanodine receptor in rat heart mitochondria. *J Biol Chem* 276: 21482-21488, 2001.

22. **Blatter L and Wier W.** Agonist-induced [Ca2+]i waves and Ca(2+)-induced Ca2+ release in mammalian vascular smooth muscle cells. *Am J Physiol* 263: H576-586, 1992.

23. **Block B, Imagawa T, Campbell K, and Franzini-Armstrong C.** Structural evidence for direct interaction between the molecular components of the transverse tubule/sarcoplasmic reticulum junction in skeletal muscle. *J Cell Biol* 107: 2587-2600, 1988.

24. **Boerman E and Jackson W.** Ca2+-activated K+ channels are controlled by Ca2+ influx through voltage-gated Ca2+ channels, not the release of Ca2+ through ryanodine receptors in arteriolar smooth muscle. *FASEB J* 22: 1142.1142, 2008.

25. **Boerman EM and Jackson W.** IP3 receptors, but not ryanodine receptors mediate subsarcolemmal Ca2+ oscillations in arteriolar smooth muscle cells. *FASEB J*: 767.763, 2009.

26. **Boittin F, Macrez N, Halet G, and Mironneau J.** Norepinephrine-induced Ca(2+) waves depend on InsP(3) and ryanodine receptor activation in vascular myocytes. *Am J Physiol* 277: C139-151, 1999.

27. **Bolton T and Imaizumi Y.** Spontaneous transient outward currents in smooth muscle cells. *Cell Calcium* 20: 141-152, 1996.

28. **Bolton TB.** Calcium events in smooth muscles and their interstitial cells; physiological roles of sparks. *J Physiol* 570: 5-11, 2006.

29. **Bonev AD, Jaggar JH, Rubart M, and Nelson MT.** Activators of protein kinase C decrease Ca2+ spark frequency in smooth muscle cells from cerebral arteries. *Am J Physiol* 273: C2090-2095, 1997.

30. **Borisova L, Wray S, Eisner DA, and Burdyga T.** How structure, Ca signals, and cellular communications underlie function in precapillary arterioles. *Circ Res* 105: 803-810, 2009.

31. **Brayden J and Nelson M.** Regulation of arterial tone by activation of calcium-dependent potassium channels. *Science* 256: 532-535, 1992.

32. **Brillantes A, Ondrias K, Scott A, Kobrinsky E, Ondriasová E, Moschella M, Jayaraman T, Landers M, Ehrlich B, and Marks A.** Stabilization of calcium release channel (ryanodine receptor) function by FK506-binding protein. *Cell* 77: 513-523, 1994.

33. **Bukoski RD, Batkai S, Jarai Z, Wang Y, Offertaler L, Jackson WF, and Kunos G.** CB(1) receptor antagonist SR141716A inhibits Ca(2+)-induced relaxation in CB(1) receptor-deficient mice. *Hypertension* 39: 251-257, 2002.

34. **Bukoski RD, Shearin S, Jackson WF, and Pamarthi MF.** Inhibition of Ca2+-induced relaxation by oxidized tungsten wires and paratungstate. *J Pharmacol Exp Ther* 299: 343-350, 2001.

35. **Bultynck G, De Smet P, Rossi D, Callewaert G, Missiaen L, Sorrentino V, De Smedt H, and Parys J.** Characterization and mapping of the 12 kDa FK506-binding protein (FKBP12)-binding site on different isoforms of the ryanodine receptor and of the inositol 1,4,5-trisphosphate receptor. *Biochem J* 354: 413-422, 2001.

36. **Burdyga T, Shmygol A, Eisner DA, and Wray S.** A new technique for simultaneous and in situ measurements of Ca2+ signals in arteriolar smooth muscle and endothelial cells. *Cell Calcium* 34: 27-33, 2003.

37. **Burdyga T, Wray S, and Noble K.** In situ calcium signaling: no calcium sparks detected in rat myometrium. *Ann N Y Acad Sci* 1101: 85-96, 2007.

38. **Burns WR, Cohen KD, and Jackson WF.** K+-induced dilation of hamster cremasteric arterioles involves both the Na+/K+-ATPase and inward-rectifier K+ channels. *Microcirculation* 11: 279-293, 2004.

39. **Cannell MB, Cheng H, and Lederer WJ.** The control of calcium release in heart muscle. *Science* 268: 1045-1049, 1995.

40. **Cardy T, Traynor D, and Taylor C.** Differential regulation of types-1 and -3 inositol trisphosphate receptors by cytosolic Ca2+. *Biochem J* 328 (Pt 3): 785-793, 1997.

41. **Carmody M, Mackrill J, Sorrentino V, and O'Neill C.** FKBP12 associates tightly with the skeletal muscle type 1 ryanodine receptor, but not with other intracellular calcium release channels. *FEBS Lett* 505: 97-102, 2001.

42. **Chelu M, Danila C, Gilman C, and Hamilton S.** Regulation of ryanodine receptors by FK506 binding proteins. *Trends Cardiovasc Med* 14: 227-234, 2004.

43. **Chen S, Li X, Ebisawa K, and Zhang L.** Functional characterization of the recombinant type 3 Ca2+ release channel (ryanodine receptor) expressed in HEK293 cells. *J Biol Chem* 272: 24234-24246, 1997.

44. **Chen S and MacLennan D.** Identification of calmodulin-, Ca(2+)-, and ruthenium red-binding domains in the Ca2+ release channel (ryanodine receptor) of rabbit skeletal muscle sarcoplasmic reticulum. *J Biol Chem* 269: 22698-22704, 1994.

45. **Chen S, Zhang L, and MacLennan D.** Characterization of a Ca2+ binding and regulatory site in the Ca2+ release channel (ryanodine receptor) of rabbit skeletal muscle sarcoplasmic reticulum. *J Biol Chem* 267: 23318-23326, 1992.

46. **Cheng H and Lederer WJ.** Calcium sparks. *Physiol Rev* 88: 1491-1545, 2008.

47. **Cheng W, Altafaj X, Ronjat M, and Coronado R.** Interaction between the dihydropyridine receptor Ca2+ channel beta-subunit and ryanodine receptor type 1 strengthens excitation-contraction coupling. *Proc Natl Acad Sci U S A* 102: 19225-19230, 2005.

48. **Cheranov SY and Jaggar JH.** TNF-alpha dilates cerebral arteries via NAD(P)H oxidase-dependent Ca2+ spark activation. *Am J Physiol Cell Physiol* 290: C964-971, 2006.

49. **Chin D and Means A.** Calmodulin: a prototypical calcium sensor. *Trends Cell Biol* 10: 322-328, 2000.

50. **Coats P, Johnston F, MacDonald J, McMurray JJ, and Hillier C.** Signalling mechanisms underlying the myogenic response in human subcutaneous resistance arteries. *Cardiovasc Res* 49: 828-837, 2001.

51. **Collier ML, Ji G, Wang Y, and Kotlikoff MI.** Calcium-induced calcium release in smooth muscle: loose coupling between the action potential and calcium release. *J Gen Physiol* 115: 653-662, 2000.

52. **Copello J, Barg S, Onoue H, and Fleischer S.** Heterogeneity of Ca2+ gating of skeletal muscle and cardiac ryanodine receptors. *Biophys J* 73: 141-156, 1997.

53. **Coronado R, Morrissette J, Sukhareva M, and Vaughan D.** Structure and function of ryanodine receptors. *Am J Physiol* 266: C1485-1504, 1994.

54. **Coussin F, Macrez N, Morel JL, and Mironneau J.** Requirement of ryanodine receptor subtypes 1 and 2 for Ca(2+)-induced Ca(2+) release in vascular myocytes. *J Biol Chem* 275: 9596-9603, 2000.

55. **Curtis TM, Tumelty J, Dawicki J, Scholfield CN, and McGeown JG.** Identification and spatiotemporal characterization of spontaneous Ca2+ sparks and global Ca2+ oscillations in retinal arteriolar smooth muscle cells. *Invest Ophthalmol Vis Sci* 45: 4409-4414, 2004.

56. **Curtis TM, Tumelty J, Stewart MT, Arora AR, Lai FA, McGahon MK, Scholfield CN, and McGeown JG.** Modification of smooth muscle Ca2+-sparks by tetracaine: evidence for sequential RyR activation. *Cell Calcium* 43: 142-154, 2008.

57. **da Fonseca P, Morris S, Nerou E, Taylor C, and Morris E.** Domain organization of the type 1 inositol 1,4,5-trisphosphate receptor as revealed by single-particle analysis. *Proc Natl Acad Sci U S A* 100: 3936-3941, 2003.

58. **Dabertrand F, Morel JL, Sorrentino V, Mironneau J, Mironneau C, and Macrez N.** Modulation of calcium signalling by dominant negative splice variant of ryanodine receptor subtype 3 in native smooth muscle cells. *Cell Calcium* 40: 11-21, 2006.

59. **Danoff S, Ferris C, Donath C, Fischer G, Munemitsu S, Ullrich A, Snyder S, and Ross C.** Inositol 1,4,5-trisphosphate receptors: distinct neuronal and nonneuronal forms derived by alternative splicing differ in phosphorylation. *Proc Natl Acad Sci U S A* 88: 2951-2955, 1991.

60. **Davis M, Donovitz J, and Hood J.** Stretch-activated single-channel and whole cell currents in vascular smooth muscle cells. *Am J Physiol* 262: C1083-1088, 1992.

61. **Davis M, Hill M, and Kuo L.** Local regulation of microvascular perfusion. In: *Handbook of Physiology: Microcirculation* (2 ed.), edited by Tuma R, Duran W and Ley K: Elsevier, 2008.

62. **Davis MJ.** Myogenic response gradient in an arteriolar network. *Am J Physiol* 264: H2168-2179, 1993.

63. **Davis MJ and Hill MA.** Signaling mechanisms underlying the vascular myogenic response. *Physiol Rev* 79: 387-423, 1999.

64. **De Smedt H, Missiaen L, Parys J, Henning R, Sienaert I, Vanlingen S, Gijsens A, Himpens B, and Casteels R.** Isoform diversity of the inositol trisphosphate receptor in cell types of mouse origin. *Biochem J* 322 (Pt 2): 575-583, 1997.

65. **Delp M, Evans M, and Duan C.** Effects of aging on cardiac output, regional blood flow, and body composition in Fischer-344 rats. *J Appl Physiol* 85: 1813-1822, 1998.

66. **Devogelaere B, Verbert L, Parys J, Missiaen L, and De Smedt H.** The complex regulatory function of the ligand-binding domain of the inositol 1,4,5-trisphosphate receptor. *Cell Calcium* 43: 17-27, 2008.

67. **Du G, Sandhu B, Khanna V, Guo X, and MacLennan D.** Topology of the Ca2+ release channel of skeletal muscle sarcoplasmic reticulum (RyR1). *Proc Natl Acad Sci U S A* 99: 16725-16730, 2002.

68. **Dulhunty A, Haarmann C, Green D, and Hart J.** How many cysteine residues regulate ryanodine receptor channel activity? *Antioxid Redox Signal* 2: 27-34, 2000.

69. **Dulhunty A and Pouliquin P.** What we don't know about the structure of ryanodine receptor calcium release channels. *Clin Exp Pharmacol Physiol* 30: 713-723, 2003.

70. **Duran W, Sanchez F, and Breslin J.** Microcirculatory Exchange Function. In: *Handbook of Physiology: Microcirculation* (2 ed.), edited by Tuma R, Duran W and Ley K. USA: Elsevier, 2008.

71. **Durham W, Wehrens X, Sood S, and Hamilton S.** Diseases associated with altered ryanodine receptor activity. *Subcell Biochem* 45: 273-321, 2007.

72. **Eager K and Dulhunty A.** Cardiac ryanodine receptor activity is altered by oxidizing reagents in either the luminal or cytoplasmic solution. *J Membr Biol* 167: 205-214, 1999.

73. **Eager K, Roden L, and Dulhunty A.** Actions of sulfhydryl reagents on single ryanodine receptor Ca(2+)-release channels from sheep myocardium. *Am J Physiol* 272: C1908-1918, 1997.

74. **Earley S, Straub SV, and Brayden JE.** Protein kinase C regulates vascular myogenic tone through activation of TRPM4. *Am J Physiol Heart Circ Physiol* 292: H2613-2622, 2007.

75. **Earley S, Waldron BJ, and Brayden JE.** Critical role for transient receptor potential channel TRPM4 in myogenic constriction of cerebral arteries. *Circ Res* 95: 922-929, 2004.

76. **Essin K and Gollasch M.** Role of ryanodine receptor subtypes in initiation and formation of calcium sparks in arterial smooth muscle: comparison with striated muscle. *J Biomed Biotechnol* 2009: 135249, 2009.

77. **Essin K, Welling A, Hofmann F, Luft FC, Gollasch M, and Moosmang S.** Indirect coupling between Cav1.2 channels and ryanodine receptors to generate Ca2+ sparks in murine arterial smooth muscle cells. *J Physiol* 584: 205-219, 2007.

78. **Farrell E, Antaramian A, Benkusky N, Zhu X, Rueda A, Gómez A, and Valdivia H.** Regulation of cardiac excitation-contraction coupling by sorcin, a novel modulator of ryanodine receptors. *Biol Res* 37: 609-612, 2004.

79. **Farrell E, Antaramian A, Rueda A, Gómez A, and Valdivia H.** Sorcin inhibits calcium release and modulates excitation-contraction coupling in the heart. *J Biol Chem* 278: 34660-34666, 2003.

80. **Fellner SK and Arendshorst WJ.** Angiotensin II Ca2+ signaling in rat afferent arterioles: stimulation of cyclic ADP ribose and IP3 pathways. *Am J Physiol Renal Physiol* 288: F785-791, 2005.

81. **Fellner SK and Arendshorst WJ.** Voltage-gated Ca2+ entry and ryanodine receptor Ca2+-induced Ca2+ release in preglomerular arterioles. *Am J Physiol Renal Physiol* 292: F1568-1572, 2007.

82. **Feng W, Tu J, Pouliquin P, Cabrales E, Shen X, Dulhunty A, Worley P, Allen P, and Pessah I.** Dynamic regulation of ryanodine receptor type 1 (RyR1) channel activity by Homer 1. *Cell Calcium* 43: 307-314, 2008.

83. **Ferris C, Cameron A, Bredt D, Huganir R, and Snyder S.** Inositol 1,4,5-trisphosphate receptor is phosphorylated by cyclic AMP-dependent protein kinase at serines 1755 and 1589. *Biochem Biophys Res Commun* 175: 192-198, 1991.

84. **Ferris C, Huganir R, Bredt D, Cameron A, and Snyder S.** Inositol trisphosphate receptor: phosphorylation by protein kinase C and calcium calmodulin-dependent protein kinases in reconstituted lipid vesicles. *Proc Natl Acad Sci U S A* 88: 2232-2235, 1991.

85. **Fill M and Copello JA.** Ryanodine receptor calcium release channels. *Physiol Rev* 82: 893-922, 2002.

86. **Finch E, Turner T, and Goldin S.** Calcium as a coagonist of inositol 1,4,5-trisphosphate-induced calcium release. *Science* 252: 443-446, 1991.

87. **Foskett J, White C, Cheung K, and Mak D.** Inositol trisphosphate receptor Ca2+ release channels. *Physiol Rev* 87: 593-658, 2007.

88. **Fruen B, Bardy J, Byrem T, Strasburg G, and Louis C.** Differential Ca(2+) sensitivity of skeletal and cardiac muscle ryanodine receptors in the presence of calmodulin. *Am J Physiol Cell Physiol* 279: C724-733, 2000.

89. **Fruen B, Black D, Bloomquist R, Bardy J, Johnson J, Louis C, and Balog E.** Regulation of the RYR1 and RYR2 Ca2+ release channel isoforms by Ca2+-insensitive mutants of calmodulin. *Biochemistry* 42: 2740-2747, 2003.

90. **Futatsugi A, Kuwajima G, and Mikoshiba K.** Tissue-specific and developmentally regulated alternative splicing in mouse skeletal muscle ryanodine receptor mRNA. *Biochem J* 305 (Pt 2): 373-378, 1995.

91. **Gao L, Balshaw D, Xu L, Tripathy A, Xin C, and Meissner G.** Evidence for a role of the lumenal M3-M4 loop in skeletal muscle Ca(2+) release channel (ryanodine receptor) activity and conductance. *Biophys J* 79: 828-840, 2000.

92. **Giannini G, Conti A, Mammarella S, Scrobogna M, and Sorrentino V.** The ryanodine receptor/calcium channel genes are widely and differentially expressed in murine brain and peripheral tissues. *J Cell Biol* 128: 893-904, 1995.

93. **Giannini G and Sorrentino V.** Molecular structure and tissue distribution of ryanodine receptors calcium channels. *Med Res Rev* 15: 313-323, 1995.

94. **Gokina NI, Knot HJ, Nelson MT, and Osol G.** Increased Ca2+ sensitivity as a key mechanism of PKC-induced constriction in pressurized cerebral arteries. *Am J Physiol* 277: H1178-1188, 1999.

95. **Gollasch M, Haase H, Ried C, Lindschau C, Morano I, Luft FC, and Haller H.** L-type calcium channel expression depends on the differentiated state of vascular smooth muscle cells. *FASEB J* 12: 593-601, 1998.

96. **Gollasch M, Lohn M, Furstenau M, Nelson MT, Luft FC, and Haller H.** Ca2+ channels, Ca2+ sparks, and regulation of arterial smooth muscle function. *Z Kardiol* 89 Suppl 2: 15-19, 2000.

97. **Gollasch M, Wellman GC, Knot HJ, Jaggar JH, Damon DH, Bonev AD, and Nelson MT.** Ontogeny of local sarcoplasmic reticulum Ca2+ signals in cerebral arteries: Ca2+ sparks as elementary physiological events. *Circ Res* 83: 1104-1114, 1998.

98. **Gorczynski R, Klitzman B, and Duling B.** Interrelations between contracting striated muscle and precapillary microvessels. *Am J Physiol* 235: H494-504, 1978.

99. **Gordienko DV and Bolton TB.** Crosstalk between ryanodine receptors and IP(3) receptors as a factor shaping spontaneous Ca(2+)-release events in rabbit portal vein myocytes. *J Physiol* 542: 743-762, 2002.

100. **Grayson TH, Haddock RE, Murray TP, Wojcikiewicz RJ, and Hill CE.** Inositol 1,4,5-trisphosphate receptor subtypes are differentially distributed between smooth muscle and endothelial layers of rat arteries. *Cell Calcium* 36: 447-458, 2004.

101. **Grunnet M and Kaufmann WA.** Coassembly of big conductance Ca2+-activated K+ channels and L-type voltage-gated Ca2+ channels in rat brain. *J Biol Chem* 279: 36445-36453, 2004.

102. **Guerrero-Hernández A, Gómez-Viquez L, Guerrero-Serna G, and Rueda A.** Ryanodine receptors in smooth muscle. *Front Biosci* 7: d1676-1688, 2002.

103. **Guia A, Wan X, Courtemanche M, and Leblanc N.** Local Ca2+ entry through L-type Ca2+ channels activates Ca2+-dependent K+ channels in rabbit coronary myocytes. *Circ Res* 84: 1032-1042, 1999.

104. **Gurrola G, Arévalo C, Sreekumar R, Lokuta A, Walker J, and Valdivia H.** Activation of ryanodine receptors by imperatoxin A and a peptide segment of the II-III loop of the dihydropyridine receptor. *J Biol Chem* 274: 7879-7886, 1999.

105. **Györke I and Györke S.** Regulation of the cardiac ryanodine receptor channel by luminal Ca2+ involves luminal Ca2+ sensing sites. *Biophys J* 75: 2801-2810, 1998.

106. **Haarmann C, Fink R, and Dulhunty A.** Oxidation and reduction of pig skeletal muscle ryanodine receptors. *Biophys J* 77: 3010-3022, 1999.

107. **Haddock RE and Hill CE.** Differential activation of ion channels by inositol 1,4,5-trisphosphate (IP3)- and ryanodine-sensitive calcium stores in rat basilar artery vasomotion. *J Physiol* 545: 615-627, 2002.

108. **Hain J, Onoue H, Mayrleitner M, Fleischer S, and Schindler H.** Phosphorylation modulates the function of the calcium release channel of sarcoplasmic reticulum from cardiac muscle. *J Biol Chem* 270: 2074-2081, 1995.

109. **Hajnóczky G and Thomas A.** Minimal requirements for calcium oscillations driven by the IP3 receptor. *EMBO J* 16: 3533-3543, 1997.

110. **Hakamata Y, Nakai J, Takeshima H, and Imoto K.** Primary structure and distribution of a novel ryanodine receptor/calcium release channel from rabbit brain. *FEBS Lett* 312: 229-235, 1992.

111. **Hakim CH, Jackson WF, and Segal SS.** Connexin isoform expression in smooth muscle cells and endothelial cells of hamster cheek pouch arterioles and retractor feed arteries. *Microcirculation* 15: 503-514, 2008.

112. **Hamada K, Terauchi A, and Mikoshiba K.** Three-dimensional rearrangements within inositol 1,4,5-trisphosphate receptor by calcium. *J Biol Chem* 278: 52881-52889, 2003.

113. **Hamilton S.** Ryanodine receptors. *Cell Calcium* 38: 253-260, 2005.

114. **Hamilton S and Serysheva I.** Ryanodine receptor structure: progress and challenges. *J Biol Chem* 284: 4047-4051, 2009.

115. **Harder D.** Pressure-induced myogenic activation of cat cerebral arteries is dependent on intact endothelium. *Circ Res* 60: 102-107, 1987.

116. **Harootunian A, Kao J, Paranjape S, and Tsien R.** Generation of calcium oscillations in fibroblasts by positive feedback between calcium and IP3. *Science* 251: 75-78, 1991.

117. **Hayashi T and Su T.** Regulating ankyrin dynamics: Roles of sigma-1 receptors. *Proc Natl Acad Sci U S A* 98: 491-496, 2001.

118. **Hennig GW, Smith CB, O'Shea DM, and Smith TK.** Patterns of intracellular and intercellular Ca2+ waves in the longitudinal muscle layer of the murine large intestine in vitro. *J Physiol* 543: 233-253, 2002.

119. **Heppner TJ, Bonev AD, Santana LF, and Nelson MT.** Alkaline pH shifts Ca2+ sparks to Ca2+ waves in smooth muscle cells of pressurized cerebral arteries. *Am J Physiol Heart Circ Physiol* 283: H2169-2176, 2002.

120. **Hill MA, Davis MJ, Meininger GA, Potocnik SJ, and Murphy TV.** Arteriolar myogenic signalling mechanisms: Implications for local vascular function. *Clin Hemorheol Microcirc* 34: 67-79, 2006.

121. **Hill MA, Falcone JC, and Meininger GA.** Evidence for protein kinase C involvement in arteriolar myogenic reactivity. *Am J Physiol* 259: H1586-1594, 1990.

122. **Hill MA, Sun Z, Martinez-Lemus L, and Meininger GA.** New technologies for dissecting the arteriolar myogenic response. *Trends Pharmacol Sci* 28: 308-315, 2007.

123. **Hill MA, Zou H, Davis MJ, Potocnik SJ, and Price S.** Transient increases in diameter and [Ca(2+)](i) are not obligatory for myogenic constriction. *Am J Physiol Heart Circ Physiol* 278: H345-352, 2000.

124. **Hill MA, Zou H, Potocnik SJ, Meininger GA, and Davis MJ.** Invited review: arteriolar smooth muscle mechanotransduction: Ca(2+) signaling pathways underlying myogenic reactivity. *J Appl Physiol* 91: 973-983, 2001.

125. **Horowitz A, Menice C, Laporte R, and Morgan K.** Mechanisms of smooth muscle contraction. *Physiol Rev* 76: 967-1003, 1996.

126. **Huang H, Wang S, Yao W, Zhang C, Zhou Y, Chen X, Zhang B, Xiong W, Wang L, Zheng L, Landry M, Hökfelt T, Xu Z, and Zhou Z.** Long latency of evoked quantal transmitter release from somata of locus coeruleus neurons in rat pontine slices. *Proc Natl Acad Sci U S A* 104: 1401-1406, 2007.

127. **Iino M.** Biphasic Ca2+ dependence of inositol 1,4,5-trisphosphate-induced Ca release in smooth muscle cells of the guinea pig taenia caeci. *J Gen Physiol* 95: 1103-1122, 1990.

128. **Iino M.** Calcium release mechanisms in smooth muscle. *Jpn J Pharmacol* 54: 345-354, 1990.

129. **Iino M.** Calcium-induced calcium release mechanism in guinea pig taenia caeci. *J Gen Physiol* 94: 363-383, 1989.

130. **Iino M, Kasai H, and Yamazawa T.** Visualization of neural control of intracellular Ca2+ concentration in single vascular smooth muscle cells in situ. *EMBO J* 13: 5026-5031, 1994.

131. **Ionescu L, Cheung K, Vais H, Mak D, White C, and Foskett J.** Graded recruitment and inactivation of single InsP3 receptor Ca2+-release channels: implications for quantal [corrected] Ca2+release. *J Physiol* 573: 645-662, 2006.

132. **Ito I, Jarajapu YP, Grant MB, and Knot HJ.** Characteristics of myogenic tone in the rat ophthalmic artery. *Am J Physiol Heart Circ Physiol* 292: H360-368, 2007.

133. **Jackson W.** Ion channels and vascular tone. *Hypertension* 35: 173-178, 2000.

134. **Jackson WF, Boerman EM, Lange EJ, Lundback SS, and Cohen KD.** Smooth muscle alpha1D-adrenoceptors mediate phenylephrine-induced vasoconstriction and increases in endothelial cell Ca2+ in hamster cremaster arterioles. *Br J Pharmacol* 155: 514-524, 2008.

135. **Jackson WF, Huebner JM, and Rusch NJ.** Enzymatic isolation and characterization of single vascular smooth muscle cells from cremasteric arterioles. *Microcirculation* 4: 35-50, 1997.

136. **Jaggar JH.** Intravascular pressure regulates local and global Ca(2+) signaling in cerebral artery smooth muscle cells. *Am J Physiol Cell Physiol* 281: C439-448, 2001.

137. **Jaggar JH, Leffler CW, Cheranov SY, Tcheranova D, E S, and Cheng X.** Carbon monoxide dilates cerebral arterioles by enhancing the coupling of Ca2+ sparks to Ca2+-activated K+ channels. *Circ Res* 91: 610-617, 2002.

138. **Jaggar JH, Porter VA, Lederer WJ, and Nelson MT.** Calcium sparks in smooth muscle. *Am J Physiol Cell Physiol* 278: C235-256, 2000.

139. **Jaggar JH, Wellman GC, Heppner TJ, Porter VA, Perez GJ, Gollasch M, Kleppisch T, Rubart M, Stevenson AS, Lederer WJ, Knot HJ, Bonev AD, and Nelson MT.** Ca2+ channels, ryanodine receptors and Ca(2+)-activated K+ channels: a functional unit for regulating arterial tone. *Acta Physiol Scand* 164: 577-587, 1998.

140. **Jarajapu YP, Guberski DL, Grant MB, and Knot HJ.** Myogenic tone and reactivity of cerebral arteries in type II diabetic BBZDR/Wor rat. *Eur J Pharmacol* 579: 298-307, 2008.

141. **Jarajapu YP and Knot HJ.** Role of phospholipase C in development of myogenic tone in rat posterior cerebral arteries. *Am J Physiol Heart Circ Physiol* 283: H2234-2238, 2002.

142. **Jeffries O, McGahon M, Bankhead P, Lozano MM, Scholfield CN, Curtis TM, and McGeown JG.** Ca-Sparks, Oscillations and SR Ca-stores are Increased in Retinal Arteriolar Myocytes via a cAMP/PKA Dependent Pathway Following Exposure to Vasopressin. *Invest Ophthalmol Vis Sci*, 2009.

143. **Jeyakumar L, Copello J, O'Malley A, Wu G, Grassucci R, Wagenknecht T, and Fleischer S.** Purification and characterization of ryanodine receptor 3 from mammalian tissue. *J Biol Chem* 273: 16011-16020, 1998.

144. **Ji G, Feldman ME, Greene KS, Sorrentino V, Xin HB, and Kotlikoff MI.** RYR2 proteins contribute to the formation of Ca(2+) sparks in smooth muscle. *J Gen Physiol* 123: 377-386, 2004.

145. **Jiang D, Xiao B, Li X, and Chen S.** Smooth muscle tissues express a major dominant negative splice variant of the type 3 Ca2+ release channel (ryanodine receptor). *J Biol Chem* 278: 4763-4769, 2003.

146. **Jiang D, Xiao B, Li X, and Chen SR.** Smooth muscle tissues express a major dominant negative splice variant of the type 3 Ca2+ release channel (ryanodine receptor). *J Biol Chem* 278: 4763-4769, 2003.

147. **Jiang D, Xiao B, Yang D, Wang R, Choi P, Zhang L, Cheng H, and Chen SR.** RyR2 mutations linked to ventricular tachycardia and sudden death reduce the threshold for store-overload-induced Ca2+ release (SOICR). *Proc Natl Acad Sci U S A* 101: 13062-13067, 2004.

148. **Joseph S.** The inositol triphosphate receptor family. *Cell Signal* 8: 1-7, 1996.

149. **Katayama E, Funahashi H, Michikawa T, Shiraishi T, Ikemoto T, Iino M, and Mikoshiba K.** Native structure and arrangement of inositol-1,4,5-trisphosphate receptor molecules in bovine cerebellar Purkinje cells as studied by quick-freeze deep-etch electron microscopy. *EMBO J* 15: 4844-4851, 1996.

150. **Kimura T, Lueck J, Harvey P, Pace S, Ikemoto N, Casarotto M, Dirksen R, and Dulhunty A.** Alternative splicing of RyR1 alters the efficacy of skeletal EC coupling. *Cell Calcium* 45: 264-274, 2009.

151. **Kimura T, Pace S, Wei L, Beard N, Dirksen R, and Dulhunty A.** A variably spliced region in the type 1 ryanodine receptor may participate in an inter-domain interaction. *Biochem J* 401: 317-324, 2007.

152. **Kirber M, Ordway R, Clapp L, Walsh JJ, and Singer J.** Both membrane stretch and fatty acids directly activate large conductance Ca(2+)-activated K+ channels in vascular smooth muscle cells. *FEBS Lett* 297: 24-28, 1992.

153. **Klein M, Cheng H, Santana L, Jiang Y, Lederer W, and Schneider M.** Two mechanisms of quantized calcium release in skeletal muscle. *Nature* 379: 455-458, 1996.

154. **Klingler W, Rueffert H, Lehmann-Horn F, Girard T, and Hopkins P.** Core myopathies and risk of malignant hyperthermia. *Anesth Analg* 109: 1167-1173, 2009.

155. **Knot HJ, Standen NB, and Nelson MT.** Ryanodine receptors regulate arterial diameter and wall [Ca2+] in cerebral arteries of rat via Ca2+-dependent K+ channels. *J Physiol* 508 (Pt 1): 211-221, 1998.

156. **Kobayashi S, Bannister M, Gangopadhyay J, Hamada T, Parness J, and Ikemoto N.** Dantrolene stabilizes domain interactions within the ryanodine receptor. *J Biol Chem* 280: 6580-6587, 2005.

157. **Kotecha N and Hill MA.** Myogenic contraction in rat skeletal muscle arterioles: smooth muscle membrane potential and Ca(2+) signaling. *Am J Physiol Heart Circ Physiol* 289: H1326-1334, 2005.

158. **Laitinen P, Swan H, Piippo K, Viitasalo M, Toivonen L, and Kontula K.** Genes, exercise and sudden death: molecular basis of familial catecholaminergic polymorphic ventricular tachycardia. *Ann Med* 36 Suppl 1: 81-86, 2004.

159. **Lamb G.** Excitation-contraction coupling in skeletal muscle: comparisons with cardiac muscle. *Clin Exp Pharmacol Physiol* 27: 216-224, 2000.

160. **Lamont C and Wier WG.** Different roles of ryanodine receptors and inositol (1,4,5)-trisphosphate receptors in adrenergically stimulated contractions of small arteries. *Am J Physiol Heart Circ Physiol* 287: H617-625, 2004.

161. **Lange EJ, Boerman EM, Segal SS, and Jackson WF.** Differences in expression and function of ryanodine receptors between arteries and arterioles in the mouse. *FASEB J* 24, 2010.

162. **Langton P.** Calcium channel currents recorded from isolated myocytes of rat basilar artery are stretch sensitive. *J Physiol* 471: 1-11, 1993.

163. **Laporte R, Hui A, and Laher I.** Pharmacological modulation of sarcoplasmic reticulum function in smooth muscle. *Pharmacol Rev* 56: 439-513, 2004.

164. **Laver D, Roden L, Ahern G, Eager K, Junankar P, and Dulhunty A.** Cytoplasmic Ca2+ inhibits the ryanodine receptor from cardiac muscle. *J Membr Biol* 147: 7-22, 1995.

165. **Ledbetter MW, Preiner JK, Louis CF, and Mickelson JR.** Tissue distribution of ryanodine receptor isoforms and alleles determined by reverse transcription polymerase chain reaction. *J Biol Chem* 269: 31544-31551, 1994.

166. **Lee CH, Poburko D, Kuo KH, Seow CY, and van Breemen C.** Ca(2+) oscillations, gradients, and homeostasis in vascular smooth muscle. *Am J Physiol Heart Circ Physiol* 282: H1571-1583, 2002.

167. **Leeb T and Brenig B.** cDNA cloning and sequencing of the human ryanodine receptor type 3 (RYR3) reveals a novel alternative splice site in the RYR3 gene. *FEBS Lett* 423: 367-370, 1998.

168. **Li XQ, Zheng YM, Rathore R, Ma J, Takeshima H, and Wang YX.** Genetic evidence for functional role of ryanodine receptor 1 in pulmonary artery smooth muscle cells. *Pflugers Arch* 457: 771-783, 2009.

169. **Li Y, Kranias E, Mignery G, and Bers D.** Protein kinase A phosphorylation of the ryanodine receptor does not affect calcium sparks in mouse ventricular myocytes. *Circ Res* 90: 309-316, 2002.

170. **Liu Q, Zheng Y, and Wang Y.** Two distinct signaling pathways for regulation of spontaneous local Ca2+ release by phospholipase C in airway smooth muscle cells. *Pflugers Arch* 453: 531-541, 2007.

171. **Lohn M, Furstenau M, Sagach V, Elger M, Schulze W, Luft FC, Haller H, and Gollasch M.** Ignition of calcium sparks in arterial and cardiac muscle through caveolae. *Circ Res* 87: 1034-1039, 2000.

172. **Lohn M, Jessner W, Furstenau M, Wellner M, Sorrentino V, Haller H, Luft FC, and Gollasch M.** Regulation of calcium sparks and spontaneous transient outward currents by RyR3 in arterial vascular smooth muscle cells. *Circ Res* 89: 1051-1057, 2001.

173. **López-López J, Shacklock P, Balke C, and Wier W.** Local calcium transients triggered by single L-type calcium channel currents in cardiac cells. *Science* 268: 1042-1045, 1995.

174. **Ma J, Hayek S, and Bhat M.** Membrane topology and membrane retention of the ryanodine receptor calcium release channel. *Cell Biochem Biophys* 40: 207-224, 2004.

175. **Mackrill J.** Ryanodine receptor calcium channels and their partners as drug targets. *Biochem Pharmacol* 79: 1535-1543, 2010.

176. **Macmillan D and McCarron JG.** The phospholipase C inhibitor U-73122 inhibits Ca(2+) release from the intracellular sarcoplasmic reticulum Ca(2+) store by inhibiting Ca(2+) pumps in smooth muscle. *Br J Pharmacol* 160: 1295-1301.

177. **Maeda N, Kawasaki T, Nakade S, Yokota N, Taguchi T, Kasai M, and Mikoshiba K.** Structural and functional characterization of inositol 1,4,5-trisphosphate receptor channel from mouse cerebellum. *J Biol Chem* 266: 1109-1116, 1991.

178. **Mahaut-Smith M, Martinez-Pinna J, and Gurung I.** A role for membrane potential in regulating GPCRs? *Trends Pharmacol Sci* 29: 421-429, 2008.

179. **Mak D, McBride S, and Foskett J.** Regulation by Ca2+ and inositol 1,4,5-trisphosphate (InsP3) of single recombinant type 3 InsP3 receptor channels. Ca2+ activation uniquely distinguishes types 1 and 3 insp3 receptors. *J Gen Physiol* 117: 435-446, 2001.

180. **Mandala M, Heppner TJ, Bonev AD, and Nelson MT.** Effect of endogenous and exogenous nitric oxide on calcium sparks as targets for vasodilation in rat cerebral artery. *Nitric Oxide* 16: 104-109, 2007.

181. **Marks A.** Cellular functions of immunophilins. *Physiol Rev* 76: 631-649, 1996.

182. **Marshall J and Tandon H.** Direct observations of muscle arterioles and venules following contraction of skeletal muscle fibres in the rat. *J Physiol* 350: 447-459, 1984.

183. **Marx S, Ondrias K, and Marks A.** Coupled gating between individual skeletal muscle Ca2+ release channels (ryanodine receptors). *Science* 281: 818-821, 1998.

184. **Marx S, Reiken S, Hisamatsu Y, Jayaraman T, Burkhoff D, Rosemblit N, and Marks A.** PKA phosphorylation dissociates FKBP12.6 from the calcium release channel (ryanodine receptor): defective regulation in failing hearts. *Cell* 101: 365-376, 2000.

185. **Marziali G, Rossi D, Giannini G, Charlesworth A, and Sorrentino V.** cDNA cloning reveals a tissue specific expression of alternatively spliced transcripts of the ryanodine receptor type 3 (RyR3) calcium release channel. *FEBS Lett* 394: 76-82, 1996.

186. **Massett MP, Ungvari Z, Csiszar A, Kaley G, and Koller A.** Different roles of PKC and MAP kinases in arteriolar constrictions to pressure and agonists. *Am J Physiol Heart Circ Physiol* 283: H2282-2287, 2002.

187. **McCarron J, Chalmers S, Bradley K, MacMillan D, and Muir T.** Ca2+ microdomains in smooth muscle. *Cell Calcium* 40: 461-493, 2006.

188. **McCarron JG, Bradley KN, MacMillan D, and Muir TC.** Sarcolemma agonist-induced interactions between InsP3 and ryanodine receptors in Ca2+ oscillations and waves in smooth muscle. *Biochem Soc Trans* 31: 920-924, 2003.

189. **McCarron JG, Crichton CA, Langton PD, MacKenzie A, and Smith GL.** Myogenic contraction by modulation of voltage-dependent calcium currents in isolated rat cerebral arteries. *J Physiol* 498 (Pt 2): 371-379, 1997.

190. **McCarron JG and Olson ML.** A single luminally continuous sarcoplasmic reticulum with apparently separate Ca2+ stores in smooth muscle. *J Biol Chem* 283: 7206-7218, 2008.

191. **McGarry S and Williams A.** Activation of the sheep cardiac sarcoplasmic reticulum Ca(2+)-release channel by analogues of sulmazole. *Br J Pharmacol* 111: 1212-1220, 1994.

192. **Mederos y Schnitzler M, Storch U, Meibers S, Nurwakagari P, Breit A, Essin K, Gollasch M, and Gudermann T.** Gq-coupled receptors as mechanosensors mediating myogenic vasoconstriction. *EMBO J* 27: 3092-3103, 2008.

193. **Meininger GA and Davis MJ.** Cellular mechanisms involved in the vascular myogenic response. *Am J Physiol* 263: H647-659, 1992.

194. **Meyers M, Pickel V, Sheu S, Sharma V, Scotto K, and Fishman G.** Association of sorcin with the cardiac ryanodine receptor. *J Biol Chem* 270: 26411-26418, 1995.

195. **Miriel VA, Mauban JR, Blaustein MP, and Wier WG.** Local and cellular Ca2+ transients in smooth muscle of pressurized rat resistance arteries during myogenic and agonist stimulation. *J Physiol* 518 (Pt 3): 815-824, 1999.

196. **Mironneau J, Coussin F, Jeyakumar L, Fleischer S, Mironneau C, and Macrez N.** Contribution of ryanodine receptor subtype 3 to ca2+ responses in Ca2+-overloaded cultured rat portal vein myocytes. *J Biol Chem* 276: 11257-11264, 2001.

197. **Miyatake R, Furukawa A, Matsushita M, Iwahashi K, Nakamura K, Ichikawa Y, and Suwaki H.** Tissue-specific alternative splicing of mouse brain type ryanodine receptor/calcium release channel mRNA. *FEBS Lett* 395: 123-126, 1996.

198. **Murrant C, Duza T, Kim M, Cohen K, and Sarelius I.** Arteriolar dilations induced by contraction of hamster cremaster muscle are dependent on changes in endothelial cell calcium. *Acta Physiol Scand* 180: 231-238, 2004.

199. **Nakade S, Maeda N, and Mikoshiba K.** Involvement of the C-terminus of the inositol 1,4,5-trisphosphate receptor in Ca2+ release analysed using region-specific monoclonal antibodies. *Biochem J* 277 (Pt 1): 125-131, 1991.

200. **Neild TO.** Measurement of arteriole diameter changes by analysis of television images. *Blood Vessels* 26: 48-52, 1989.

201. **Nelson M and Quayle J.** Physiological roles and properties of potassium channels in arterial smooth muscle. *Am J Physiol* 268: C799-822, 1995.

202. **Nelson MT, Cheng H, Rubart M, Santana LF, Bonev AD, Knot HJ, and Lederer WJ.** Relaxation of arterial smooth muscle by calcium sparks. *Science* 270: 633-637, 1995.

203. **Nelson MT, Conway MA, Knot HJ, and Brayden JE.** Chloride channel blockers inhibit myogenic tone in rat cerebral arteries. *J Physiol* 502 (Pt 2): 259-264, 1997.

204. **Nelson MT, Patlak JB, Worley JF, and Standen NB.** Calcium channels, potassium channels, and voltage dependence of arterial smooth muscle tone. *Am J Physiol* 259: C3-18, 1990.

205. **Nelson MT and Quayle JM.** Physiological roles and properties of potassium channels in arterial smooth muscle. *Am J Physiol* 268: C799-822, 1995.

206. **Neylon CB, Richards SM, Larsen MA, Agrotis A, and Bobik A.** Multiple types of ryanodine receptor/Ca2+ release channels are expressed in vascular smooth muscle. *Biochem Biophys Res Commun* 215: 814-821, 1995.

207. **Nixon G, Mignery G, and Somlyo A.** Immunogold localization of inositol 1,4,5-trisphosphate receptors and characterization of ultrastructural features of the sarcoplasmic reticulum in phasic and tonic smooth muscle. *J Muscle Res Cell Motil* 15: 682-700, 1994.

208. **Nizami S, Lee V, Davies J, Long P, Jovanovic J, and Sihra T.** Presynaptic roles of intracellular Ca(2+) stores in signalling and exocytosis. *Biochem Soc Trans* 38: 529-535, 2010.

209. **Ogawa Y.** Distinct mechanisms for dysfunctions of mutated ryanodine receptor isoforms. *Biochem Biophys Res Commun* 369: 208-212, 2008.

210. **Ohya Y, Adachi N, Nakamura Y, Setoguchi M, Abe I, and Fujishima M.** Stretch-activated channels in arterial smooth muscle of genetic hypertensive rats. *Hypertension* 31: 254-258, 1998.

211. **Orlova E, Serysheva I, van Heel M, Hamilton S, and Chiu W.** Two structural configurations of the skeletal muscle calcium release channel. *Nat Struct Biol* 3: 547-552, 1996.

212. **Osol G, Laher I, and Cipolla M.** Protein kinase C modulates basal myogenic tone in resistance arteries from the cerebral circulation. *Circ Res* 68: 359-367, 1991.

213. **Osol G, Laher I, and Kelley M.** Myogenic tone is coupled to phospholipase C and G protein activation in small cerebral arteries. *Am J Physiol* 265: H415-420, 1993.

214. **Patterson R, Boehning D, and Snyder S.** Inositol 1,4,5-trisphosphate receptors as signal integrators. *Annu Rev Biochem* 73: 437-465, 2004.

215. **Patterson R, van Rossum D, Barrow R, and Snyder S.** RACK1 binds to inositol 1,4,5-trisphosphate receptors and mediates Ca2+ release. *Proc Natl Acad Sci U S A* 101: 2328-2332, 2004.

216. **Peng H, Matchkov V, Ivarsen A, Aalkjaer C, and Nilsson H.** Hypothesis for the initiation of vasomotion. *Circ Res* 88: 810-815, 2001.

217. **Percival A, Williams A, Kenyon J, Grinsell M, Airey J, and Sutko J.** Chicken skeletal muscle ryanodine receptor isoforms: ion channel properties. *Biophys J* 67: 1834-1850, 1994.

218. **Perez P, Ramos-Franco J, Fill M, and Mignery G.** Identification and functional reconstitution of the type 2 inositol 1,4,5-trisphosphate receptor from ventricular cardiac myocytes. *J Biol Chem* 272: 23961-23969, 1997.

219. **Perkel J.** How to troubleshoot sample preparation for cryo-electron microscopy, an up-and-coming structural biology technique. *The Scientist* 23: 56, 2009.

220. **Poole J, Lawrenson L, Kim J, Brown C, and Richardson R.** Vascular and metabolic response to cycle exercise in sedentary humans: effect of age. *Am J Physiol Heart Circ Physiol* 284: H1251-1259, 2003.

221. **Porter VA, Bonev AD, Knot HJ, Heppner TJ, Stevenson AS, Kleppisch T, Lederer WJ, and Nelson MT.** Frequency modulation of Ca2+ sparks is involved in regulation of arterial diameter by cyclic nucleotides. *Am J Physiol* 274: C1346-1355, 1998.

222. **Potocnik SJ and Hill MA.** Pharmacological evidence for capacitative Ca(2+) entry in cannulated and pressurized skeletal muscle arterioles. *Br J Pharmacol* 134: 247-256, 2001.

223. **Prakash Y, Kannan M, and Sieck G.** Regulation of intracellular calcium oscillations in porcine tracheal smooth muscle cells. *Am J Physiol* 272: C966-975, 1997.

224. **Pries A and Secomb T.** Blood flow in microvascular networks. In: *Handbook of Physiology: Microcirculation* (2 ed.), edited by Tuma R, Duran W and Ley K. USA: Elsevier, 2008.

225. **Proctor D, Koch D, Newcomer S, Le K, and Leuenberger U.** Impaired leg vasodilation during dynamic exercise in healthy older women. *J Appl Physiol* 95: 1963-1970, 2003.

226. **Proctor D and Parker B.** Vasodilation and vascular control in contracting muscle of the aging human. *Microcirculation* 13: 315-327, 2006.

227. **Protasi F.** Structural interaction between RYRs and DHPRs in calcium release units of cardiac and skeletal muscle cells. *Front Biosci* 7: d650-658, 2002.

228. **Pucovsky V and Bolton TB.** Localisation, function and composition of primary Ca(2+) spark discharge region in isolated smooth muscle cells from guinea-pig mesenteric arteries. *Cell Calcium* 39: 113-129, 2006.

229. **Radermacher M, Rao V, Grassucci R, Frank J, Timerman A, Fleischer S, and Wagenknecht T.** Cryo-electron microscopy and three-dimensional reconstruction of the calcium release channel/ryanodine receptor from skeletal muscle. *J Cell Biol* 127: 411-423, 1994.

230. **Reggiani C and te Kronnie T.** RyR isoforms and fibre type-specific expression of proteins controlling intracellular calcium concentration in skeletal muscles. *J Muscle Res Cell Motil* 27: 327-335, 2006.

231. **Remillard CV, Zhang WM, Shimoda LA, and Sham JS.** Physiological properties and functions of Ca(2+) sparks in rat intrapulmonary arterial smooth muscle cells. *Am J Physiol Lung Cell Mol Physiol* 283: L433-444, 2002.

232. **Robinson R, Carpenter D, Shaw M, Halsall J, and Hopkins P.** Mutations in RYR1 in malignant hyperthermia and central core disease. *Hum Mutat* 27: 977-989, 2006.

233. **Rossi A and Taylor C.** Ca2+ regulation of inositol 1,4,5-trisphosphate receptors: can Ca2+ function without calmodulin? *Mol Pharmacol* 66: 199-203, 2004.

234. **Rueda A, Song M, Toro L, Stefani E, and Valdivia HH.** Sorcin modulation of Ca2+ sparks in rat vascular smooth muscle cells. *J Physiol* 576: 887-901, 2006.

235. **Ruehr M, Russell M, Ferguson D, Bhat M, Ma J, Damron D, Scott J, and Bond M.** Targeting of protein kinase A by muscle A kinase-anchoring protein (mAKAP) regulates phosphorylation and function of the skeletal muscle ryanodine receptor. *J Biol Chem* 278: 24831-24836, 2003.

236. **Ríos E, Ma J, and González A.** The mechanical hypothesis of excitation-contraction (EC) coupling in skeletal muscle. *J Muscle Res Cell Motil* 12: 127-135, 1991.

237. **Salomone S, Soydan G, Moskowitz M, and Sims J.** Inhibition of cerebral vasoconstriction by dantrolene and nimodipine. *Neurocrit Care* 10: 93-102, 2009.

238. **Schiefer A, Meissner G, and Isenberg G.** Ca2+ activation and Ca2+ inactivation of canine reconstituted cardiac sarcoplasmic reticulum Ca(2+)-release channels. *J Physiol* 489 (Pt 2): 337-348, 1995.

239. **Schneider M.** Control of calcium release in functioning skeletal muscle fibers. *Annu Rev Physiol* 56: 463-484, 1994.

240. **Segal SS.** Regulation of blood flow in the microcirculation. *Microcirculation* 12: 33-45, 2005.

241. **Sencer S, Papineni R, Halling D, Pate P, Krol J, Zhang J, and Hamilton S.** Coupling of RYR1 and L-type calcium channels via calmodulin binding domains. *J Biol Chem* 276: 38237-38241, 2001.

242. **Serysheva I, Bare D, Ludtke S, Kettlun C, Chiu W, and Mignery G.** Structure of the type 1 inositol 1,4,5-trisphosphate receptor revealed by electron cryomicroscopy. *J Biol Chem* 278: 21319-21322, 2003.

243. **Serysheva I, Schatz M, van Heel M, Chiu W, and Hamilton S.** Structure of the skeletal muscle calcium release channel activated with Ca2+ and AMP-PCP. *Biophys J* 77: 1936-1944, 1999.

244. **Setoguchi M, Ohya Y, Abe I, and Fujishima M.** Stretch-activated whole-cell currents in smooth muscle cells from mesenteric resistance artery of guinea-pig. *J Physiol* 501 (Pt 2): 343-353, 1997.

245. **Sharma M, Jeyakumar L, Fleischer S, and Wagenknecht T.** Three-dimensional structure of ryanodine receptor isoform three in two conformational states as visualized by cryo-electron microscopy. *J Biol Chem* 275: 9485-9491, 2000.

246. **Simmerman H and Jones L.** Phospholamban: protein structure, mechanism of action, and role in cardiac function. *Physiol Rev* 78: 921-947, 1998.

247. **Sitsapesan R and Williams A.** Regulation of current flow through ryanodine receptors by luminal Ca2+. *J Membr Biol* 159: 179-185, 1997.

248. **Slish DF, Welsh DG, and Brayden JE.** Diacylglycerol and protein kinase C activate cation channels involved in myogenic tone. *Am J Physiol Heart Circ Physiol* 283: H2196-2201, 2002.

249. **Sorrentino V and Volpe P.** Ryanodine receptors: how many, where and why? *Trends Pharmacol Sci* 14: 98-103, 1993.

250. **Soulsby M, Alzayady K, Xu Q, and Wojcikiewicz R.** The contribution of serine residues 1588 and 1755 to phosphorylation of the type I inositol 1,4,5-trisphosphate receptor by PKA and PKG. *FEBS Lett* 557: 181-184, 2004.

251. **Straub S, Wagner Ln, Bruce J, and Yule D.** Modulation of cytosolic calcium signaling by protein kinase A-mediated phosphorylation of inositol 1,4,5-trisphosphate receptors. *Biol Res* 37: 593-602, 2004.

252. **Sun X, Gu XQ, and Haddad GG.** Calcium influx via L- and N-type calcium channels activates a transient large-conductance Ca2+-activated K+ current in mouse neocortical pyramidal neurons. *J Neurosci* 23: 3639-3648, 2003.

253. **Sutko J and Airey J.** Ryanodine receptor Ca2+ release channels: does diversity in form equal diversity in function? *Physiol Rev* 76: 1027-1071, 1996.

254. **Takasago T, Imagawa T, Furukawa K, Ogurusu T, and Shigekawa M.** Regulation of the cardiac ryanodine receptor by protein kinase-dependent phosphorylation. *J Biochem* 109: 163-170, 1991.

255. **Takeshima H, Nishimura S, Matsumoto T, Ishida H, Kangawa K, Minamino N, Matsuo H, Ueda M, Hanaoka M, and Hirose T.** Primary structure and expression from complementary DNA of skeletal muscle ryanodine receptor. *Nature* 339: 439-445, 1989.

256. **Tasker PN, Michelangeli F, and Nixon GF.** Expression and distribution of the type 1 and type 3 inositol 1,4, 5-trisphosphate receptor in developing vascular smooth muscle. *Circ Res* 84: 536-542, 1999.

257. **Tasker PN, Taylor CW, and Nixon GF.** Expression and distribution of InsP(3) receptor subtypes in proliferating vascular smooth muscle cells. *Biochem Biophys Res Commun* 273: 907-912, 2000.

258. **Taylor C, da Fonseca P, and Morris E.** IP(3) receptors: the search for structure. *Trends Biochem Sci* 29: 210-219, 2004.

259. **Taylor CW and Laude AJ.** IP3 receptors and their regulation by calmodulin and cytosolic Ca2+. *Cell Calcium* 32: 321-334, 2002.

260. **Thorneloe KS and Nelson MT.** Ion channels in smooth muscle: regulators of intracellular calcium and contractility. *Can J Physiol Pharmacol* 83: 215-242, 2005.

261. **Tostes RC, Leite R, and Webb C.** Vascular smooth muscle contraction and relaxation. In: *Hypertension Primer: The essentials of high blood pressure: basic science, population science, and clinical management* (4 ed.), edited by Izzo J, Sica D and Black H. Philadelphia, PA: Lippencott, Williams & Wilkins, 2008.

262. **Tripathy A and Meissner G.** Sarcoplasmic reticulum lumenal Ca2+ has access to cytosolic activation and inactivation sites of skeletal muscle Ca2+ release channel. *Biophys J* 70: 2600-2615, 1996.

263. **Tu H, Wang Z, and Bezprozvanny I.** Modulation of mammalian inositol 1,4,5-trisphosphate receptor isoforms by calcium: a role of calcium sensor region. *Biophys J* 88: 1056-1069, 2005.

264. **Tu J, Xiao B, Yuan J, Lanahan A, Leoffert K, Li M, Linden D, and Worley P.** Homer binds a novel proline-rich motif and links group 1 metabotropic glutamate receptors with IP3 receptors. *Neuron* 21: 717-726, 1998.

265. **Tumelty J, Scholfield N, Stewart M, Curtis T, and McGeown G.** Ca2+-sparks constitute elementary building blocks for global Ca2+-signals in myocytes of retinal arterioles. *Cell Calcium* 41: 451-466, 2007.

266. **Tunwell R, Wickenden C, Bertrand B, Shevchenko V, Walsh M, Allen P, and Lai F.** The human cardiac muscle ryanodine receptor-calcium release channel: identification, primary structure and topological analysis. *Biochem J* 318 (Pt 2): 477-487, 1996.

267. **Vaithianathan T, Narayanan D, Asuncion-Chin M, Jeyakumar L, Liu J, Fleischer S, Jaggar J, and Dopico A.** Subtype identification and functional

characterization of ryanodine receptors in rat cerebral artery myocytes. *Am J Physiol Cell Physiol* 299: C264-278, 2010.

268. **Valdivia H, Kaplan J, Ellis-Davies G, and Lederer W.** Rapid adaptation of cardiac ryanodine receptors: modulation by Mg2+ and phosphorylation. *Science* 267: 1997-2000, 1995.

269. **Vallot O, Combettes L, Jourdon P, Inamo J, Marty I, Claret M, and Lompré A.** Intracellular Ca(2+) handling in vascular smooth muscle cells is affected by proliferation. *Arterioscler Thromb Vasc Biol* 20: 1225-1235, 2000.

270. **Vermassen E, Parys J, and Mauger J.** Subcellular distribution of the inositol 1,4,5-trisphosphate receptors: functional relevance and molecular determinants. *Biol Cell* 96: 3-17, 2004.

271. **Wagenknecht T, Radermacher M, Grassucci R, Berkowitz J, Xin H, and Fleischer S.** Locations of calmodulin and FK506-binding protein on the three-dimensional architecture of the skeletal muscle ryanodine receptor. *J Biol Chem* 272: 32463-32471, 1997.

272. **Wagenknecht T and Samsó M.** Three-dimensional reconstruction of ryanodine receptors. *Front Biosci* 7: d1464-1474, 2002.

273. **Webb R.** Smooth muscle contraction and relaxation. *Adv Physiol Educ* 27: 201-206, 2003.

274. **Wehrens X, Lehnart S, Huang F, Vest J, Reiken S, Mohler P, Sun J, Guatimosim S, Song L, Rosemblit N, D'Armiento J, Napolitano C, Memmi M, Priori S, Lederer W, and Marks A.** FKBP12.6 deficiency and defective calcium release channel (ryanodine receptor) function linked to exercise-induced sudden cardiac death. *Cell* 113: 829-840, 2003.

275. **Wehrens X, Lehnart S, Reiken S, Deng S, Vest J, Cervantes D, Coromilas J, Landry D, and Marks A.** Protection from cardiac arrhythmia through ryanodine receptor-stabilizing protein calstabin2. *Science* 304: 292-296, 2004.

276. **Wehrens X, Lehnart S, Reiken S, and Marks A.** Ca2+/calmodulin-dependent protein kinase II phosphorylation regulates the cardiac ryanodine receptor. *Circ Res* 94: e61-70, 2004.

277. **Weisleder N, Brotto M, Komazaki S, Pan Z, Zhao X, Nosek T, Parness J, Takeshima H, and Ma J.** Muscle aging is associated with compromised Ca2+ spark signaling and segregated intracellular Ca2+ release. *J Cell Biol* 174: 639-645, 2006.

278. **Welch W, Rheault S, West D, and Williams A.** A model of the putative pore region of the cardiac ryanodine receptor channel. *Biophys J* 87: 2335-2351, 2004.

279. **Wellman GC, Nathan DJ, Saundry CM, Perez G, Bonev AD, Penar PL, Tranmer BI, and Nelson MT.** Ca2+ sparks and their function in human cerebral arteries. *Stroke* 33: 802-808, 2002.

280. **Wellman GC, Santana LF, Bonev AD, and Nelson MT.** Role of phospholamban in the modulation of arterial Ca(2+) sparks and Ca(2+)-activated K(+) channels by cAMP. *Am J Physiol Cell Physiol* 281: C1029-1037, 2001.

281. **Welsh DG, Morielli AD, Nelson MT, and Brayden JE.** Transient receptor potential channels regulate myogenic tone of resistance arteries. *Circ Res* 90: 248-250, 2002.

282. **Wesselman JP, VanBavel E, Pfaffendorf M, and Spaan JA.** Voltage-operated calcium channels are essential for the myogenic responsiveness of cannulated rat mesenteric small arteries. *J Vasc Res* 33: 32-41, 1996.

283. **Witcher D, Kovacs R, Schulman H, Cefali D, and Jones L.** Unique phosphorylation site on the cardiac ryanodine receptor regulates calcium channel activity. *J Biol Chem* 266: 11144-11152, 1991.

284. **Wray S and Burdyga T.** Sarcoplasmic reticulum function in smooth muscle. *Physiol Rev* 90: 113-178, 2010.

285. **Wray S, Burdyga T, and Noble K.** Calcium signalling in smooth muscle. *Cell Calcium* 38: 397-407, 2005.

286. **Wu X and Davis M.** Characterization of stretch-activated cation current in coronary smooth muscle cells. *Am J Physiol Heart Circ Physiol* 280: H1751-1761, 2001.

287. **Xi Q, Adebiyi A, Zhao G, Chapman KE, Waters CM, Hassid A, and Jaggar JH.** IP3 constricts cerebral arteries via IP3 receptor-mediated TRPC3 channel activation and independently of sarcoplasmic reticulum Ca2+ release. *Circ Res* 102: 1118-1126, 2008.

288. **Xi Q, Umstot E, Zhao G, Narayanan D, Leffler CW, and Jaggar JH.** Glutamate regulates Ca2+ signals in smooth muscle cells of newborn piglet brain slice arterioles through astrocyte- and heme oxygenase-dependent mechanisms. *Am J Physiol Heart Circ Physiol* 298: H562-569.

289. **Xu L, Tripathy A, Pasek D, and Meissner G.** Potential for pharmacology of ryanodine receptor/calcium release channels. *Ann N Y Acad Sci* 853: 130-148, 1998.

290. **Yang XR, Lin MJ, Yip KP, Jeyakumar LH, Fleischer S, Leung GP, and Sham JS.** Multiple ryanodine receptor subtypes and heterogeneous ryanodine receptor-gated Ca2+ stores in pulmonary arterial smooth muscle cells. *Am J Physiol Lung Cell Mol Physiol* 289: L338-348, 2005.

291. **Yang Y, Murphy TV, Ella SR, Grayson TH, Haddock R, Hwang YT, Braun AP, Peichun G, Korthuis RJ, Davis MJ, and Hill MA.** Heterogeneity in function of small artery smooth muscle BKCa: involvement of the beta1-subunit. *J Physiol* 587: 3025-3044, 2009.

292. **Yeon DS, Kim JS, Ahn DS, Kwon SC, Kang BS, Morgan KG, and Lee YH.** Role of protein kinase C- or RhoA-induced Ca(2+) sensitization in stretch-induced myogenic tone. *Cardiovasc Res* 53: 431-438, 2002.

293. **Yin C, D'Cruz L, and Lai F.** Ryanodine receptor arrays: not just a pretty pattern? *Trends Cell Biol* 18: 149-156, 2008.

294. **Yuan J, Kiselyov K, Shin D, Chen J, Shcheynikov N, Kang S, Dehoff M, Schwarz M, Seeburg P, Muallem S, and Worley P.** Homer binds TRPC family channels and is required for gating of TRPC1 by IP3 receptors. *Cell* 114: 777-789, 2003.

295. **Yuill KH and Smirnov SV.** Calcium-dependent regulation of voltage-gated sodium channels in cardiac myocytes: just the beginning? *Cardiovasc Res* 85: 411-412.

296. **Zacharia J, Zhang J, and Wier W.** Ca2+ signaling in mouse mesenteric small arteries: myogenic tone and adrenergic vasoconstriction. *Am J Physiol Heart Circ Physiol* 292: H1523-1532, 2007.

297. **Zalk R, Lehnart S, and Marks A.** Modulation of the ryanodine receptor and intracellular calcium. *Annu Rev Biochem* 76: 367-385, 2007.

298. **Zhang J, Wu Y, Williams B, Rodney G, Mandel F, Strasburg G, and Hamilton S.** Oxidation of the skeletal muscle Ca2+ release channel alters calmodulin binding. *Am J Physiol* 276: C46-53, 1999.

299. **Zhang WM, Yip KP, Lin MJ, Shimoda LA, Li WH, and Sham JS.** ET-1 activates Ca2+ sparks in PASMC: local Ca2+ signaling between inositol trisphosphate and ryanodine receptors. *Am J Physiol Lung Cell Mol Physiol* 285: L680-690, 2003.

300. **Zhao G, Adebiyi A, Blaskova E, Xi Q, and Jaggar JH.** Type 1 inositol 1,4,5-trisphosphate receptors mediate UTP-induced cation currents, Ca2+ signals, and vasoconstriction in cerebral arteries. *Am J Physiol Cell Physiol* 295: C1376-1384, 2008.

301. **Zhao G, Adebiyi A, Xi Q, and Jaggar JH.** Hypoxia reduces KCa channel activity by inducing Ca2+ spark uncoupling in cerebral artery smooth muscle cells. *Am J Physiol Cell Physiol* 292: C2122-2128, 2007.

302. **Zheng YM, Wang QS, Liu QH, Rathore R, Yadav V, and Wang YX.** Heterogeneous gene expression and functional activity of ryanodine receptors in resistance and conduit pulmonary as well as mesenteric artery smooth muscle cells. *J Vasc Res* 45: 469-479, 2008.

303. **Zheng YM, Wang QS, Rathore R, Zhang WH, Mazurkiewicz JE, Sorrentino V, Singer HA, Kotlikoff MI, and Wang YX.** Type-3 ryanodine receptors mediate hypoxia-, but not neurotransmitter-induced calcium release and contraction in pulmonary artery smooth muscle cells. *J Gen Physiol* 125: 427-440, 2005.

304. **ZhuGe R, Sims S, Tuft R, Fogarty K, and Walsh JJ.** Ca2+ sparks activate K+ and Cl- channels, resulting in spontaneous transient currents in guinea-pig tracheal myocytes. *J Physiol* 513 (Pt 3): 711-718, 1998.

305. **Zimmermann PA, Knot HJ, Stevenson AS, and Nelson MT.** Increased myogenic tone and diminished responsiveness to ATP-sensitive K+ channel openers in cerebral arteries from diabetic rats. *Circ Res* 81: 996-1004, 1997.

306. **Zorzato F, Fujii J, Otsu K, Phillips M, Green N, Lai F, Meissner G, and MacLennan D.** Molecular cloning of cDNA encoding human and rabbit forms of the Ca2+ release channel (ryanodine receptor) of skeletal muscle sarcoplasmic reticulum. *J Biol Chem* 265: 2244-2256, 1990.

307. **Zou H, Ratz P, and Hill M.** Role of myosin phosphorylation and [Ca2+]i in myogenic reactivity and arteriolar tone. *Am J Physiol* 269: H1590-1596, 1995.

308. **Zucchi R and Ronca-Testoni S.** The sarcoplasmic reticulum Ca2+ channel/ryanodine receptor: modulation by endogenous effectors, drugs and disease states. *Pharmacol Rev* 49: 1-51, 1997.